INFORMATION TO USERS

This manuscript has been reproduced from the microfilm master. UMI films the text directly from the original or copy submitted. Thus, some thesis and dissertation copies are in typewriter face, while others may be from any type of computer printer.

The quality of this reproduction is dependent upon the quality of the copy submitted. Broken or indistinct print, colored or poor quality illustrations and photographs, print bleedthrough, substandard margins, and improper alignment can adversely affect reproduction.

In the unlikely event that the author did not send UMI a complete manuscript and there are missing pages, these will be noted. Also, if unauthorized copyright material had to be removed, a note will indicate the deletion.

Oversize materials (e.g., maps, drawings, charts) are reproduced by sectioning the original, beginning at the upper left-hand corner and continuing from left to right in equal sections with small overlaps.

Photographs included in the original manuscript have been reproduced xerographically in this copy. Higher quality 6" x 9" black and white photographic prints are available for any photographs or illustrations appearing in this copy for an additional charge. Contact UMI directly to order.

ProQuest Information and Learning
300 North Zeeb Road, Ann Arbor, MI 48106-1346 USA
800-521-0600

DISSERTATION

DOSE-VOLUME RELATIONSHIPS OF RADIATION INJURY TO CANINE LUNG: EARLY EFFECTS

Submitted by

Jean Marie Poulson

Department of Radiological Health Sciences

In partial fulfillment of the requirements

for the degree of Doctor of Philosophy

Colorado State University

Fort Collins, Colorado

Summer 2001

ProQuest Information and Learning Company
300 North Zeeb Road
P.O. Box 1346
Ann Arbor, MI 48106-1346

COLORADO STATE UNIVERSITY

July 5, 2001

WE HEREBY RECOMMEND THAT THE DISSERTATION PREPARED UNDER OUR SUPERVISION BY JEAN MARIE POULSON ENTITLED *DOSE-VOLUME RELATIONSHIPS OF RADIATION INJURY TO CANINE LUNG: EARLY EFFECTS* BE ACCEPTED AS FULFILLING IN PART REQUIREMENTS FOR THE DEGREE OF DOCTOR OF PHILOSOPHY.

Committee on Graduate Work

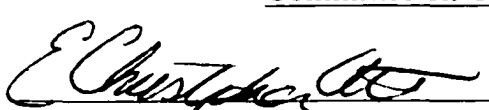

E. Christopher Orton

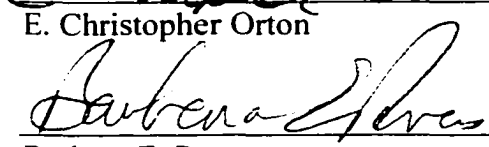

Barbara E. Powers

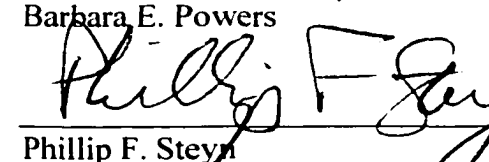

Phillip F. Steyn

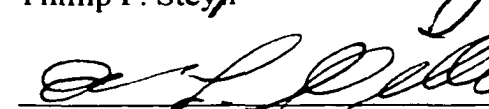

Edward L. Gillette, Advisor

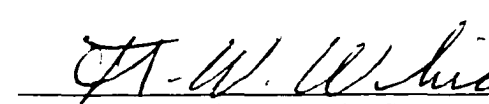

F. Ward Whicker, Interim Department Head

ABSTRACT OF DISSERTATION

DOSE-VOLUME RELATIONSHIPS OF RADIATION INJURY TO CANINE LUNG: EARLY EFFECTS

Tolerance of lung is a critical limiting factor in radiotherapy of tumors involving the thorax. The influence of volume on radiation tolerance of lung is an effect that has not been adequately quantified. The goal of our studies was to determine the dose-volume relationship of lung injury in normal dogs. A three-dimensional treatment planning system was used to design mediastinal fields of increasing width to irradiate 33%, 67% or 100% of both lungs combined. Radiation was delivered in 1.5 Gy fractions over 6 weeks using x rays from a 6 MV clinical linear accelerator. This study was part of a larger study investigating volume and tolerance-dose relationships for early and late effects in normal canine lung. The early effects reported here were evaluated at 3 months after irradiation. The late effects were evaluated 24 months after irradiation and will be reported elsewhere. No dogs irradiated to 33% of their total lung volume developed severe symptomatic pneumonitis, and a clear volume effect was observed in the 67% and 100% lung volume groups. Serotonin uptake and changes in plain thoracic radiographs were other endpoints demonstrating a volume effect. Other pulmonary function endpoints were evaluated, but were either not sensitive enough to demonstrate a volume

effect, considering the great compensatory capacity of normal, nonirradiated lung, or they demonstrated a threshold effect, independent of lung volume irradiated. Radiation injury as assessed by histology was independent of volume irradiated. Volume relationships in lung depend on the endpoint being considered. Volume effects in the lung are consistent with increased morbidity due to the same effect in a larger volume of tissue. Volume effects in the lung are also critically dependent on the compensatory capacity of the nonirradiated lung. Underlying pathophysiology of irradiated tissue, as well as decreased compensatory capacity of nonirradiated tissue may have a strong effect on the dose-volume response. When small volumes of lung are irradiated (33% or less) the dose-limiting complications are more likely to be related to the structural tolerance of vessels or airways rather than loss of pulmonary function.

Jean Marie Poulson
Department of Radiological Health Sciences
Colorado State University
Fort Collins, Colorado 80523
Summer 2001

ACKNOWLEDGEMENTS

A project of the magnitude of this lung volume study could not have been considered, much less undertaken, without the inspiration, expertise, and hard work of a team made up of many, many dedicated individuals. What follows are the names of many, but certainly not all, of the people who were involved in carrying out this research. Grant CA 13899-20, awarded by the National Institutes of Health, supported this work.

Dr. Edward L. Gillette and "normal tissue studies" are synonymous in the field of radiobiology. Dr. Gillette was a pioneer in the field of comparative oncology and has remained on the leading edge of cancer research. It is a privilege to be a part of his outstanding program and to be counted in the number of radiobiologists who have trained under Dr. Gillette's guidance. The excellence that has been the hallmark of Dr. Gillette's distinguished and prolific research career is notably reflected in the work of his students who came before me. To follow in such footsteps is a daunting task, to say the least. But it is a challenge I feel lucky and privileged to be faced with. I thank Dr. Gillette for his support and guidance, and for affording me the opportunity of a lifetime in participating in these lung volume studies.

Dr. E. Christopher Orton has been a patient and skillful mentor to me for many years, and I sincerely appreciate everything he has taught me about surgery, cardiopulmonary physiology and cycling. Dr. Orton's input regarding the interpretation

of these lung volume data has been insightful and invaluable. I would like to thank Dr. Phillip Steyn for his help with the thoracic radiography studies described here, and the extensive nuclear medicine studies yet to be described elsewhere. Dr. Steyn was always available to discuss a set of films or help with a new aspect of the project. His enthusiasm, expertise, and friendly smile are all very much appreciated.

Dr. Barbara E. Powers provided excellent guidance and encouragement throughout every step of this project, as well as her unequalled expertise in doing the post mortem examinations and evaluating the histologic results presented in this manuscript. Dr. Powers is the busiest person I know, yet she somehow always found the time to help when I asked. Dr. Chuck Hibler provided very helpful guidance as well.

Dr. Sharon McChesney Gillette, blazed a trail before me and laid the groundwork for the studies described here. Her important work on radiation effects in normal canine heart and lung were the foundation for this lung volume study.

Dr. Susan LaRue has been not only a great mentor and teacher during these years, but a diehard coach and cheerleader as well. Her support has been enthusiastic and sincere, and it got me across the finish line.

Dr. Howard D. Thames helped design these experiments and has been a great friend and collaborator on this project. Cyndi Smith spent many hours carefully organizing data and crunching numbers on our behalf.

Dr. David A. Rickaby and Dr. Christopher A. Dawson helped to design the indicator dilution assays and provided the indicator dilution assay results from our blood

sample data. Dr. Rickaby was incredibly helpful and always willing and happy to explain a procedure or discuss the latest results.

My colleagues at Duke University Medical Center have been a great help in the completion of this manuscript. Dr. Lawrence B. Marks has taught me a great deal about clinical lung volume considerations in human patients. He is a dynamic and enthusiastic investigator and it has been my privilege to work with him on his lung volume studies as a natural extension of our work in dogs. Gunilla Bentel was a great teacher who always had an encouraging word, and she was a great friend. I miss her dearly. Dr. Marlene Hauck makes every day a great day. Dr. H. Cecil Charles has been a valuable source of encouragement, insight, and guidance. Dr. Zeljko Vujaskovic has been a great collaborator and colleague for many years. He has been a tremendous help, on this project and others. He and his wife Sanja give generously of their time and ideas, and I have been fortunate to have them as supporters and friends. Dr. Mark W. Dewhirst has been encouraging and supportive, and I appreciate the time he has afforded me to finish this project. Phil Antoine has been not only a great source of encouragement, but also a lifesaver during the process of changing from Windows to Macintosh computer platforms and back again.

Drs. Kelly Hepworth, Sue McKelvey, LuAnn Aki and Beth Mewshaw each took their turns, carefully processing the indicator dilution assay samples. They were cheerful and helpful and did a great job. They also did the follow-up physical exams on dogs after they were irradiated.

Billie Arceneaux did a CT study on each dog and shipped the tape to the University of North Carolina (UNC), where Kathy Deschesne and William Bird designed three-dimensional treatment plans and dose-volume histograms to irradiate a specific volume of lung in each dog. Dr. Ed Chaney helped design the experiments and supervised the three-dimensional treatment planning and dose-volume histogram generation at UNC.

Bob Scott and John Gerwig kept the linear accelerator running like clockwork. They built much of the other equipment we used as well. We couldn't have done this project without them. Eric Berns was a great help with the lung mechanics studies. Dr. Tom Borak lent his expertise in treatment planning and dose calculations.

Jennifer Johnston Devitt, Mark Jensen, Heidi Woog, and the many other "Beagle Nurses" did an outstanding job caring for and spoiling the beagles. This is a group without whom the studies would not have gone on. They were cheerful, enthusiastic and very hard working, and we were lucky to have such a great beagle team! The beagles themselves deserved nothing but the best of care, and that is just what this team gave them.

My graduate school mates, Dr. E. J. Ehrhart and Dr. Greg Harris were also great friends and supporters. Surviving radiation physics class together means a bond for life!

Thanks to Carol Horner and Lynda Reed for always having a smile and sunshine for everyone who comes into the oncology office.

Dr. Richard L. Johnson gave generously of his time as a 4-H leader, and it is due to his mentorship that I decided build my scientific education around veterinary medicine. Dr. Johnson was a great teacher and a great doc, and a great influence on my career. Dr. A. Simon Turner was another great influence on my career. His zest for life and his love of research was contagious, and clinched my decision to pursue an academic career.

Last, but far from least, I want to thank my family and friends (in addition to those listed above) who have given so much love and encouragement through these years of graduate school, and without whom I could not have completed this manuscript. They have been tireless in their support, and their love and friendship are the most precious gifts I will ever receive. Thanks to my parents, Dr. Richard and Alyce Poulson, my sisters, Sharon Graf and Mary Ellen Donahue, and my brother, David Poulson. The Kennedy Families have kept me going through thick and thin with their sharp Wyoming wit, and have made me feel like a part of their family for as long as I can remember. The Bakers and the Chesebros have always made me feel like part of their families as well. I am so lucky to have so many families! Dr. Cynthia and Jay Johnson, Dr. Amy and Craig Shenkenberg, and Dr. Cynthia Ballenger have been cheering for me the whole time. My deepest appreciation and gratitude goes to each and every one.

DEDICATION

This manuscript is dedicated with love to my parents, Dr. Richard E. Poulson and Alyce Jean Thompson Poulson. They instilled in me a love of learning, encouraged my interest in science and medicine, and set a wonderful example with their own scientific careers. Their love, support and encouragement has been unwavering, not only during the writing of this dissertation but always. I am truly fortunate to be the daughter of the two best parents and best scientists in the world. Thank you so very much, Mom and Dad!

TABLE OF CONTENTS

Page

LIST OF TABLES

LIST OF FIGURES

INTRODUCTION

The ideal outcome in the treatment of any cancer with any type of therapy would be the death of all cancerous cells without affecting the normal tissues. The challenge of cancer therapy continues to be to spare the normal tissues to the greatest degree possible while delivering a treatment regimen with a high probability for tumor control.

Radiation therapy has an increasing role in the treatment of lung cancer, breast cancer, Hodgkin's disease, and other malignancies involving the thorax. Lung cancer is the leading cause of cancer death for both men and women. The American Cancer Society estimates that in the United States during the year 2000 there were 164,100 new cases of lung cancer, 7,400 new cases of Hodgkin's disease, and 182,800 women were diagnosed with invasive breast cancer [1]. All of these patients who receive radiation therapy for their disease will have a portion of normal lung irradiated as well. The extreme sensitivity of lung to radiation-induced damage is a critical limiting factor in radiation therapy of these diseases. Irradiated volume is the most important factor in curative radiation therapy of lung cancer [21], and irradiated volume is the factor with primary influence on normal lung tolerance as well. However, the influence of volume on the radiation tolerance of lung is an effect that has not been adequately quantified, and the maximum allowable volumes have not been defined.

These studies were designed to determine volume and tolerance-dose relationships for lung by investigating these relationships in normal dogs. The first hypothesis was that the probability for developing a significant deficit in pulmonary function after a given dose of radiation to the lung would increase with volume irradiated. Physiologic endpoints include decreased compliance, decreased lung volume and decreased endothelial cell function. The second hypothesis was that there is a dose-volume relationship for the frequency and severity of radiographic changes in lung. Radiographic endpoints include presence, degree, and distribution of fissure lines, decreased vascular detail and increased opacity. The third hypothesis tested in this study was that there is a dose-volume relationship for the frequency and severity of histologic changes in lung. Histomorphometric endpoints include percentages of type II epithelial cells and alveolar macrophages, and areas of consolidated lung and interstitial fibrosis.

The assumption that dose-volume relationships exist in normal tissues is based largely on clinical observations [45]. Clinical dose-volume relationships have been compiled for the incidence of radiation pneumonitis [81]. Methods to predict overall pulmonary function loss based on dose-volume relationships and patient- and treatment-related factors have been investigated by several groups [14, 23, 32, 105, 164]. The ongoing development of elegant three-dimensional imaging and treatment planning systems has been accompanied by the development of numerous theoretical, mathematical models of dose-volume relationships in an effort to predict the influence of volume on normal tissue injury [70, 72, 79, 95, 124, 155, 178, 193, 196, 197]. These

models attempt to incorporate volume variations, dose-response models for normal tissues, and, in some cases, structure and function of the tissues irradiated. Biological data with which to test these models are sparse, and none has yet been validated. The goal of this study was to investigate volume and tolerance-dose relationships of early radiation injury to the lung in normal beagle dogs. The dog is a large enough model that we were able to use treatment fields similar to those used clinically for humans. We evaluated pulmonary function sequentially using relevant physiologic studies similar to those used clinically in humans. This study was part of a larger study also investigating late effects in irradiated normal canine lung. Our goal for this project was not to create a new model, but to develop a better understanding of dose-volume relationships in normal lung. Ideally, these data may now be used to test and further develop existing or new models of volume effects and normal tissue complication probability.

REVIEW OF THE LITERATURE

Clinical Significance

Lung tolerance is the primary limiting factor in radiation therapy of tumors involving the thorax and lung has long been recognized as one of the tissues most sensitive to radiation. Radiation therapy plays a significant role in the treatment of thoracic malignancies. The most common radiotherapy settings in which pulmonary damage constitutes a limiting factor are breast cancer, malignant lymphoma and lung cancer. Breast cancer irradiation involves the apical lung region included in the supraclavicular field and/or anterolateral part of the lung included within the tangential chest wall fields. Mantle field irradiation for Hodgkin's and non-Hodgkin's lymphomas includes the perihilar and retrocardiac lung zones. A variable volume of lung is irradiated during radiation therapy for lung cancer. Whole lung tolerance is a dose-limiting factor for half-body and total body irradiation. Reduction in pulmonary function has been reported following radiotherapy in all of these situations [2, 14, 22, 32, 63, 65, 69, 75, 94, 105, 106].

Early reports of radiation therapy of breast cancer patients described an irritative, unproductive cough that developed around the time of appearance of an erythematous skin reaction. Shortly afterward infiltrative changes were demonstrated radiographically,

coincident with dyspnea that seemed related to the spread of the infiltration [57]. The time to the development of these changes varied with the time of exposure and treatment number in each case. Hines [67] documented pathologic fibrosis in normal lung and pleurae on postmortem examination of two patients treated with thoracic irradiation.

It is generally accepted that the clinical sequelae of radiation lung injury usually start with the acute onset of radiation pneumonitis at 1 to 8 months after radiotherapy with symptoms that range from cough, chest pain, fever and dyspnea to death from respiratory failure. Depending on radiation dose, volume and pre-existing lung pathology, radiation pneumonitis may resolve without further changes or may progress to pulmonary fibrosis over the next 6 to 12 months. Radiation fibrosis is asymptomatic in most patients, but severe respiratory impairment and chronic respiratory failure may develop [58, 104, 117].

Among the many clinical situations in which pulmonary toxicity represents a major therapeutic limitation, clinical data on the relationship between local control and survival of non-small cell lung cancer (NSCLC) patients underscore the importance of studies involving radiation-induced lung damage. NSCLC is a common tumor with a poor prognosis. For inoperable patients radiation therapy is the treatment of choice. However, the median survival time for this group of patients is 7 to 10 months. The 2-year survival rates range from 10% to 25%, and the 5-year survival is only 3% to 10% [7, 53, 56, 78, 121, 154]. A relationship between local control and survival has been demonstrated in several studies [108, 128, 129, 131, 153]. Improvement in the control of

local disease is important for several reasons. First, locoregional disease is often the direct cause of death due to mechanical effects within the lung and mediastinum. Second, locally persistent or recurrent thoracic disease can serve as a focus for metastatic dissemination. Finally, with the development of more effective systemic therapies, and with them the ability to eradicate distant microscopic metastases, effective local control becomes even more important.

Numerous approaches are being investigated to improve local control, and thereby survival. Studies indicate that shortening the overall treatment time by hyperfractionated and accelerated radiotherapy may increase tumor control [76, 90, 151]. Chemotherapy given prior to [78, 152, 161], or concurrent with [18, 85, 154] radiotherapy results in a small but significant improvement in survival. However, chemotherapy often cannot be given in geriatric cases or in patients with hepatic, renal or cardiac disorders.

Clinical data suggest a strong relationship between total tumor dose and rate of local control. In an extensive review of the literature from studies in patients with inoperable NSCLC, Vijayakumar *et al.* [182] determined a dose-effect relationship for local control, with 50% local control at a dose of 53 Gy. They estimated that for 90% local control 80 Gy might be required. In the studies reviewed, local control was assessed only radiologically. Arriagada *et al.* [5] found a local control rate of only 10% at a dose of 65 Gy/26 fractions. In contrast to the previous study, local control was more strictly defined as radiologic, bronchoscopic, histologic, and clinical complete response.

The results of two RTOG trials [29, 128] indicate that total doses higher than the standard 60 Gy are associated with improved outcome [17]. However, increasing the radiation dose may also result in increased in normal tissue injury. New treatment techniques such as three-dimensional conformal radiotherapy may help spare as much normal tissue as possible. In a study of 37 patients with Stage III NSCLC receiving high-dose conformal radiotherapy, survival rates compared favorably with trials of chemoradiotherapy or conventional radiotherapy with a low treatment-associated morbidity. However, local progression remained a significant problem despite median radiotherapy doses of 66 Gy [156]. To be able to design the optimal treatment plan, it would be ideal to be able to estimate not only the tumor control probability associated with a certain treatment plan, but also the expected normal tissue injury.

Radiation-Induced Pulmonary Injury

Although clinically important, the mechanisms of radiation-induced lung damage are not well understood. Lung tissue is sensitive to radiation, yet as an organ, lung has considerable anatomical and functional reserve. Due to this functional reserve, symptomatic changes are uncommon among radiotherapy patients despite radiation damage to portions of the lung [169]. The clinical sequelae of radiation lung injury usually start with the acute onset of radiation pneumonitis 1 to 6 months after radiotherapy. Symptoms range from mild dyspnea and cough to death from respiratory failure. Depending on the radiation dose and the volume of lung irradiated, radiation

pneumonitis may resolve without further problems, or may progress to chronic pulmonary fibrosis over 6 to 12 months.

The histopathological changes in lung tissue after irradiation have been very well documented in animals [40, 49, 50, 51, 83, 84, 116, 120, 138, 147, 167, 168, 172, 186]. However, data for humans are less complete [34, 46, 60, 145, 146]. The response of the lung to radiation injury is characterized by an acute exudative phase, an organizing or proliferative phase, and a chronic fibrotic phase [74]. The exudative and proliferative phases correspond to the clinical and radiologic stage of radiation pneumonitis. The third phase corresponds to the radiation fibrosis stage [58]. Evidence suggests that injury to the type II pneumocytes and endothelial cells may be closely associated with the pneumonitic process, and an initial latent period reflects the inherent turnover time of the affected cells [25, 58, 127, 167, 172, 187, 190]. This process is characterized by exudation of proteinaceous material into the alveoli, desquamation of epithelial cells from the alveolar walls, alveolar edema and infiltration of inflammatory cells, leading to impairment of gas exchange, thickening of the alveolar septa, and reduced lung compliance. Decreased surfactant production by type II pneumocytes likely results directly from irradiation and leads to alterations in alveolar surface tension and low lung compliance. [127, 149, 150]. A lack of surfactant also leads to transudation of serum proteins into the alveoli [60]. Endothelial cell damage results in changes in perfusion and permeability of capillaries. The cells become pleomorphic, vacuolated, producing areas of denuded basement membrane and occlusion of the capillary lumen by debris and

thrombi [59]. These lesions are seen very early after irradiation and may extend even beyond the phase of pneumontis.

Characteristic of late lung injury is progressive fibrosis of alveolar septae that become thickened by bundles of elastic fibers and collagen [58, 146, 147, 168, 188]. The time course of collagen deposition varies according to the species and strain of animal, suggesting a genetic variability [43]. The alveoli later collapse and are obliterated by connective tissue. The mechanism of radiation-induced inflammatory response and pulmonary fibrosis is not completely understood. It may be related to the effects of radiation on vasculature combined with effects on epithelium and other stromal cells of the lung [145, 188]. Recently has been suggested that a perpetual cascade of proinflammatory and profibrotic cytokines produced immediately after irradiation prompts collagen genes to be activated, and persists until the fibrosis becomes apparent [148].

Pulmonary fibrosis is a repair process that follows the acute inflammatory response. While some cellular and biochemical changes that follow lung irradiation have been investigated, the biological mechanisms that underlie radiation-induced pneumonitis and the subsequent development of pulmonary fibrosis are still not well understood. Recent advances in molecular biology may make way for better understanding of the mechanisms of radiation injury to normal tissue and repair. Injury and repair of normal tissue induced by radiation, as well as other agents, is related to activation of cells that produce biological modifiers [38, 165]. Of the multiple growth factors involved in

normal tissue injury and repair, transforming growth factor β (TGF-β) is of particular interest [143]. TGF-β has been found to be elevated in wound healing [30], inflammation and tissue repair [122, 133, 144, 160]. This cytokine has been shown to be chemotactic for lymphocytes and fibroblasts [133], mitogenic for fibroblasts and a stimulator for the cellular production of collagen and fibronectin [3, 15, 19]. TGF-β has also been shown to increase the production of type I plasminogen activator inhibitor (PAI-1) while significantly decreasing the production of plasminogen activators u-PA and t-Pa in human lung fibroblasts [93]. Thus, TGF-β is a cytokine known not only to stimulate connective tissue formation, but also to limit its breakdown, leading to connective tissue maturation. Several studies have reported TGF-β as a radiation-induced cytokine responsible for the fibrotic reaction in many normal tissues [3, 6, 19, 110, 136, 148].

Dose-Volume Relationships

The radiation dose and volume irradiated appear to be the most important factors affecting lung tolerance. The specific aim of three-dimensional, conformal radiation therapy is to improve the target dose distribution while concomitantly reducing the normal tissue dose, primarily by reducing the normal tissue volume at risk.

The influence of treatment volume on tissue tolerance is not well understood. The assumption that dose-volume relationships exist in normal tissues is based largely on clinical experience, observations, and reports. Early on Coutard [28] noted that for a given dose and short time course a patient could be irradiated through a small field without "grave accidents", while a patient given the same dose and time course but

irradiated through a large field would suffer ill effects. Clinical dose-volume relationships for normal tissue have been compiled [45], but there are few experimental studies documenting such relationships. Emami *et al.* [45] presented a paper with estimations for TD_5 and TD_{50} for radiation pneumonitis, for homogeneous irradiation of partial lung volumes. The TD_5 and TD_{50} for whole lung irradiation were 17.5 Gy and 24.5 Gy, for irradiation of 2/3 of the lung 30 Gy and 40 Gy, and for 1/3 of the lung 40 Gy and 65 Gy, respectively.

The relationships between the volume effect and tissue type, dose fractionation pattern, level of response, field shape, radiation quality and tissue dimensionality (such as area for skin versus length for spinal cord) are all important questions that have yet to be answered definitively [194]. Several possible mechanisms of a volume effect have been speculated on. Decreased tolerance with increased treatment volume could result from increased morbidity due to the same effect in a larger volume of tissue, an increase in effect per unit of dose with increasing treatment area or volume, or an increased probability for the same effect with an increase in the amount of tissue at risk [193].

Numerous theoretical, mathematical models have been developed in an effort to predict the influence of volume on normal tissue injury [68, 70, 79, 95, 124, 125, 155, 177, 178, 193]. These models attempt to incorporate volume variations, dose response models for normal tissues, and, in some cases, structure and function, of the tissues irradiated. Biological data with which to test these models are sparse, and none has yet

been validated. Powers *et al.* [134] tested data from a study of irradiated canine spinal cord and found that it did not fit the probability model of Schultheiss, *et al.* [155].

The concept of integral dose has been investigated to relate complication probability to dose and volume. Mayneord [112] originally defined "integral dose" as the total energy absorbed from the beam by the patient. Early attempts to correlate integral dose with radiation injury without making distinctions between tissue types lacked good correlation with clinical experience [71, 112]. Dritschilo, *et al.* [44] and Wolbarst, *et al.* [195] proposed the complication probability factor, a variant of integral dose based on sparse clinical data available to them at the time.

The "power law" class of volume effect models relate the dependence of the "effective", "equivalent", or "tolerance" dose, to the size or shape of the treated region. In a power law formula, the biologically equivalent dose level for a treated radiation field is equal to the dose for a standard field multiplied by a correction factor based on the size and shape of the new volume. The independent variable in these relationships is length, area, or volume, or some combination of parameters. The dose correction factor is given by the independent variable raised to a negative, fractional power. Power law volume corrections require a homogeneous dose distribution, and most models do not specify different exponents for different types of tissues or organs irradiated so are of limited use for general application. The general volume effect, or probability model of Schultheiss, *et al.* [155] uses power law and integral dose relationships in an attempt to define the variation in response of normal tissues as a function of the volume of these tissues

irradiated and shows that earlier volume effect models are special cases of this general model. Tissue specific correction factors are derived to take into account the differential sensitivity of organs and tissues within the irradiated volume. The complication probability factor is used to address the problem of inhomogeneous dose distributions. This model attempts to predict an increased probability for the same effect with an increase in the amount of tissue at risk.

Models to predict normal tissue complication probabilities (NTCPs) can be divided into two categories: Phenomenological models and more biological models [11]. The most widely used phenomenological model uses a sigmoidal relationship between dose and NTCP, for homogeneous irradiation of a partial volume of an organ at risk [95]. This model describes the dependence of the dose-effect relationship on the irradiated volume. The description of this volume effect is a power-law relationship between tolerance dose and irradiated volume [95]. This type of model describes dose-effect relationships for homogeneous irradiation of a partial volume. To use this model to predict the NTCP for a given, the inhomogeneous dose distribution of that treatment plan must be converted to a homogeneous dose distribution with the same complication probability. The three-dimensional dose distribution is summarized in a dose volume histogram (DVH), showing the fraction of the target volume raised to a particular dose value (differential DVH) or the volume receiving the specified dose value or greater (integral DVH) [189].

Biological models are based on the concept of tissues being arranged into parallel or serial structural functional subunits (FSUs) [193]. It has been proposed that the number of FSUs, the tissue architecture (parallel or serial arrangement), variations in cellular content within FSU's, variations in cellular radiosensitivity, different levels of cell depletion per FSU and the relationship between the number of surviving FSUs and the probability of complication for a given end-point are all parameters governing the radiobiological response of a particular organ [193]. Dose-volume models incorporating these functional factors have been proposed to take into account differences in the radiation response of specific tissues [70, 72, 124]. The critical volume model [124] allows calculation of NTCPs for functional endpoints, and takes into account three intrinsic aspects of radiotherapy: Spatial heterogeneity of the dose distribution, variable sensitivity of the irradiated tissues (both intra-variability within a patient and inter-variability among patients) and fractionation of dose. Parallel FSU-models [70, 124, 197] use a dose-effect relationship for the destruction of an FSU and calculate the NTCP as a cumulative binomial probability of destroying a certain fraction of FSUs.

Clinical Studies of Volume Effects in Lung

Numerous clinical assays have been employed to evaluate radiation-induced lung damage, especially in the pneumonitis phase. Scoring of the patient's symptoms has obvious clinical relevance, but low sensitivity since even severe changes in a small volume of lung do not always give rise to clinical symptoms [89, 135].

Several groups have used the Lyman and Wolbarst [96, 97] and Kutcher *et al.* [80] models to investigate whether the estimated NTCP for pneumonitis was correlated with the observed incidence of pneumonitis. For patients treated for malignant lymphoma a reasonably good correlation was found [105, 109], but for lung cancer patients the correlation was usually weak [55, 105, 109]. Marks *et al.* [105] observed that when patients with poor pulmonary function prior to radiotherapy were excluded, the correlation improved considerably. The only group to find a good correlation in lung and esophageal cancer patients was Oetzel *et al.* [126]. All of these groups used different values for TD_{50} (the probability of 50% complication), ranging from 24.5 Gy to 29.5 Gy. For the purposes of dose-volume effects modeling it is not yet clear whether the lungs should be considered to be a paired organ or to be independent separate organs.

The FSU-model [70, 124, 197] was applied to the clinical data of 25 patients treated for malignant lymphoma, using a dose-effect relationship for local changes in perfusion [12, 13, 14, 105, 107]. An overall response parameter (ORP) was calculated [14], representing the average reduction of local perfusion over the whole lung (analogous to the fraction of nonfunctioning FSUs if the dose-effect relationship for perfusion represents the dose-effect relationship for the function of FSUs). A strong correlation was observed between the ORP and the incidence of radiation pneumonitis. However, the limited number of patients and the low incidence of pneumonitis did not allow a reliable comparison with the other NTCP models [33].

Graham *et al.* [56] found that a simple parameter, the lung volume that received >20 Gy, was related to the incidence of radiation pneumonitis. Similar findings were reported by Marks *et al.* [105] for the lung volume receiving ≥30 Gy. Another simple parameter, the mean lung dose, seems to be correlated with the incidence of pneumonitis as well [55, 109, 126]. The results of these studies have been elaborated recently by Kwa *et al.* [81], in cooperation with Marks *et al.*, Oetzel *et al.*, Graham *et al.* and Ten Haken *et al.* This large multi-center study of 540 patients demonstrated that a clear dose-effect relationship is present between the mean lung dose and the incidence of radiation pneumonitis [81].

Experimental Studies of Volume Effects in Lung

Extensive studies of radiation effects on lung have been done in small animal models using radiographic and histologic changes, breathing frequency, and respiratory death due to pneumonitis as the endpoints [48, 61, 130, 171].

Among the non-invasive assays available in mice and rats for assessing overall lung function after radiation, the measurement of breathing frequency and carbon monoxide uptake have proved to be the most informative [37, 137, 167, 176]. Radiation-induced changes in these parameters compare well with the histopathological appearance of alveolar damage [47, 167] and provide the opportunity to monitor the progress of lung injury at sub-lethal as well as lethal radiation dose levels. The breathing frequency assay has been extensively used to measure the radiation dose-modifying effects of

fractionation [170, 174, 179], low dose-rate irradiation [41] and chemotherapy [26, 27, 91, 92, 183].

Plain chest radiographs have been evaluated by several groups as a tool to assess both radiation-induced lung changes [9, 58, 98, 116, 118, 157] and response to radiotherapy [82]. The chest radiograph may reveal a diffuse infiltrate corresponding to the radiation field [58]. Radiographic changes are often present even in patients who do not develop symptomatic pneumonitis [132]. Herrmann, *et al.* [66] evaluated chest radiographs as an endpoint for volume effects in irradiated pig lung, but a clear cut volume effect was not observed.

Computed tomography (CT) represents another non-invasive approach to evaluating lung damage in animals as well as clinical human patients by exploiting changes in tissue electron density associated either with pneumonitis or fibrosis [42, 86, 99, 119, 123]. CT is especially valuable for resolving both regional lung density and volume changes following more localized irradiation of the thorax [184]. CT has the benefit of three-dimensional spatial resolution not available with plain chest radiographs. Comparisons of plain chest radiographs and computed tomography (CT) of the chest have shown CT to be more sensitive for detecting abnormalities in irradiated lung [8, 88, 100]. Still, plain chest radiographs remain a standard diagnostic test for the evaluation of pulmonary changes during and after radiation therapy of the thorax.

In addition to radiographic and CT density changes, regional hypoperfusion concurrent with radiation pneumonitis is consistently seen in other investigations in mice

[52], rats [185] and humans [16, 23, 62]. With the advent of the single photon emission computed tomography technique, a higher resolution and quantification of these regional functional changes has become possible [77]. With the use of both CT and SPECT, radiation-induced local changes were related to the locally delivered doses enabling construction of dose-effect curves for perfusion, ventilation and lung density within each individual patient [13]. While such an approach is difficult to apply in small laboratory animals, it can be used in large animals, such as dogs. Incorporation of functional endpoints, other than breathing frequency and death, in the evaluation of radiation lung injury has enormous potential for directly addressing a number of topical issues in clinical radiation lung injury including the roles of treatment volume, combined chemotherapy and cytokines.

Larger animals, such as dogs, are models in which pulmonary function tests similar to those given to human patients may be used as experimental endpoints to evaluate radiation injury in the lung. [49, 50, 51, 113, 114, 115, 116]. Early and late responses of irradiated canine lung were evaluated and described in these studies. Experimental methods for the measurement of pulmonary function in dogs, including lung mechanics, hemodynamics, and indicator dilution assays were developed and used to assess the changes in lung function in dogs after partial or whole lung irradiation. Alpha beta ratios were determined for lung based on histomorphometric measurement of alveolar air space ($\alpha/\beta = 3$ Gy), and radiographic evidence of alveolar consolidation

(α/β = 4 Gy), both measured at 6 months after irradiation [116]. Early observations about the volume effect in lung were made during the course of these experiments.

Experimental studies addressing the influence of volume on functional capacity of the lung are scarce. A few recent studies have focused on the effect the volume of lung irradiated has on pulmonary function [66, 87, 173]. Liao *et al.* [87] studied damage and morbidity from pneumonitis after irradiation of partial volumes of mouse lung. Fractional volumes of lung ranging from 94% to 17% of the lungs of mice were irradiated with single doses ranging from 12 to 22 Gy. The objectives of the study were to define dose-volume relationship, determine the threshold volume for morbidity after partial lung irradiation and to determine whether the response to radiation of mouse lung was independent of the region irradiated. Two assays of total lung function, breathing rate and mortality were used in this study. These experiments showed a threshold volume for morbidity from radiation pneumonitis in mouse lung. They also suggested that the threshold was dependent on the end point. The breathing rate assay was more sensitive than mortality. Although the functional tolerance of the lung was volume dependent, the histopathological changes observed were in the irradiated lung only and were independent of the volume of lung irradiated. This supports the hypothesis that lungs are parallel architecture tissue consisting of functional subunits and exhibiting a critical volume phenomenon. However, Liao *et al.* [87, 173] found the response of mouse lung to be heterogeneous, showing a greater sensitivity of the base than of the apex for both breathing rate and death. This is in contrast with the idea that all FSUs are

equally important and that the volume distribution of surviving FSU is irrelevant to tissue response [124]. Heterogeneous distribution of FSUs with optimal functional status was suggested as a possible cause of the non-uniform response of mouse lung.

Herrmann *et al.* [66] studied the effect of irradiated volume on radiation pneumonitis and lung fibrosis in pigs after fractionated irradiation. The whole right lung, or to the lower part of the right lung of pigs were irradiated in five fractions given over five days with total doses ranging from 14.3-38.0 Gy (whole lung) or 21.3-31.2 Gy (half lung). Early lung damage was assessed by weekly chest radiographs and by twice weekly determinations of breathing frequency at rest. Fibrosis was quantified at necropsy by histological evaluation and by determination of the hydroxyproline content of the lung tissue. The investigators did not find any significant differences for the incidence of lung damage after half lung and whole lung irradiation when injury was assessed by radiography, histology or hydroxyproline content. However, using increased breathing frequency as an experimental endpoint, significant differences in radiation-induced morbidity were observed. Their conclusion was that a volume effect can only be demonstrated for functional lung morbidity, whereas induction of structural lung damage is independent of the volume irradiated.

During the past several years there has been considerable evidence suggesting that alterations in the metabolic function of lung endothelial cells may provide a method for detecting various lung injuries *in vivo* [10, 24, 31, 35, 36, 39, 64, 102, 139, 140, 142, 159, 162, 181, 192]. The pulmonary vascular endothelium, a metabolically active tissue, is a

target site for many types of lung injury including radiation. Serotonin is a vasoactive amine that is normally removed from the circulation very efficiently by endothelial cells. Seventy to ninety percent of injected serotonin has been shown to be removed in one passage through the pulmonary circulation by pulmonary endothelial cells [192]. Removal of serotonin from the circulation represents one of the metabolic functions of endothelial cells that is decreased early in the course of lung injury.

Summary

Clinical data indicate that a dose-effect relationship exists between radiation dose and local control. Since local control seems to be associated with an increase in survival, dose-escalation may not only lead to an increase in local control but also to better survival. There are a number of complicated theoretical models which have been developed to estimate the risk of developing radiation induced lung damage. Currently available models that describe the effect of treatment volume and NTCP are yet to be sufficiently validated with clinical or experimental data. One study in mice has indicated a non-uniform response of the lung. Such a phenomenon needs to be investigated in more detail using a larger animal model. In a larger model, such as the dog, pulmonary function tests approximating those done in human patients could be used as experimental endpoints to evaluate pulmonary injury. Various non-invasive methods for monitoring the development of radiation-induced pulmonary injury have been described in both rodents and patients. The most notable are radiography, CT, SPECT, breathing frequency and carbon monoxide uptake. Application of such endpoints can provide

valuable and complementary information on locoregional and overall lung function and injury with respect to different treatment volumes. For the most part, to date, only physical parameters such as the radiation dose and irradiated volume have been taken into account. Possibly, the estimation of the functional outcome can be improved by incorporation of biological factors in the models, for example, pulmonary endothelial cell function prior to and during the course of radiation therapy, the distribution of the local lung function prior to radiotherapy and time course of the plasma level of TGF-β. Therefore, more clinical data as well as experimental data are needed to optimize the models.

MATERIALS AND METHODS

Location

This study was conducted at the Colorado State University (CSU) Veterinary Teaching Hospital (VTH), Fort Collins, Colorado, USA.

Animals and Maintenance

One hundred twenty-eight beagle dogs of both sexes were used. The dogs ranged in age from 8 to 37 months with a mean age of 16 months at the time of irradiation. Appendix A is the detailed dog census and schedule. Adult dogs were obtained from Ridglan Farms, Inc., Mount Horeb, WI, and Marshall Farms, North Rose, NY. All studies were conducted according to a protocol approved by the Colorado State University Institutional Animal Care and Use Committee. Dogs were identified by a five-digit number tattoo in the right ear (Ridglan Farms) or a seven-digit number tattoo in the left ear (Marshall Farms) and on entry into this study a unique prefix was assigned to each dog. Animals were housed indoors in large runs with expanded metal floors at the CSU Foothills campus. Water and dry commercial dog food were provided *ad libitum*. All dogs were given routine vaccinations for distemper, infectious hepatitis, parainfluenza, parvovirus, rabies, and *Bordetella bronchiseptica* (kennel cough). All male dogs were castrated when entered into the study.

Beginning one month prior to the start of irradiation dogs were housed indoors in expanded metal runs in the VTH. Animals were given water *ad libitum* and dry commercial dog food once daily. During the irradiation period the dogs were also fed canned dog food once a day. Dogs were kept in the hospital and observed closely for three weeks after irradiation, then moved back to indoor runs at the Foothills campus. Animals were returned to the veterinary hospital at 3 months and 24 months after the end of irradiation for evaluation of cardiopulmonary changes. Following the 24-month evaluation the dogs were humanely killed and necropsy was performed at the VTH. Only the results from the 3-month followup studies will be described here.

Experimental Design

One hundred twenty-eight adult beagle dogs were randomized into 26 groups. Three volume groups of 33%, 67% and 100% lung volume were divided into ten, eight and seven radiation dose groups, respectively. Total doses ranged from 27 to 72 Gy, given in 1.5 Gy fractions over six weeks. Five dogs were randomized into a nonirradiated control group. Total numbers of dogs randomized to each dose-volume group are shown in Table 1.

Dose Calculation

A whole thorax computed tomography (CT) study was carried out on each dog. A three-dimensional treatment planning system (PLUNC, University of North Carolina, USA) was used to design mediastinal fields of increasing width to irradiate 33%, 67% or 100% of both lungs combined (Figure 1). The surfaces of the lungs were defined by

Table 1. Experimental design

Total Dose (Gy)		Lung Volume Irradiated	
(1.5 Gy/fxn)	33%	67%	100%
0	—	—	5
27	—	—	5
31.5	4	4	6
36	6	6	6
40.5	6	6	8
45	6	5	5
49.5	5	6	2
54	7	5	1
58.5	5	4	—
63	5	1	—
67.5	4	—	—
72	5	—	—
Totals: (128)	**53**	**37**	**38**

Figure 1. Diagrams of ventrodorsal views of mediastinal fields designed to irradiate 33% (A.), 67% (B.) or 100% (C.) of both lungs combined. Fields of increasing width were designed using a three-dimensional treatment planning system. Doses were calculated at the midline and delivered through bilateral parallel opposed dorsoventral and ventrodorsal portals.

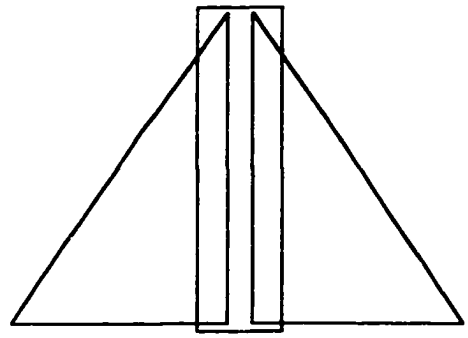

A. 33% lung volume field

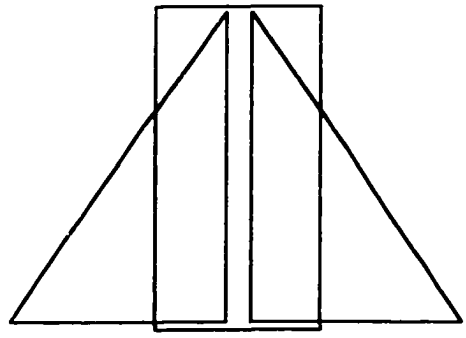

B. 67% lung volume field

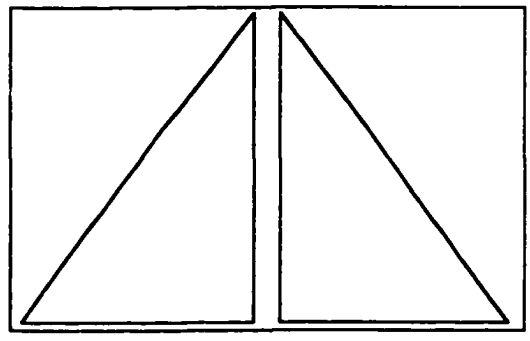

C. 100% lung volume field

contours so that they could be recognized for computer calculations of irradiated lung volume and calculation of dose-volume histograms. Doses were calculated so that the desired lung volume received a minimum of the prescribed dose (1.5 Gy/fraction). Dose-volume histograms were generated to represent the dose versus the fractional volume of lung receiving at least that dose. Doses were calculated at the midline and delivered through bilateral parallel opposed dorsoventral and ventrodorsal portals. Corrections for tissue inhomogeneities were included in the dose calculations. The dorsoventral doses were weighted slightly less to increase the dose sparing of the spinal cord. A source-axis distance of 100 cm was used. Field sizes ranged from 4 to 16 cm in width and 15 to 22 cm in length, depending on dog size and the volume of lung to be irradiated. Tissues in the radiation field included the specified volume of lung and heart, and portions of the esophagus, trachea, spinal cord, aorta, vena cava, thoracic duct, phrenic nerves, vagus nerves, thymus, diaphragm, stomach and liver.

Anesthesia

Irradiation, CT, lung mechanics and hemodynamics studies, indicator dilution assays and nuclear medicine procedures were carried out on dogs under general anesthesia. The dogs were given 0.044 mg/kg atropine sulfate subcutaneously prior to induction of anesthesia for all procedures except lung mechanics and hemodynamics studies. Anesthesia was induced using thiopental sodium given intravenously, titrated to effect (maximum dose of 18 mg/kg). The dogs were then intubated and anesthesia was

maintained using isoflurane gas (1.5% in 100% oxygen) for the irradiation procedures and halothane gas (1.5% in 100% oxygen) for all other procedures.

Irradiation

Radiation was delivered in 1.5 Gy fractions using x rays from a 6 MV clinical linear accelerator with a dose rate of 2.5 Gy per minute. Fractions were administered on weekdays and spaced evenly over 6 weeks. Dogs receiving total doses above 45 Gy were given two fractions per day not less than six hours apart spaced at regular intervals throughout the 6 week treatment time. Each dog was fitted with a rigid foam whole body cradle. Anesthetized dogs were stably positioned in dorsal recumbency in these cradles for the CT study and for each irradiation to ensure that the same positioning was maintained throughout treatment planning and irradiation. Portal films were made weekly to evaluate field placement and positioning Appendix B details the irradiation procedure.

Baseline and Follow-Up Evaluation Schedule

This study was part of a larger study investigating volume and tolerance-dose relationships for early and late effects in normal canine lung. The early effects on lung mechanics, hemodynamics and indicator dilution assays reported here were evaluated 3 months after irradiation. Appendix C is a detailed list of the endpoints measured.

The late effects in the surviving dogs were evaluated 24 months after irradiation, and will be reported elsewhere.

Physical Examinations

The dogs were carefully monitored by a veterinarian during and after irradiation. Dogs were observed daily for signs of respiratory distress or abnormal behavior. Heart rate and respiration were monitored weekly by auscultation throughout irradiation and for the three months following. Dogs developing severe symptomatic pneumonitis (respiratory rate > 150 breaths per minute, arterial pO_2 < 65 mm Hg, severe respiratory distress) were humanely killed. Supplemental oxygen was the only therapy administered for symptomatic pneumonitis.

Blood Gases

Arterial blood was drawn from the femoral artery while the dogs were non-sedated and breathing room air prior to and 3 months after irradiation. Paired blood gas samples were drawn simultaneously from the pulmonary artery and the femoral artery during the right heart catheterization procedure (below) while the dogs were breathing 100% oxygen. Samples were immediately processed on an ABL30 Radiometer Copenhagen acid-base analyzer. The blood PO_2 was determined for each sample. The blood pH, PCO_2, HCO_3 and percent saturation of hemoglobin by oxygen were also determined (data not shown).

Lung Mechanics

Functional residual capacity (FRC) was determined using a whole body plethysmograph. Anesthetized beagles were placed in an airtight chamber with their endotracheal tubes attached to a portal to the outside of the box. A pressure transducer

and strip chart recorder were used to measure and record pressure changes in the box. Mouth pressure and box pressure were measured before and during an occluded inspiratory effort. Boyle's law states that the product of pressure and volume is constant (at constant temperature). Applying Boyle's law, the following equations were used to calculate the FRC. P_1 and P_2 were the pressures in the box before and after the inspiratory effort, respectively, V_1 was the known preinspiratory box volume, and ΔV equals the change in volume of the box. The change in box volume equals lung volume and was obtained using the equation $P_1V_1 = P_2(V_1 - \Delta V)$. By applying Boyle's law to the gas in the lungs, the FRC was calculated: $P_3(FRC) = P_4[(FRC) + \Delta V]$, where P_3 and P_4 were the mouth pressures before and after the inspiratory effort [191]. A decrease in FRC of 25 percent or more was considered significant.

Tidal volume was measured using a volume-calibrated pneumotachometer. A small balloon was passed down the esophagus of the anesthetized dog and the intrapleural pressure was measured indirectly by a pressure transducer attached to the balloon. Changes in volume and pressure were recorded at the points of no flow.

Dynamic compliance (change in lung volume per unit pressure, C_D) was calculated as follows: $C_D = \Delta V$ liters / ΔP cm H_2O [111].

Appendix D details the protocol followed for the lung mechanics measurements.

Hemodynamics

Right heart catheterization was done on anesthetized dogs prior to treatment and three months after treatment. In these studies atropine sulfate was not given until after the cardiac pressure measurements had been completed to prevent alteration of physiologic parameters by this drug. The right heart was catheterized using a flow-directed 5F balloon-tip thermodilution catheter introduced via jugular venipuncture. The tip of the catheter was directed through the right heart and into the pulmonary artery. The location of the catheter tip during pressure measurements was assessed based on the size and shape of the pressure tracing. Right ventricular pressure, mean pulmonary artery pressure, and pulmonary artery wedge pressure were measured and recorded using a fluid filled pressure transducer and a Series 7010 Marquette Electronics, Inc. patient monitor. The thermodilution technique was used to measure cardiac output. Appendix D details the protocol followed for the hemodynamics measurements.

A 7F catheter was placed percutaneously in the femoral artery in the region of the femoral triangle. Systemic arterial blood pressures were measured and recorded via this catheter. Multiple arterial blood samples were drawn from this catheter for the indicator dilution assays (below).

Indicator Dilution Assay

Pulmonary endothelial cell damage and extravascular lung water were quantified prior to and 3 months after irradiation using a multiple indicator dilution technique [20] [101] [141, 166]. The anesthetized dogs were mechanically ventilated during this

procedure. Appendices D and E detail the indicator dilution assay procedure. Appendix F is the indicator dilution assay data form. A bolus of 370 kBq tritiated water (Amersham), 74 kBq [^{14}C]5-hydroxytryptamine (serotonin, 5-HT) (Amersham) and 5 mg indocyanine green dye (Cardiogreen, Sigma Chemical Co.) was injected into the right heart via a 5F balloon-tip thermodilution catheter in the right jugular vein. Multiple arterial blood samples were immediately drawn from the aorta via the femoral artery and collected into a fraction collector (Gilson, Inc., Middleton, WI). Forty-five samples were collected over the 30 s sampling time at a rate of 1.67 samples per second. Sampling vials were simultaneously filled with 3 ml ethanol and approximately 0.9 ml arterial blood to clear the samples for ^{3}H and ^{14}C measurement by liquid scintillation counting. The samples were stored at -15°C for at least 48 h prior to analysis. After the samples were centrifuged, the indocyanine green was measured spectrophotometrically and ^{14}C and ^{3}H were counted in a Beckman LS 6000 liquid scintillation counter. Outflow concentration curves (the concentration of each component over time) were calculated for each component [141].

Mean transit time was calculated for both the indocyanine green dye and tritiated water boluses as follows:

$$\text{mean transit time} = \int tC(t)\,dt \,/\, \int C(t)\,dt,$$

where C is the concentration of indocyanine green dye or tritiated water and t is the time at which C had decreased to 1% of its peak value. Pulmonary blood flow was calculated from the green dye dilution curve. Central blood volume was the product of the mean

transit time for green dye and pulmonary blood flow. Extravascular volume (Q_{ev}) accessible to the tritiated water was the product of the mean transit time for tritiated water and the perfusate flow rate.

The percentage of injected serotonin taken up by the lung during passage of the bolus ($\%U$) was calculated as follows:

$$\%U = (Q \int [C_R(t) - C_S(t)]\, dt) \times 100,$$

where Q is flow rate in ml/s and C_R and C_S are the concentrations of green dye and serotonin, respectively, divided by the amounts injected.

The permeability surface area (PS) for serotonin was calculated as follows:

$$PS = -Q \ln (1-U),$$

where U is the fraction of injected serotonin taken up by the lung during passage of the bolus. Using this parameter, serotonin uptake corrected for permeability surface area (serotonin PS) was calculated. A decrease in cardiac output will cause an increase in serotonin uptake. Calculation of serotonin PS is a method to evaluate this effect.

Cardiac output was calculated from the green dye dilution curve generated the indicator dilution assays (data not shown).

Thoracic Radiography

Ventrodorsal, and right and left lateral thoracic radiographs were made prior to treatment to screen for pre-existing lung conditions. Follow-up radiographs were taken 3 months after treatment. Pre treatment and 3 months post treatment radiographs were

compared and evaluated for changes in and out of the field. Radiographs were evaluated by a single observer (J. M. Poulson) and graded for presence of radiographic fissure lines, decreased vascular detail, degree and distribution of increased opacity in the treatment field, peribronchial changes and air bronchograms according to a four grade scoring system (0 = absent, 1 = mild, 2 = moderate, 3 = severe) devised for this study (Appendices G, H). Scores for the presence of radiographic fissure lines (0-3 points), decreased vascular detail (0-3 points), increased opacity (ventrodorsal view, 0-3 points) and increased opacity (lateral view, 0-3 points) were summed for a composite radiographic changes score. A total of 12 points was possible for the composite score. A score of 0 was graded as no change. The range of possible scores was divided evenly: Scores of 1 - 4 were considered mild radiographic changes, 5 - 8 were graded as moderate changes, and 9 - 12 were considered severe radiographic changes. Dogs with scores of 5 and above were considered responders for logit analysis to determine ED_{50} and ED_5 for moderate to severe radiographic changes.

Perfusion SPECT Lung Imaging

Perfusion single photon emission computed tomography (SPECT) studies were done prior to and 3 months after irradiation on four dogs from the 40.5 Gy, 33% volume group, three dogs from the 40.5 Gy, 67% volume group and three dogs from the 40.5 Gy, 100% volume group. Our funds did not allow for SPECT imaging of every dog in the study, so we chose a sample from each volume group at the 40.5 Gy dose level and imaged dogs from all three volume groups that had received the same dose. Perfusion

imaging was done using technetium-99m labeled macroaggregated albumin (^{99m}Tc-MAA) prepared from commercially available kits (Mallinckrodt Medical). Anesthetized dogs were positioned in ventral recumbency in a foam trough and administered 37 MBq of ^{99m}Tc-MAA via the lateral saphenous vein. Ninety (90) thirty-second images were acquired in a 360° radius around the dog.

Using the field dimensions for each dog and the portal films made during the treatment period a region of interest (ROI) representing the volume of lung irradiated was drawn on the reconstructed pre-treatment SPECT studies. Two more ROIs were drawn representing the volumes of nonirradiated right lung and nonirradiated left lung. Time activity curves (activity in counts versus image frame) were calculated and drawn for each ROI (Nuclear Mac). The total perfused lung volume equals the sum of the areas under the curve (AUC) activity in counts for all three ROIs. The volume of perfused lung irradiated was estimated to be the percentage of functional lung volume in the "irradiated" ROI.

Post Mortem Evaluation

Complete necropsies were performed on all dogs that were euthanatized prior to the planned 2-year follow-up term. The dogs were anesthetized, heparinized and administered an overdose of halothane anesthetic, immediately followed by perfusion with buffered zinc formalin (Z-Fix, Anatech Ltd.). Zinc formalin was used to provide good morphologic detail and preserve immunoreactivity. Tissues were perfused with buffered zinc formalin. The lungs were inflated with buffered zinc formalin. Eight lung

sections were made per dog. One section each was taken from the right and left cranial, middle and caudal lobes, and the accessory lobe (Appendix I).

Histomorphometric Analysis

Tissue samples were routinely and automatically processed by dehydration in increasing concentrations of alcohol and embedding in paraffin. Sections were cut at 5 μm, and stained with Masson's trichrome stain. Sections of lung, heart, pericardium, and liver were evaluated qualitatively.

For automated image analysis the BioQuant True Color Windows System was used. For each dog, the right cranial, right middle, right caudal, left cranial, left caudal and accessory lung lobes were evaluated. For each lung lobe three separate regions of interest within the irradiated portion of lung were drawn so that the total area per lung lobe was at least 500 mm^2. For each region of interest, using automated thresholding techniques, the following areas were automatically calculated: Total area, total area of air space density, total area of tissue density, total area of non-functional air space density (large bronchi or blood vessels), percentage of air space, percentage of non-functional air space density and percentage of tissue density. The values for the three regions of interest for each field in a given lung lobe were added to give a single value for each lung lobe.

Additional histomorphometric analysis was done using point count techniques. For each dog, the right cranial, right caudal, left cranial and left caudal lung lobes were evaluated. For each lung lobe at least 500 points were counted using a 36 point grid fitted

in the microscope eyepiece. At 400x magnification, the tissue type under each intersection of grid lines was categorized as air space, edema fluid, fibrin exudate, interstitial fibrosis, type II epithelial cell, alveolar macrophage, mononuclear inflammatory cell (lymphocyte or plasma cell), vessels larger than capillaries, or normal interstitium. The percentage of each tissue component was determined by dividing the specific tissue component by the total count.

Volume Enhancement Ratio

The volume enhancement ratio (VER) is defined as:

$$VER = \frac{Radiation\ dose\ for\ smaller\ volume}{Radiation\ dose\ for\ larger\ volume}$$

required to produce the same biological effect.

Statistical Analysis

Arithmetic means and standard error of the means were calculated on all data collected from lung mechanics, hemodynamics, and histomorphometry studies, and indicator dilution assays. The box plot method was used to test for outliers where appropriate. The paired two sample t-test was used to test differences between pre- and post-irradiation groups. The unpaired t-test assuming unequal variances was used to test differences between post-irradiation dose-volume groups and pooled pre-irradiation values from dogs in the respective volume groups (33%, 67%, 100%). The unpaired t-test assuming unequal variances was also used to test differences between post-irradiation dose-volume groups and pooled pre-irradiation values from all dogs, and post-irradiation

dose-volume groups and sham-irradiated controls. *P*-values less than 0.05 (two sided) were accepted as significantly different from the pre-irradiation value or the sham-irradiated control. Individual data points were plotted against dose. Where appropriate, a response threshold was determined and the fraction of animals with a response greater than this threshold were plotted against dose. Dose-response curves were fitted to determine the dose at which fifty percent (ED_{50}) and five percent (ED_5) probability for severe symptomatic pneumonitis, decreased serotonin uptake, and moderate to severe radiographic changes were expected. ED_{50} and ED_5 values and their 95% confidence intervals were calculated by logit analysis on the quantal data using the probit procedure of the SAS 6.12 software package (SAS Institute, Inc., Cary, NC, USA). Survival of severe symptomatic pneumonitis was calculated from the date of the end of irradiation to the date the dog was humanely killed and plotted as a step function using the Kaplan-Meier product limit method [73] feature of the JMP 3.2.2 software package (SAS Institute, Inc., Cary, NC, USA). Comparison of survival curves was done using the log-rank test [103].

RESULTS

Overall Survival

During the first six months after irradiation 23 dogs were humanely killed due to radiation-induced complications (Table 2). In the group of animals irradiated to 33% of their total lung volume there was no morbidity related directly to lung toxicity. In this group three dogs were humanely killed due to esophagitis and one dog after development of severe pericarditis. One developed chylothorax, and one developed severe liver complications related to the size and shape of the radiation field. (Table 2).

Six dogs in the 67% lung volume group were humanely killed after they developed severe radiation pneumonitis.

In the 100% lung volume group one dog developed severe pneumonia three weeks after the end of irradiation and was killed humanely. Another dog developed severe liver complications related to the size and shape of the radiation field four weeks after the end of irradiation (Table 2). Nine dogs in this group were euthanatized as a result of severe lung toxicity. Five of the dogs developed severe symptomatic pneumonitis, and four also had severe pulmonary hypertension.

Three Month Follow-Up Studies

Table 3 lists the follow-up studies completed on the 23 dogs humanely killed during the first six months after irradiation. One of twelve dogs humanely killed due to

Table 2. Morbidity and reason for sacrifice during the first six months after irradiation

Total Dose (Gy)	Lung Volume Irradiated					
	33%		67%		100%	
	Number	Cause	Number	Cause	Number	Cause
0	—		—		0/5	
27	—		—		1/5	pneumonia
31.5	0/4		0/4		0/6	
36	0/6		0/6		0/6	
40.5	0/6		0/6		3/8	pneumonitis (1), pulm. hyperten. (2)
45	1/6	chylothorax	0/5		4/5	pneumonitis (3), pulm. hyperten. (1)
49.5	0/5		1/6	pneumonitis	2/2	pneumonitis, liver complications
54	1/7	liver complications	1/5	pneumonitis	1/1	pneumonitis
58.5	0/5		3/4	pneumonitis		
63	1/5	esophagitis	1/1	pneumonitis	—	
67.5	0/4		—		—	
72	3/5	esophagitis (2), heart complications (1)	—		—	

Table 3. Three month follow-up studies completed on dogs humanely killed during the first six months after irradiation.

Total Dose (Gy)	Lung Volume Irradiated								
	33%			67%			100%		
	Cause	3m Lung Assays*	3m Thoracic Radiographs	Cause	3m Lung Assays*	3m Thoracic Radiographs	Cause	3m Lung Assays*	3m Thoracic Radiographs
0									
27							pneumonia	NO	NO
31.5									
36									
40.5							pneumonitis	NO	7 wks
							pulm. hyperten. (2)	YES NO	YES 11 wks
45	chylothorax	NO	NO				pneumonitis (3)	NO NO NO	9 wks 9 wks NO
							pulm. hyperten.	YES	YES
49.5				pneumonitis	YES	YES	pneumonitis	9 wks	9 wks
							liver complications	NO	NO
54	liver complications	NO	9 wks	pneumonitis	YES	YES	pneumonitis	NO	9 wks
58.5				pneumonitis (3)	YES (3)	YES (3)			
63	esophagitis	NO	NO	pneumonitis	NO	11 wks			
67.5									
72	esophagitis (2)	NO NO	NO NO						
	heart complications	YES	YES						

* Lung Assays = Lung mechanics, hemodynamics and indicator dilution assay studies.

the development of severe symptomatic pneumonitis was evaluated for changes in lung mechanics, hemodynamics and indicator dilution assay endpoints 9 weeks after the end of irradiation (total dose 49.5 Gy, lung volume 100%). These data were included with the 3-month results. Five of these dogs were humanely killed after their 3-months post-irradiation evaluations had been completed (all in the 67% lung volume group). The other six dogs were not evaluated for changes lung mechanics, hemodynamics, or indicator dilution assays before they were humanely killed due to the development of severe symptomatic pneumonitis prior to 3 months post-irradiation (one in the 67% lung volume group, 5 in the 100% lung volume group).

Eight of eleven dogs humanely killed due to other causes were euthanatized prior to 3 months post-irradiation and were not evaluated for changes in lung mechanics, hemodynamics, or indicator dilution assays post-irradiation. Two dogs were evaluated prior to being humanely killed due to the development of severe symptomatic pulmonary hypertension and one after the development of heart complications, all at 3 months post-irradiation (Table 3).

Thoracic radiographs were taken of eight dogs that developed severe complications and were humanely killed prior to 3 months post-irradiation. Six of these dogs developed severe symptomatic pneumonitis and were radiographed 7 to 11 weeks post-irradiation. One dog developed severe liver complications and was radiographed 9 weeks post-irradiation. One dog developed severe pulmonary hypertension and was

radiographed 11 weeks post-irradiation. These radiographs were included in the analysis of the 3 month studies of the surviving dogs (Table 3).

Severe Symptomatic Pneumonitis

In the 67% volume group six (of 37) dogs were humanely killed as a consequence of severe symptomatic pneumonitis (Table 4). Logistic fit of the data showed a dose response curve with a 50% probability of developing severe symptomatic pneumonitis (ED_{50}) after 56.0 Gy in 1.5 Gy fractions (52.2-66.0 Gy, 95% confidence interval (CI)) (Figure 2). No dogs in this group developed lung toxicity at doses less than 49.5 Gy. The more clinically relevant ED_5 for the first 6 months after irradiation of 67% of the lung was 48.1 Gy (18.5-52.0 Gy, 95% CI). The latency for the development of severe pneumonitis in the 67% volume group ranged from 11 to 17 weeks with a mean latency of 14 weeks. There was a trend toward shorter latency with higher doses (Table 4). Six (of 33) dogs receiving whole lung irradiation with doses of $\geq$ 40.5 Gy developed severe pneumonitis and were humanely killed 7 to 9 weeks after the end of irradiation (Table 4). The Kaplan-Meier log rank survival curve showed a significant difference ($p = 0.0003$) in survival probability related to the volume of lung irradiated in the dose range from 40.5 to 63 Gy (Figure 3). Dogs irradiated to 33% of their lung volume with doses in the range of 40.5 Gy to 63 Gy showed a 100% survival probability, whereas dogs irradiated to 67% and 100% of their lung volume had a survival probability of 78% and 60% respectively. Three dogs in the 100% lung volume group, given total doses of 40.5 to 45 Gy, developed severe pulmonary hypertension secondary to increased pulmonary resistance

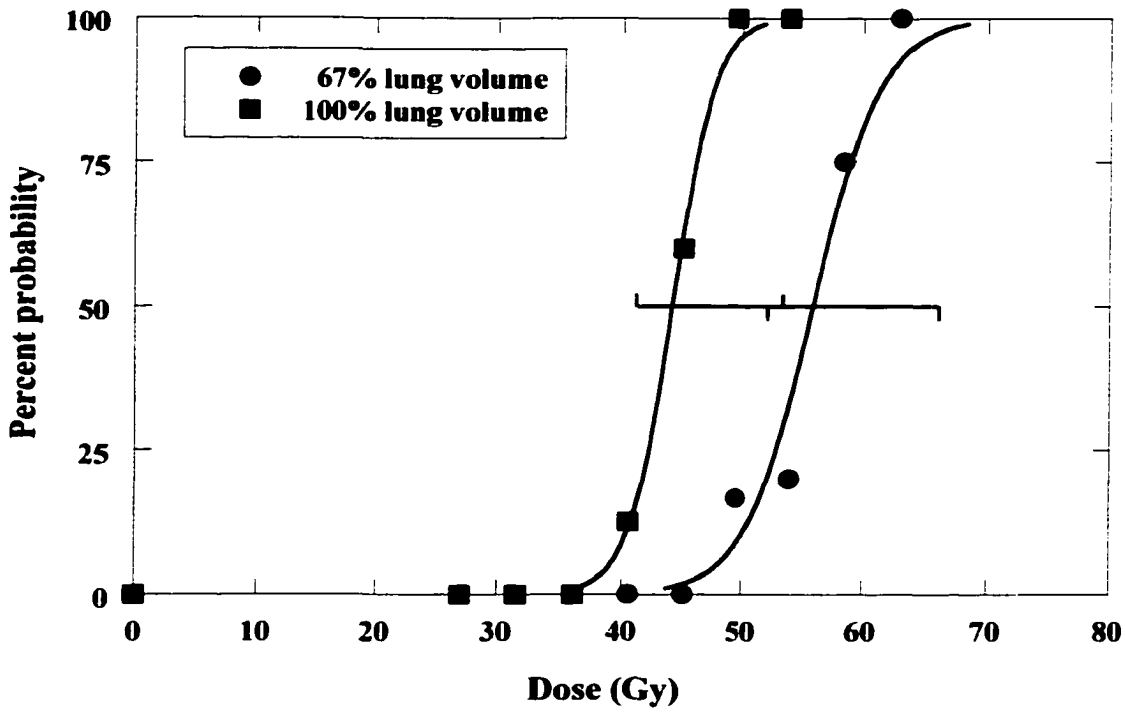

Figure 2. Dose-response curves for development of severe symptomatic pneumonitis based on logistic fit showed significant differences in the ED_{50} and ED_5 for 67% and 100% irradiated lung volumes. The ED_{50} and ED_5 for the 67% irradiated lung volume group were 56.0 Gy (52.2-66.0 Gy, 95% CI) and 48.1 Gy (18.5-52.0 Gy, 95% CI) respectively (● data points). The ED_{50} and ED_5 for the 100% irradiated lung volume group were 44.1 Gy (41.2-53.5 Gy, 95% CI) and 39.1 Gy (8.8-41.8 Gy, 95% CI) respectively (■ data points). Error bars represent 95% confidence intervals.

Table 4. Morbidity related to pneumonitis during the first six months after irradiation

Total Dose (Gy)	Lung Volume Irradiated					
	33%		67%		100%	
	Number	Latency (wks)	Number	Latency (wks)	Number	Latency (wks)
0	—		—		0/5	
27	—		—		0/5	
31.5	0/4		0/4		0/6	
36	0/6		0/6		0/6	
40.5	0/6		0/6		1/8	7
45	0/6		0/5		3/5	8, 9, 9
49.5	0/5		1/6	15	1/2	9
54	0/7		1/5	14	1/1	9
58.5	0/5		3/4	12, 15, 17	—	
63	0/5		1/1	11	—	
67.5	0/4		—		—	
72	0/5		—		—	

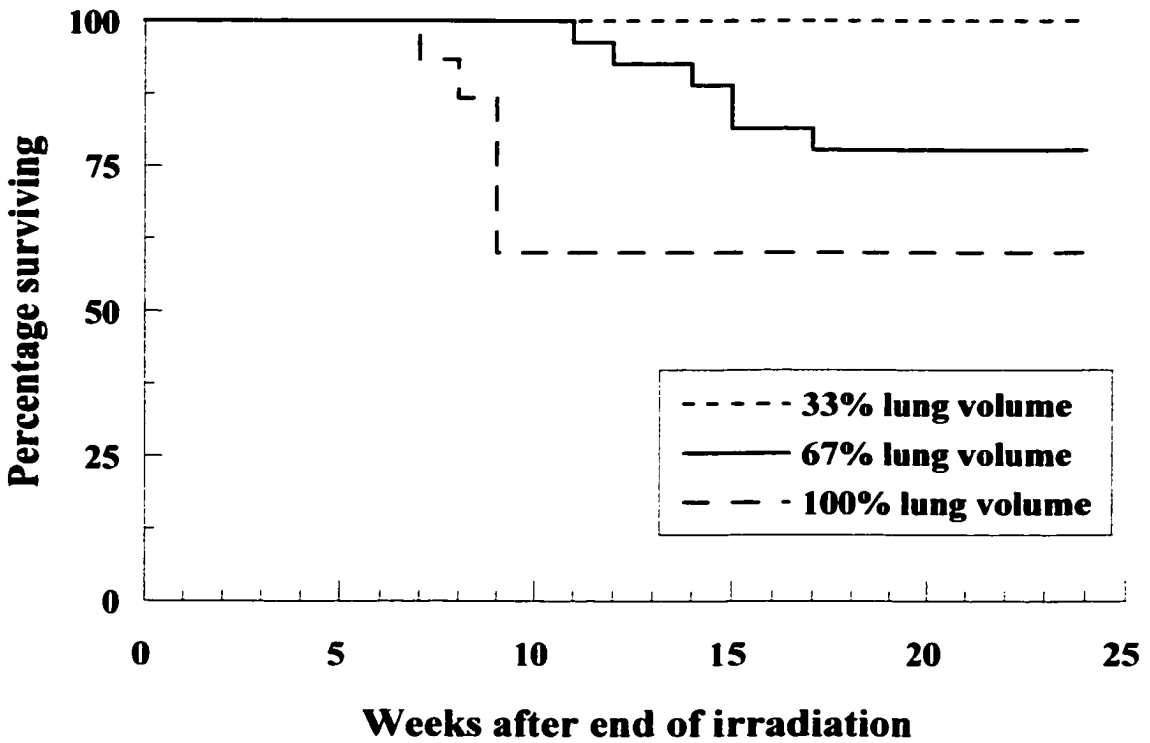

Figure 3. Kaplan-Meier log rank curve for pneumonitis survival of dogs irradiated in the dose range of 40.5 to 63 Gy. Dogs in the 67% irradiated lung volume group had a higher survival rate (78%) and survived longer ($p = 0.0003$) than dogs in the 100% irradiated lung volume group (60% survival rate). No dogs in the 33% irradiated lung volume group developed signs of pulmonary toxicity.

due to radiation-induced lung damage and were humanely killed 9 to 25 weeks after the end of irradiation (Table 2). The probability of developing severe pneumonitis after whole lung irradiation was significantly higher than in the 67% lung volume group. Calculated ED_{50} and ED_5 values were 44.1 Gy (41.2-53.5 Gy, 95% CI) and 39.1 Gy (8.8-41.8 Gy, 95% CI) respectively.

The volume enhancement ratios (VER) comparing 67% and 100% lung volumes irradiated at the ED_{50} and ED_5 levels of effect for severe symptomatic pneumonitis were 1.27 and 1.23, respectively.

Arterial Blood Gases

There was a trend toward decreased arterial oxygen tension (PaO_2) (mm Hg) values at the higher doses in all three lung volume groups while the dogs were awake and breathing room air 3 months after irradiation (Table 5, Figure 4). The average $PaCO_2$ was while awake and breathing room air was 34.5 (2.8) mm Hg, (range 25.7 - 40.7 mm Hg) prior to treatment. The average $PaCO_2$ was 35.0 (3.7) mm Hg, (range 23.8 - 49.3 mm Hg) three months after treatment. There was a trend toward decreased PaO_2 in the higher dose groups while the dogs were under general anesthesia and breathing 100% oxygen, with significant decreases only at the highest doses in all three lung volume groups (Table 6, Figure 5). The average $PaCO_2$ while anesthetized and breathing 100% oxygen was 49.0 (2.8) mm Hg, (range 27.2 - 72.8 mm Hg) prior to treatment. The average $PaCO_2$ was 49.4 (7.0) mm Hg, (range 34.1 - 70.3 mm Hg) three months after treatment.

Table 5. Arterial oxygen tension (PaO_2, mm Hg) while awake and breathing room air, three months after irradiation[§]

	Lung Volume Irradiated											
	33%				67%				100%			
Dose (Gy)	n	PaO_2 (mm Hg)	n	% Change	n	PaO_2 (mm Hg)	n	% Change	n	PaO_2 (mmHg)	n	% Change
Pre Tx	52	79.7 (0.9)			37	81.4 (1.0)			36	80.9 (1.0)		
Sham	—	—	—	—	—	—	—	—	5	80.2 (1.7)	4	-0.5 (2.3)
27.0	—	—	—	—	—	—	—	—	4	78.8 (5.0)	4	3.0 (4.6)
31.5	4	83.5 (0.4)	3	9.5 (7.7)	4	75.7 (3.9)	4	-0.9 (5.2)	6	**73.8 (2.1)***	6	-9.0 (2.8)
36.0	6	77.5 (2.7)	6	-1.3 (4.8)	6	79.5 (1.3)	6	-3.4 (2.3)	5	78.1 (1.1)	5	-0.7 (4.5)
40.5	6	75.9 (1.8)	6	-1.3 (3.1)	6	79.6 (2.3)	6	-5.1 (3.2)	6	75.8 (2.2)	6	-5.6 (2.4)
45.0	5	85.1 (2.5)	5	3.2 (4.1)	5	**73.5 (1.5)***	5	-8.0 (1.2)	2	**68.7 (3.4)***	2	-18.2 (3.1)
49.5	4	84.1 (3.1)	5	2.0 (6.5)	6	78.4 (2.5)	6	-2.4 (2.3)	1	67.3	0	—
54.0	7	74.4 (2.5)	7	-8.3 (2.0)	5	**72.7 (2.1)***	5	-10.4 (4.9)	0	No survivors	0	—
58.5	5	81.8 (1.4)	5	3.1 (4.3)	3	75.5 (6.6)	3	-6.8 (5.1)	—	—	—	—
63.0	4	78.9 (4.7)	4	7.7 (5.6)	1	74.5	0	—	—	—	—	—
67.5	4	76.9 (5.8)	4	-4.6 (2.5)	—	—	—	—	—	—	—	—
72.0	3	**72.5 (1.8)***	3	-7.6 (2.2)	—	—	—	—	—	—	—	—

[§] Mean (standard error of the mean). * Significantly different from pre-treatment values and sham-irradiated controls ($p \leq 0.05$).

Figure 4. Arterial oxygen tension while awake and breathing room air (PaO_2) (mmHg) three months after irradiation as a function of dose. There was a trend toward decreased PaO_2 values at the higher doses in all three lung volume groups. (◊) data points represent pre-treatment values. (◆) data points represent sham-irradiated controls. Error bars represent standard error of the mean. Points without error bars represent single animals. * Points significantly different from pre-treatment values and sham-irradiated controls ($p \leq 0.05$).

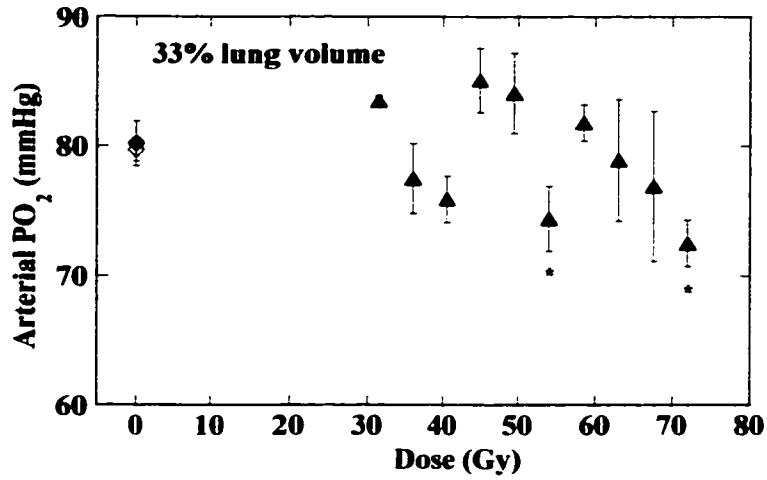

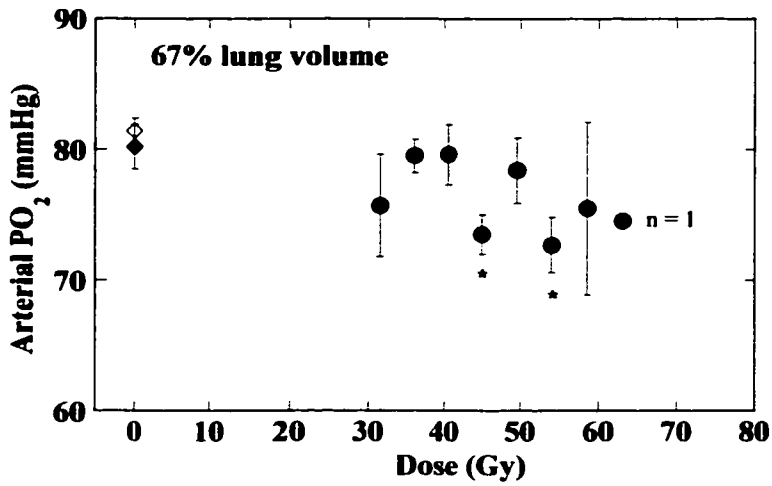

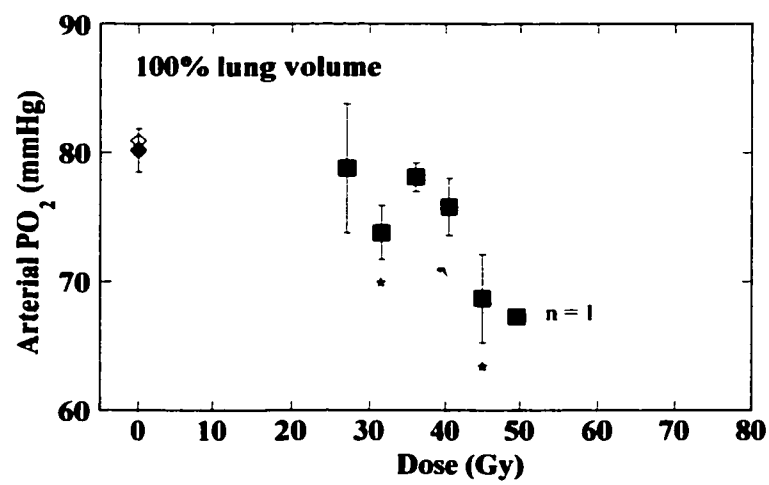

Table 6. Arterial oxygen tension (PaO_2, mm Hg) while anesthetized and breathing 100% oxygen, three months after irradiation

	Lung Volume Irradiated											
	33%				67%				100%			
Dose (Gy)	n	PaO_2 (mm Hg)	n	% Change	n	PaO_2 (mm Hg)	n	% Change	n	PaO_2 (mmHg)	n	% Change
Pre Tx	47	457.0 (5.1)			34	469.5 (4.8)			36	465.3 (5.1)		
Sham	—	—	—	—	—	—	—	—	5	476.8 (11.3)	5	0.5 (5.4)
27.0	—	—	—	—	—	—	—	—	3	472.5 (14.0)	3	4.1 (6.4)
31.5	4	464.9 (8.2)	3	9.4 (10.3)	4	464.3 (12.6)	4	3.1 (5.4)	6	474.1 (9.9)	6	0.3 (3.0)
36.0	6	477.4 (18.0)	6	5.6 (2.8)	5	479.9 (12.7)	5	-1.6 (2.6)	6	469.4 (8.3)	5	2.0 (2.2)
40.5	6	482.8 (9.0)	5	7.0 (5.1)	6	467.2 (15.9)	6	-1.7 (3.7)	5	483.9 (4.9)	5	7.6 (5.1)
45.0	5	450.3 (7.0)	5	-4.0 (2.4)	5	448.7 (12.5)	3	6.2 (7.3)	4	**441.5 (3.4)***	2	-5.5 (3.1)
49.5	5	460.0 (14.8)	3	8.4 (6.7)	6	456.7 (11.8)	5	-6.4 (3.3)	1	417.7	1	11.7
54.0	6	445.2 (10.9)	6	-4.6 (2.7)	5	470.4 (9.8)	5	0.8 (4.3)	0	No survivors	0	—
58.5	5	453.4 (14.0)	5	-2.3 (5.8)	4	**438.2 (11.5)***	4	-6.8 (4.1)	—	—	—	—
63.0	4	453.1 (18.7)	3	-1.1 (4.8)	—	—	—	—	—	—	—	—
67.5	3	452.2 (15.4)	3	-6.9 (2.9)	—	—	—	—	—	—	—	—
72.0	3	**428.2 (14.7)***	3	-6.5 (6.0)	—	—	—	—	—	—	—	—

[§] Mean (standard error of the mean). * Significantly different from sham-irradiated controls ($p \leq 0.05$).

Figure 5. Arterial oxygen tension while anesthetized, breathing 100% oxygen (PaO_2) (mmHg) three months after irradiation as a function of dose. There was a trend toward decreased PaO_2 values at the higher doses in all three lung volume groups. (◊) data points represent pre-treatment values. (◆) data points represent sham-irradiated controls. Error bars represent standard error of the mean. Points without error bars represent single animals. * Points significantly different from sham-irradiated controls ($p \leq 0.05$).

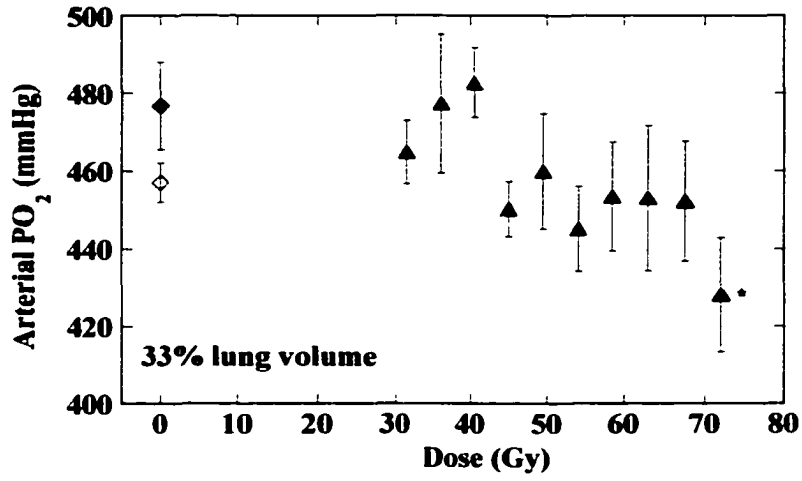

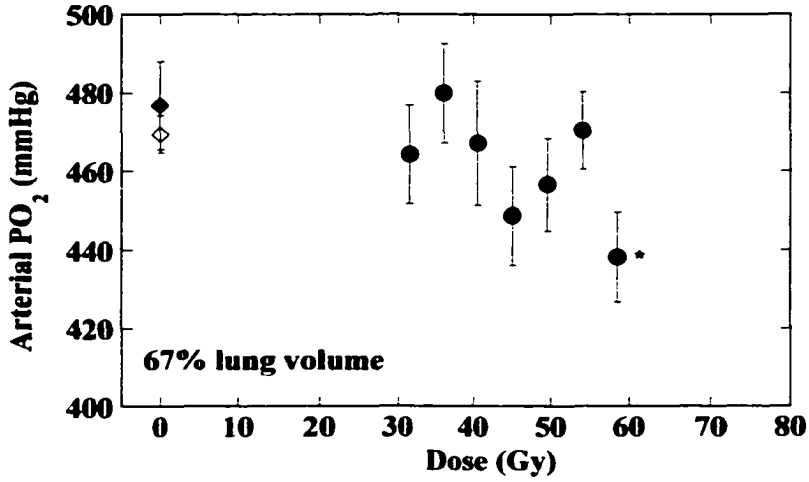

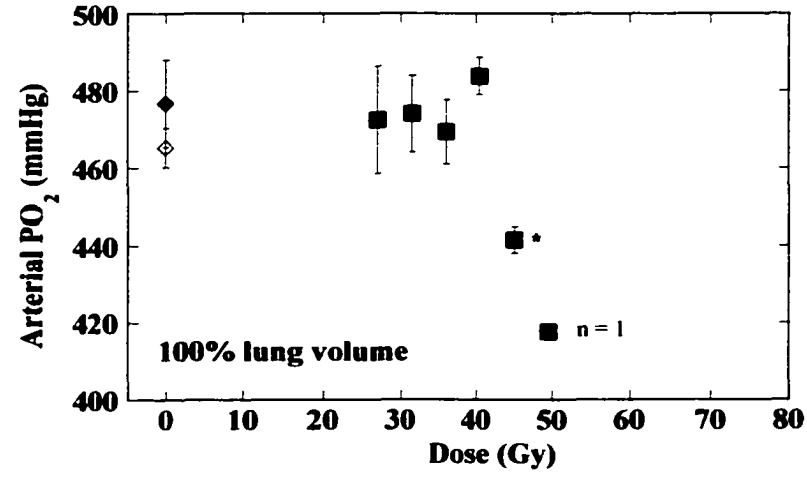

Lung Mechanics

Functional Residual Capacity

There was no significant difference in functional residual capacity three months after irradiation in comparison with pre-treatment values and sham-irradiated controls. (Table 7, Figure 6).

Tidal Volume

Tidal volume was significantly decreased from pre-treatment values at the higher doses in the 67% irradiated lung volume group three months after irradiation (Table 8, Figure 7). There was a statistically significant decrease in tidal volume compared to pre-treatment values throughout the range of doses in the 100% irradiated lung volume group.

Dynamic Compliance

Dynamic compliance (l/cm H_2O) was significantly decreased from pre-treatment values after doses of 49.5 Gy or more in the 67% irradiated lung volume group, and after doses of 40.5 Gy or more in the 100% irradiated lung volume group three months after irradiation (Table 9, Figure 8).

Hemodynamics

Right Ventricular Systolic Pressure

There was no significant difference in right ventricular (RV) systolic pressure in the 33% and 67% irradiated lung volume groups compared with pre-treatment values and sham-irradiated controls (Table 10, Figure 9). RV systolic pressure was markedly

Table 7. Functional residual capacity (FRC) (ml) three months after irradiation[§]

Dose (Gy)	Lung Volume Irradiated											
	33%				67%				100%			
	n	FRC (ml)	n	% Change	n	FRC (ml)	n	% Change	n	FRC (ml)	n	% Change
Pre Tx	46	373 (13)			33	391 (16)			38	389 (12)		
Sham	—	—	—	—	—	—	—	—	5	330 (62)	4	-5 (16)
27.0	—	—	—	—	—	—	—	—	4	361 (16)	4	-3 (5)
31.5	4	391 (47)	2	-13 (14)	4	455 (20)	4	15 (11)	4	335 (45)	4	-11 (11)
36.0	5	376 (30)	5	14 (22)	4	449 (22)	4	14 (4)	5	409 (47)	3	-1 (11)
40.5	6	395 (40)	4	2 (16)	6	433 (28)	6	30 (24)	6	380 (32)	6	-13 (8)
45.0	5	424 (12)	4	3 (11)	5	398 (20)	4	1 (7)	2	386 (64)	2	29 (1)
49.5	5	418 (41)	4	5 (5)	6	422 (44)	4	-13 (11)	0	—	0	—
54.0	6	415 (35)	6	50 (25)	4	364 (36)	4	-5 (3)	0	No survivors	0	—
58.5	4	458 (58)	4	47 (30)	3	435 (35)	3	40 (45)	—	—	—	—
63.0	4	304 (72)	4	-16 (17)	0	No survivors	0	—	—	—	—	—
67.5	3	364 (57)	3	-4 (24)	—	—	—	—	—	—	—	—
72.0	2	482 (65)	2	38 (16)	—	—	—	—	—	—	—	—

[§] Mean (standard error of the mean). No values significantly different from pre-treatment values or sham-irradiated controls ($p \leq 0.05$).

Figure 6. Functional residual capacity (ml) three months after irradiation as a function of dose. There was no significant difference in functional residual capacity three months after irradiation compared with pre-treatment values (◊) and sham-irradiated controls (♦). Error bars represent standard error of the mean. Points without error bars represent single animals.

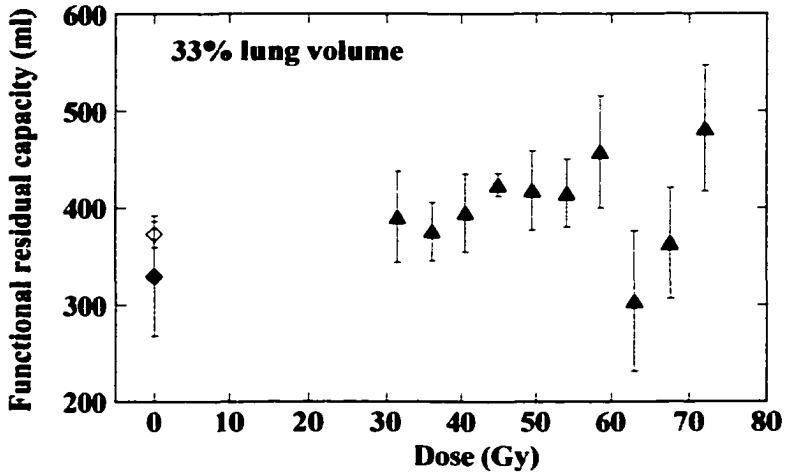

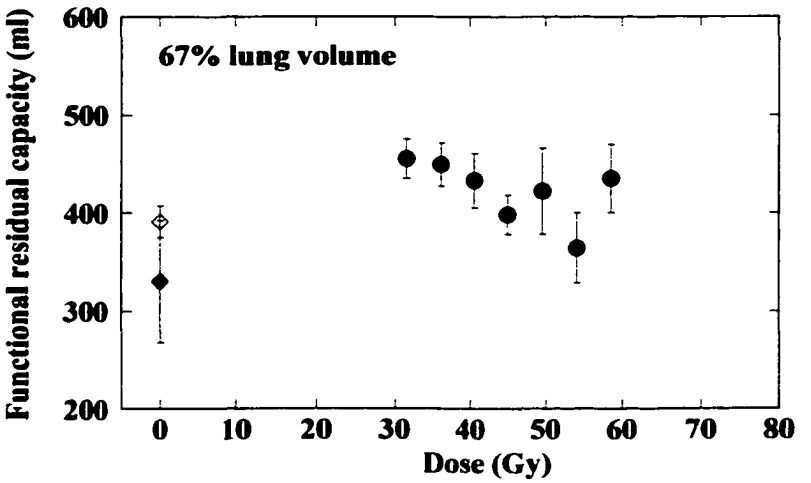

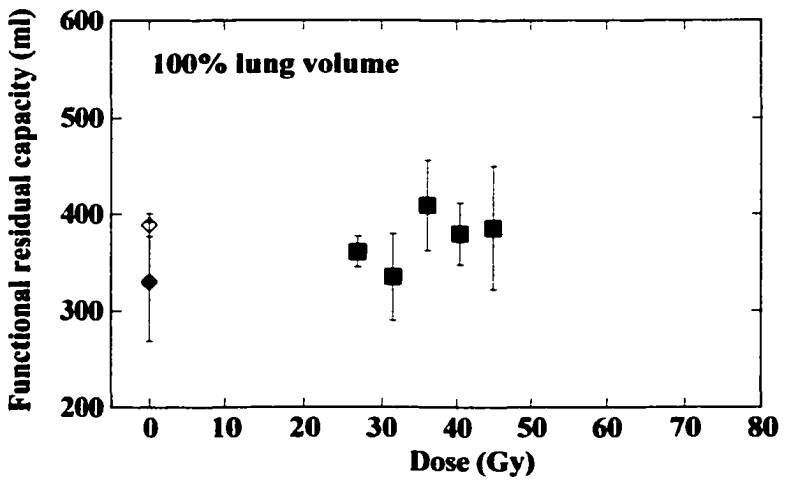

Table 8. Tidal volume (ml) and percent change three months after irradiation[§]

	Lung Volume Irradiated											
	33%				67%				100%			
Dose (Gy)	**n**	**Tidal volume (ml)**	**n**	**% Change**	**n**	**Tidal Volume (ml)**	**n**	**% Change**	**n**	**Tidal Volume (ml)**	**n**	**% Change**
Pre Tx	51	142 (8)			37	169 (10)			38	160 (13)		
Sham	—	—	—	—	—	—	—	—	4	127 (20)	4	-11 (9)
27.0	—	—	—	—	—	—	—	—	4	**109 (8)***	4	23 (10)
31.5	4	162 (23)	4	-2 (11)	4	186 (38)	4	-1 (5)	5	124 (14)	5	17 (12)
36.0	6	137 (14)	6	9 (14)	6	139 (14)	6	14 (5)	6	**121 (12)***	6	-5 (18)
40.5	6	124 (12)	6	21 (16)	6	140 (20)	6	-15 (8)	8	**110 (7)$^{+}$**	8	-24 (10)
45.0	5	157 (33)	5	13 (13)	5	144 (11)	5	-8 (6)	2	**89 (5)$^{+}$**	2	-34 (22)
49.5	5	163 (15)	5	-1 (15)	6	173 (18)	6	9 (24)	1	91	1	42
54.0	6	124 (16)	6	-1 (9)	5	**115 (20)***	5	-34 (2)	0	No survivors	0	—
58.5	5	180 (36)	4	-16 (7)	4	**107 (18)***	4	-34 (6)	—	—	—	—
63.0	4	169 (46)	3	10 (5)	0	No survivors	0	—	—	—	—	—
67.5	4	113 (31)	4	-21 (17)	—	—	—	—	—	—	—	—
72.0	3	140 (39)	3	17 (49)	—	—	—	—	—	—	—	—

[§] Mean (standard error of the mean). Significantly different from pre-treatment values (* $p \leq 0.05$, $^{+}$ $p \leq 0.001$).

Figure 7. Tidal volume (ml) three months after irradiation as a function of dose. There was a statistically significant decrease from pre-treatment values at the higher doses in the 67% irradiated lung volume group. There was a statistically significant decrease from pre-treatment values throughout the range of doses in the 100% irradiated lung volume group. (◊) data points represent pre-treatment values. (◆) data points represent sham-irradiated controls. Error bars represent standard error of the mean. Points without error bars represent single animals. Points significantly different from pre-treatment values (* $p \leq 0.05$, $^{+}$ $p \leq 0.001$).

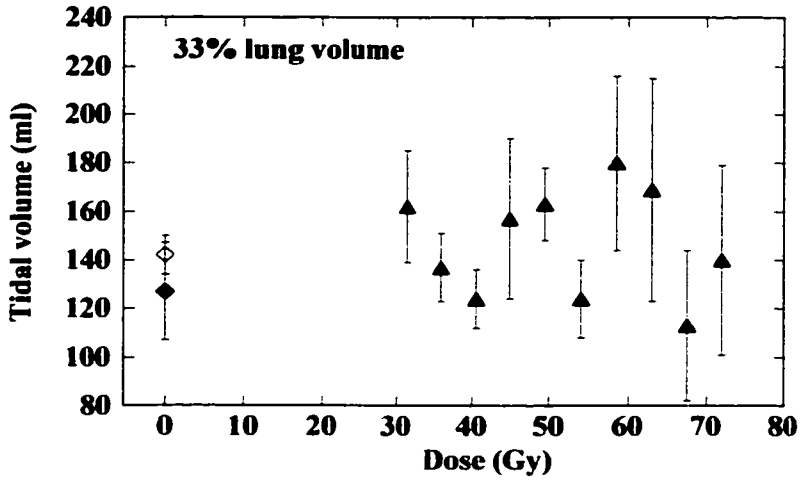

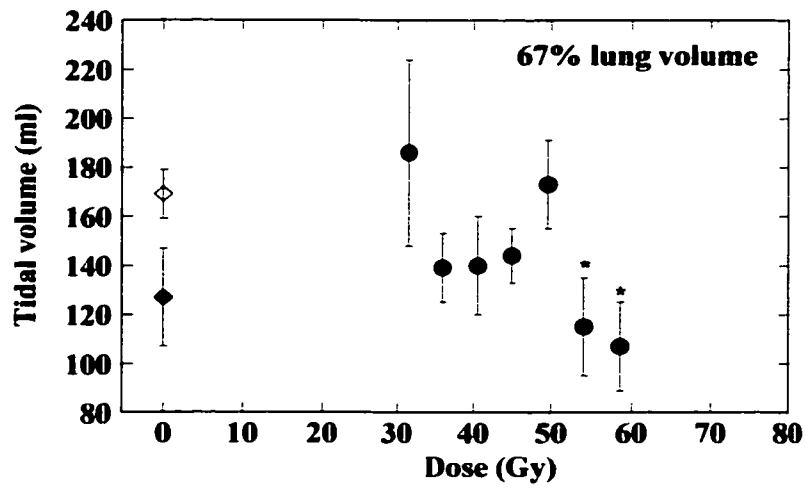

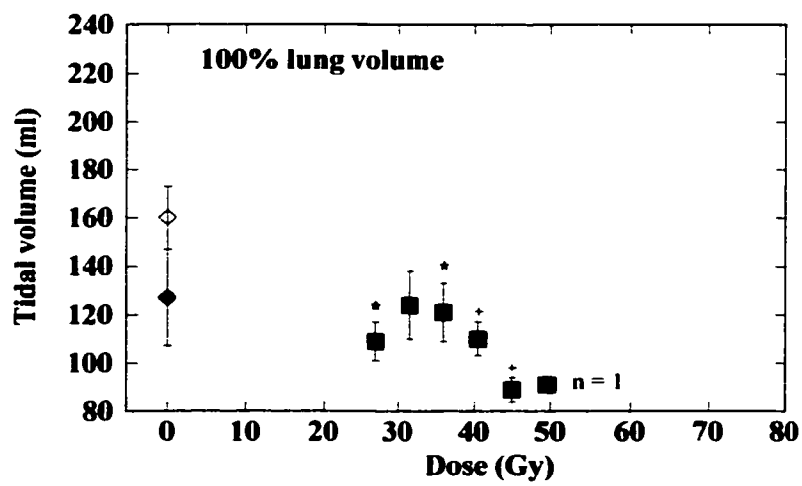

Table 9. Dynamic compliance (CDyn) (volume change per unit pressure change) and percent change three months after irradiation[§]

	Lung Volume Irradiated											
	33%				67%				100%			
Dose (Gy)	n	CDyn (l/cm H_2O)	n	% Change	n	CDyn (l/cm H_2O)	n	% Change	n	CDyn (l/cm H_2O)	n	% Change
Pre Tx	52	0.063 (0.003)			37	0.065 (0.003)			30	0.065 (0.005)		
Sham	—	—	—	—	—	—	—	—	5	0.054 (0.009)	5	-17 (16)
27.0	—	—	—	—	—	—	—	—	4	0.058 (0.013)	4	-16 (14)
31.5	4	0.057 (0.007)	4	2 (12)	4	0.057 (0.006)	4	37 (26)	6	0.051 (0.007)	6	14 (20)
36.0	6	0.057 (0.005)	6	6 (13)	4	**0.057 (0.001)***	4	-8 (7)	5	0.048 (0.015)	5	-22 (13)
40.5	5	0.068 (0.005)	5	48 (17)	6	0.056 (0.010)	6	-17 (15)	6	**0.040 (0.009)***	5	-46 (15)
45.0	4	0.058 (0.004)	4	-24 (8)	5	0.054 (0.006)	5	-8 (11)	2	**0.036 (0.004)***	2	-18 (1)
49.5	5	0.054 (0.006)	5	-24 (8)	6	**0.040 (0.008)***	6	-33 (19)	1	0.068	1	42
54.0	6	0.049 (0.005)	6	4 (19)	5	**0.029 (0.006)**$^{+}$	5	-57 (10)	0	No survivors	0	—
58.5	5	0.062 (0.007)	5	-13 (16)	4	**0.047 (0.003)**$^{+}$	4	-32 (6)	—	—	—	—
63.0	4	0.043 (0.007)	4	-29 (12)	0	No survivors	0	—	—	—	—	—
67.5	4	0.042 (0.015)	4	-39 (21)	—	—	—	—	—	—	—	—
72.0	1	0.058	1	85	—	—	—	—	—	—	—	—

[§] Mean (standard error of the mean). Significantly different from pre-treatment values (* $p \leq 0.05$, $^{+}$ $p \leq 0.001$).

Figure 8. Dynamic compliance (l/cm H_2O) three months after irradiation as a function of dose. There was a statistically significant decrease from pre-treatment values after doses of 49.5 Gy in the 67% irradiated lung volume group, and after doses of 40.5 Gy in the 100% irradiated lung volume group. (◊) data points represent pre-treatment values. (◆) data points represent sham-irradiated controls. Error bars represent standard error of the mean. Points without error bars represent single animals. Points significantly different from pre-treatment values (* $p \leq 0.05$, $^{+}$ $p \leq 0.001$).

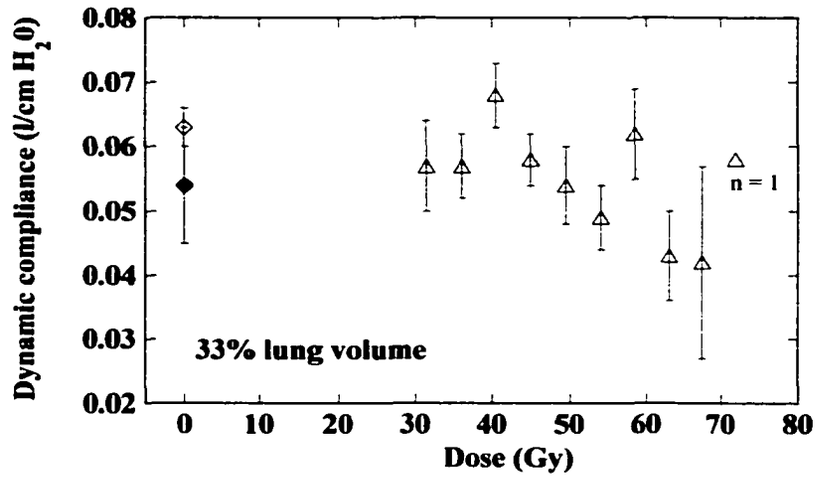

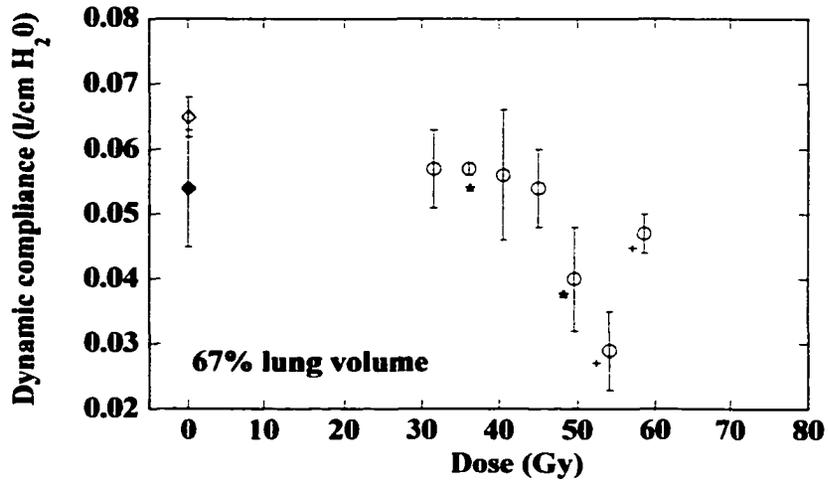

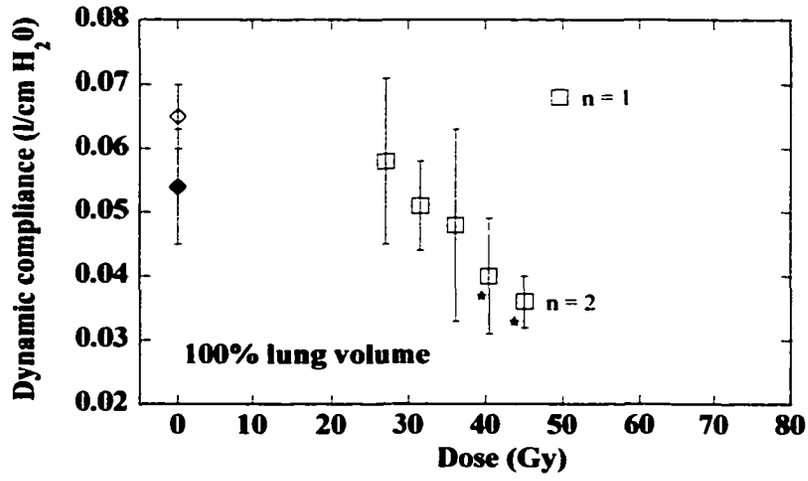

Table 10. Right ventricular systolic pressure (torr) and percent change three months after irradiation[§]

	Lung Volume Irradiated											
	33%				67%				100%			
Dose (Gy)	n	RV systolic pressure (torr)	n	% Change	n	RV systolic pressure (torr)	n	% Change	n	RV systolic pressure (torr)	n	% Change
Pre Tx	53	25.7 (0.5)			37	27.1 (0.7)			38	25.3 (0.7)		
Sham	—	—	—	—	—	—	—	—	5	27.6 (3.0)	5	11.4 (17.1)
27.0	—	—	—	—	—	—	—	—	4	26.5 (3.0)	4	-9.3 (10.4)
31.5	4	26.3 (2.2)	4	-7.0 (14.7)	4	27.8 (1.7)	4	4.9 (12.5)	6	25.2 (2.4)	6	3.1 (16.0)
36.0	6	27.3 (1.6)	6	1.1 (6.5)	6	23.5 (1.9)	6	-8.2 (7.6)	6	25.7 (3.3)	6	6.3 (10.6)
40.5	6	25.3 (2.1)	6	-1.9 (6.6)	6	25.7 (1.4)	6	-2.5 (5.5)	6	26.8 (2.3)	6	19.7 (10.9)
45.0	5	23.6 (1.0)	5	0.7 (6.5)	5	25.8 (1.7)	5	-2.0 (7.9)	2	48.5 (22.5)	2	121.0 (117.0)
49.5	5	23.6 (1.7)	5	-0.6 (6.7)	6	27.2 (1.5)	6	4.4 (9.8)	1	57.0	1	119.2
54.0	6	24.0 (1.4)	6	0.8 (9.4)	5	29.4 (3.3)	5	-2.8 (14.2)	0	No survivors	0	—
58.5	5	24.0 (1.3)	5	-5.3 (9.9)	4	22.7 (2.4)	4	-12.0 (7.2)	—	—	—	—
63.0	4	26.0 (2.7)	4	7.8 (18.1)	0	No survivors	0	—	—	—	—	—
67.5	4	24.5 (1.7)	4	14.9 (14.3)	—	—	—	—	—	—	—	—
72.0	3	25.3 (3.4)	3	-9.0 (3.0)	—	—	—	—	—	—	—	—

[§] Mean (standard error of the mean). No values significantly different from pre-treatment values or sham-irradiated controls ($p \leq 0.05$).

Figure 9. Right ventricular (RV) systolic pressure (torr) three months after irradiation as a function of dose. There was no significant difference in RV systolic pressure in the 33% and 67% irradiated lung volume groups compared with pre-treatment values (◊) and sham-irradiated controls (♦). RV systolic pressure was markedly elevated at the higher doses in the 100% irradiated lung volume group. However, few animals survived to be evaluated in these groups, and the differences were not significant. Error bars represent standard error of the mean. Points without error bars represent single animals.

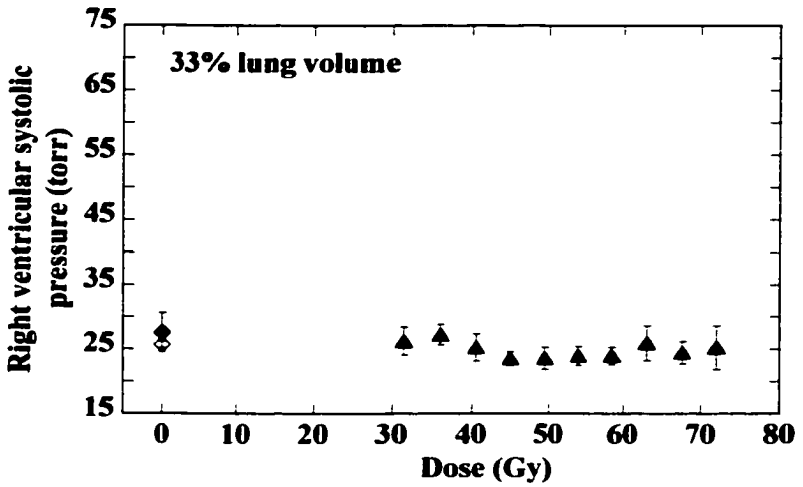

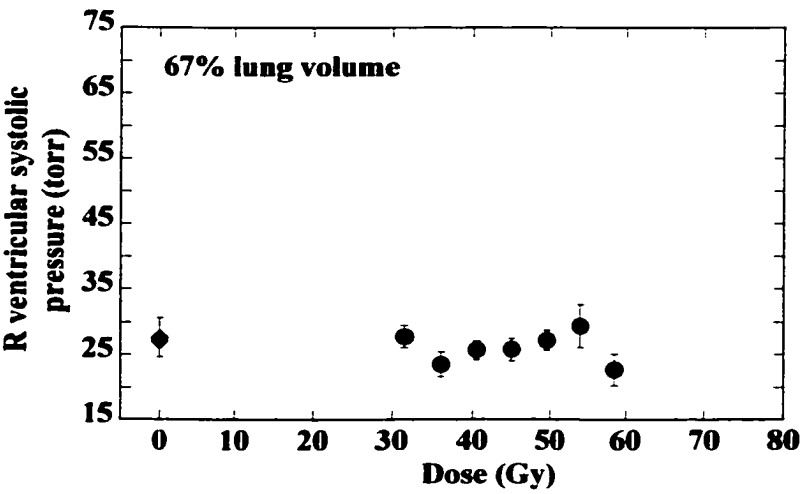

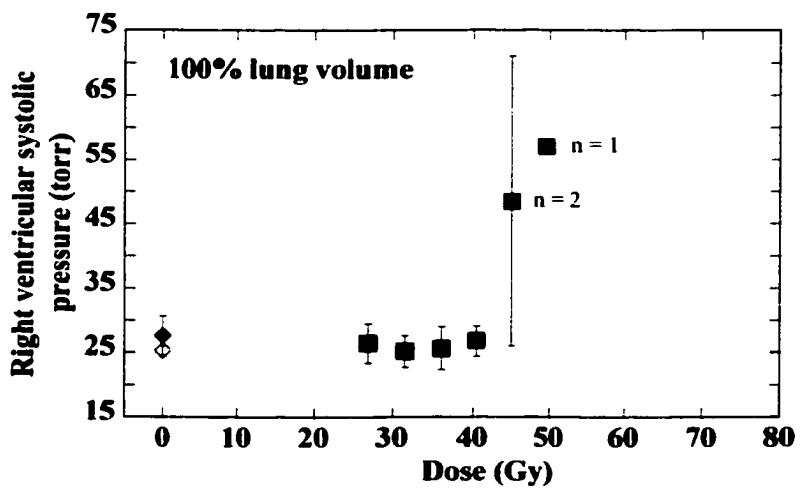

elevated at the higher doses in the 100% irradiated lung volume group. However, few animals survived to be evaluated in these groups, and the differences were not significant.

Mean Pulmonary Artery Pressure

There was a trend toward increased mean pulmonary artery pressures in the 67% lung volume group, but the increases were not statistically significant compared with pre-treatment values and sham-irradiated controls (Table 11, Figure 10). Mean pulmonary artery pressures were markedly elevated at the higher doses in the 100% irradiated lung volume group. However, few animals survived to be evaluated in these groups, and the differences were not significant.

Pulmonary Artery Wedge Pressure

No significant changes in pulmonary artery wedge pressure were found three months after irradiation (Table 12, Figure 11).

Cardiac Output

Three months after irradiation there was a trend toward reduction in cardiac output in all three lung volume groups, compared with pretreatment values. There were significant decreases from pretreatment values at some, but not all of the higher doses in the 67% and 100% irradiated lung volume groups (Table 13, Figure 12).

Table 11. Mean pulmonary artery pressure (torr) and percent change three months after irradiation[§]

	Lung Volume Irradiated											
	33%				67%				100%			
Dose (Gy)	n	Mean PA pressure (torr)	n	% Change	n	Mean PA pressure (torr)	n	% Change	n	Mean PA pressure (torr)	n	% Change
Pre Tx	53	17.8 (0.3)			37	18.2 (0.3)			38	18.1 (0.4)		
Sham	—	—	—	—	—	—	—	—	5	20.0 (1.3)	5	9.1 (3.6)
27.0	—	—	—	—	—	—	—	—	4	19.3 (2.0)	4	1.1 (6.7)
31.5	4	19.5 (2.6)	4	2.4 (14.6)	4	17.0 (0.7)	4	1.4 (7.6)	6	17.3 (0.8)	6	-4.0 (10.5)
36.0	6	17.2 (0.5)	6	-2.9 (5.1)	6	16.3 (0.5)	6	-7.3 (2.9)	5	19.6 (3.2)	5	5.6 (6.2)
40.5	6	16.7 (0.8)	6	-2.6 (4.2)	6	17.8 (0.7)	6	-3.3 (2.8)	6	21.0 (2.1)	6	19.3 (9.2)
45.0	5	16.8 (1.0)	5	-3.1 (9.4)	5	18.4 (1.2)	5	2.8 (6.8)	2	36.5 (11.5)	2	133.3 (66.7)
49.5	5	19.0 (1.3)	5	15.9 (14.6)	6	19.3 (1.1)	6	10.2 (3.9)	1	33.0	1	73.7
54.0	6	16.7 (0.5)	6	-10.9 (3.8)	5	22.2 (2.4)	5	9.2 (8.6)	0	No survivors	0	—
58.5	5	17.8 (0.7)	5	-0.5 (4.6)	4	19.0 (0.9)	4	1.2 (2.5)	—	—	—	—
63.0	4	17.8 (0.9)	4	0.9 (11.2)	0	No survivors	0	—	—	—	—	—
67.5	4	17.5 (0.6)	4	2.5 (9.7)	—	—	—	—	—	—	—	—
72.0	3	16.0 (1.5)	3	-14.6 (5.1)	—	—	—	—	—	—	—	—

[§] Mean (standard error of the mean). No values significantly different from pre-treatment values or sham-irradiated controls ($p \leq 0.05$).

Figure 10. Mean pulmonary artery pressure (torr) three months after irradiation as a function of dose. There was a trend toward increased pressures in the 67% irradiated lung volume group, but the increases were not statistically significant compared with pre-treatment values (◊) and sham-irradiated controls (♦). Mean pulmonary artery pressures were markedly elevated at the higher doses in the 100% irradiated lung volume group. However, few animals survived to be evaluated in these groups, and the differences were not significant. Error bars represent standard error of the mean. Points without error bars represent single animals.

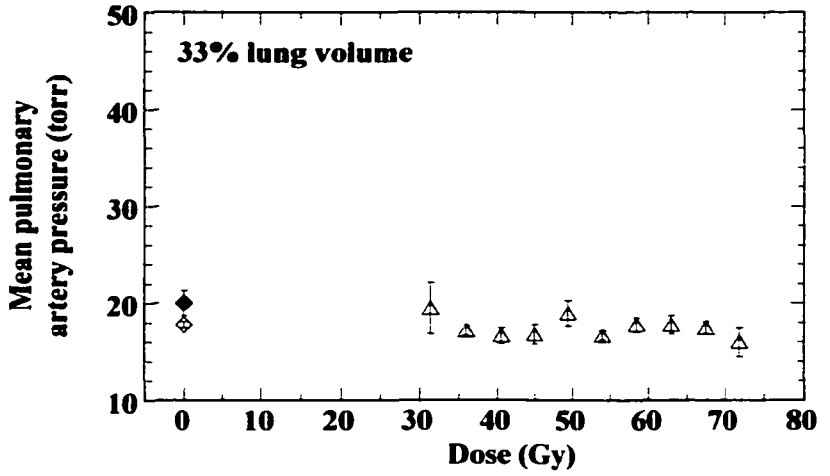

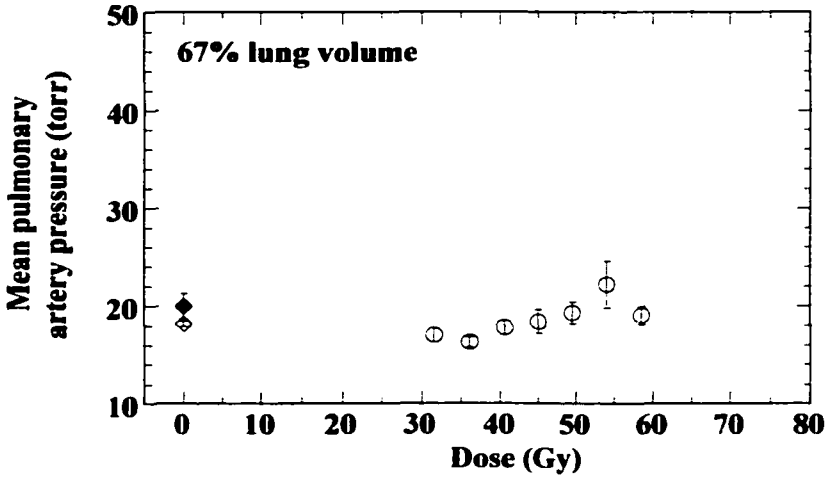

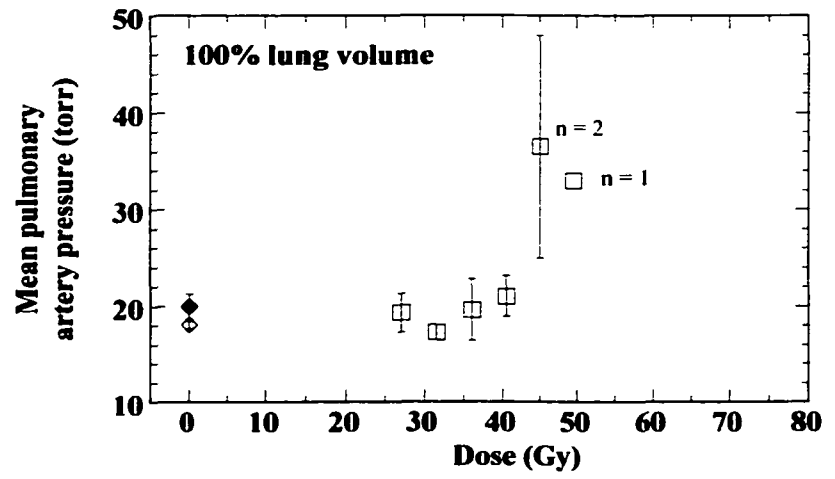

Table 12. Pulmonary artery wedge pressure (torr) and percent change three months after irradiation[§]

	Lung Volume Irradiated											
	33%				67%				100%			
Dose (Gy)	n	PA wedge pressure (torr)	n	% Change	n	PA wedge pressure (torr)	n	% Change	n	PA wedge pressure (torr)	n	% Change
Pre Tx	53	8.4 (0.2)			37	8.4 (0.2)			38	8.6 (0.3)		
Sham	—	—	—	—	—	—	—	—	5	9.6 (1.1)	5	6.6 (14.9)
27.0	—	—	—	—	—	—	—	—	4	6.8 (0.9)	4	-19.4 (12.3)
31.5	4	6.8 (0.8)	4	-27.3 (14.3)	4	6.8 (0.9)	4	-0.4 (5.5)	6	7.2 (0.7)	6	-11.7 (16.5)
36.0	6	7.3 (0.5)	6	-11.2 (9.3)	6	**6.3 (0.9)**$^{+}$	6	-21.2 (9.6)	5	**6.4 (0.7)***$^{+}$	5	-27.2 (7.0)
40.5	6	7.0 (0.9)	6	-18.3 (6.5)	6	6.8 (0.7)	6	-16.8 (7.4)	6	**6.5 (0.8)***	6	0.6 (31.7)
45.0	5	7.4 (1.1)	5	-9.6 (12.3)	5	7.6 (0.7)	5	-4.7 (13.0)	2	6.5 (1.5)	2	-28.8 (8.8)
49.5	5	8.0 (0.7)	5	6.8 (12.7)	6	**7.0 (0.4)***	6	-19.9 (5.1)	1	30.0	1	—
54.0	6	**6.0 (0.4)***$^{+}$	6	-34.5 (4.1)	5	6.8 (1.0)	5	-29.8 (9.4)	0	No survivors	0	—
58.5	5	7.8 (1.0)	5	-7.9 (8.7)	4	**6.3 (0.5)***$^{+}$	4	-30.4 (4.9)	—	—	—	—
63.0	4	7.3 (0.6)	4	-9.9 (17.7)	0	No survivors	0	—	—	—	—	—
67.5	4	6.5 (0.9)	4	1.8 (41.1)	—	—	—	—	—	—	—	—
72.0	3	6.3 (1.5)	3	-25.8 (19.4)	—	—	—	—	—	—	—	—

[§] Mean (standard error of the mean). Significantly different from pre-treatment values (*) and sham-irradiated controls ($^{+}$) ($p \leq 0.05$).

Figure 11. Pulmonary artery wedge pressure (torr) three months after irradiation as a function of dose. There was no significant difference in pulmonary artery wedge pressure three months after irradiation in comparison with pre-treatment values (◊) and sham-irradiated controls (◆). Error bars represent standard error of the mean. Points without error bars represent single animals.

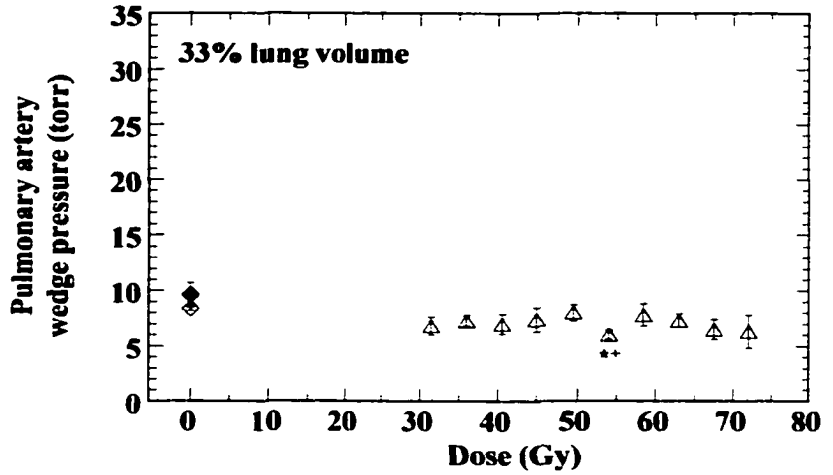

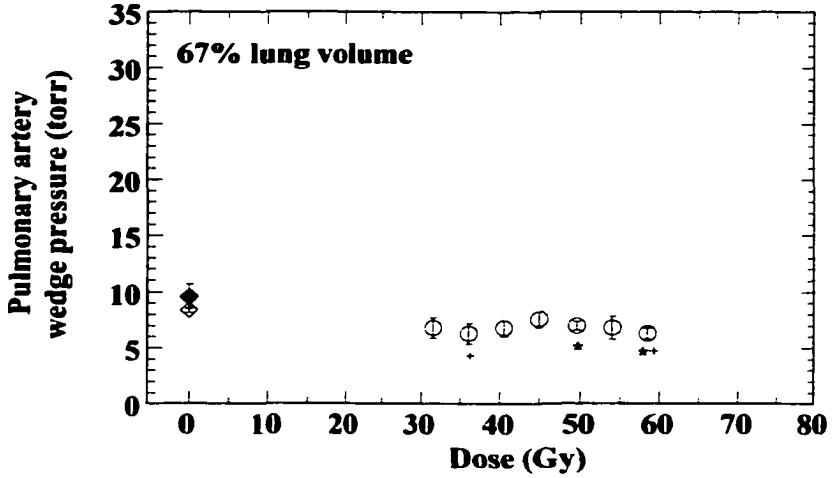

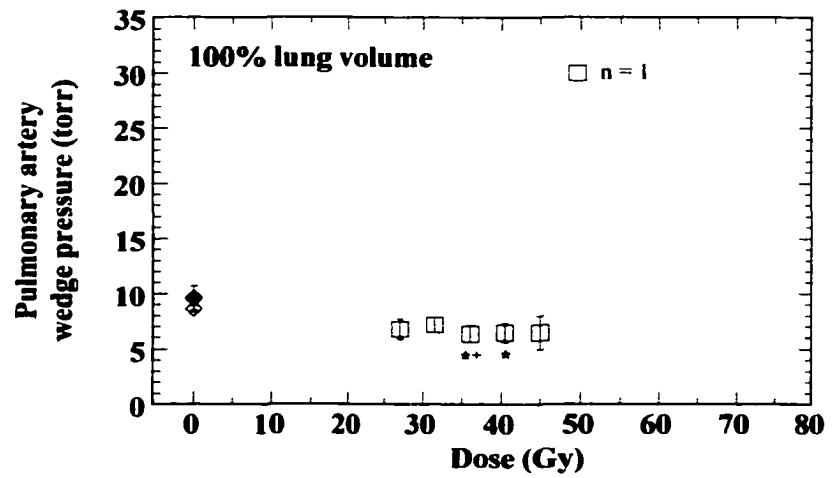

Table 13. Cardiac output (ml/min) and percent change three months after irradiation[§]

	Lung Volume Irradiated											
	33%				67%				100%			
Dose (Gy)	n	Cardiac output (ml/min)	n	% Change	n	Cardiac output (ml/min)	n	% Change	n	Cardiac output (ml/min)	n	% Change
Pre Tx	53	1.6 (0.1)			37	1.8 (0.1)			38	1.7 (0.1)		
Sham	—	—	—	—	—	—	—	—	5	1.8 (0.3)	5	-2.3 (6.7)
27.0	—	—	—	—	—	—	—	—	4	1.6 (0.3)	4	-6.4 (12.4)
31.5	4	1.4 (0.1)	4	-11.3 (9.3)	4	1.7 (0.2)	4	6.1 (21.5)	6	**1.3 (0.1)***	6	4.0 (14.4)
36.0	6	1.5 (0.1)	6	8.1 (6.6)	6	1.8 (0.1)	6	14.5 (11.3)	6	1.6 (0.2)	6	31.9 (27.2)
40.5	6	1.5 (0.1)	6	10.8 (11.3)	6	1.5 (0.2)	6	-18.8 (7.3)	5	1.5 (0.2)	5	-15.9 (9.5)
45.0	5	1.5 (0.2)	5	-7.4 (18.6)	5	1.9 (0.2)	5	24.3 (15.1)	2	**1.0 (0.1)***	2	-24.7 (6.5)
49.5	5	1.5 (0.1)	5	-16.8 (2.4)	6	**1.3 (0.1)***	6	-13.4 (16.2)	1	2.0	1	-16.7
54.0	6	**1.2 (0.1)***	6	-17.2 (12.2)	5	1.5 (0.1)	5	-28.0 (11.2)	0	No survivors	0	—
58.5	5	1.4 (0.1)	5	-18.2 (10.1)	4	**1.1 (0.1)***	4	-31.1 (8.1)	—	—	—	—
63.0	4	1.2 (0.2)	4	-21.4 (11.9)	0	No survivors	0	—	—	—	—	—
67.5	4	1.3 (0.2)	4	-32.5 (7.8)	—	—	—	—	—	—	—	—
72.0	3	1.0 (0.3)	3	-15.1 (33.2)	—	—	—	—	—	—	—	—

[§] Mean (standard error of the mean). * Significantly different from pre-treatment values ($p \leq 0.01$).

Figure 12. Cardiac output (ml/min) three months after irradiation as a function of dose. There was a trend toward decreased cardiac output at the higher doses in all three lung volume groups compared with pre-treatment values. There were significant decreases at some, but not all of the higher doses in the 67% and 100% irradiated lung volume groups. (◊) data points represent pre-treatment values. (×) data points represent sham-irradiated controls. Points without error bars represent single animals. Points significantly different from pre-treatment values (* $p \leq 0.01$).

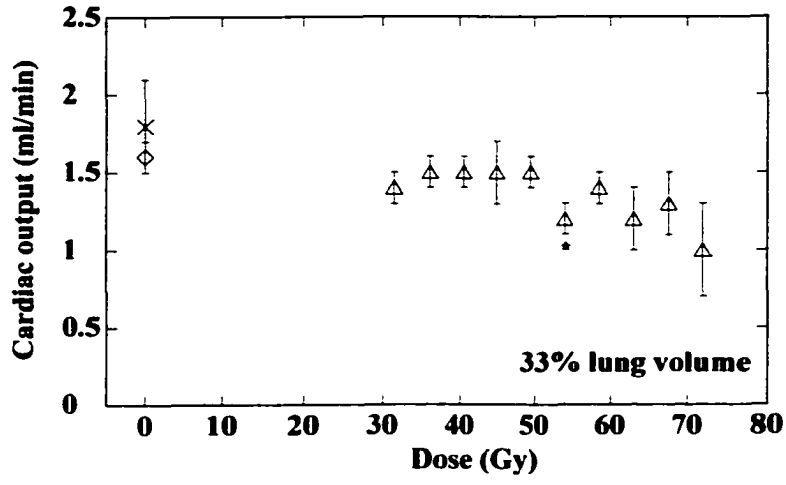

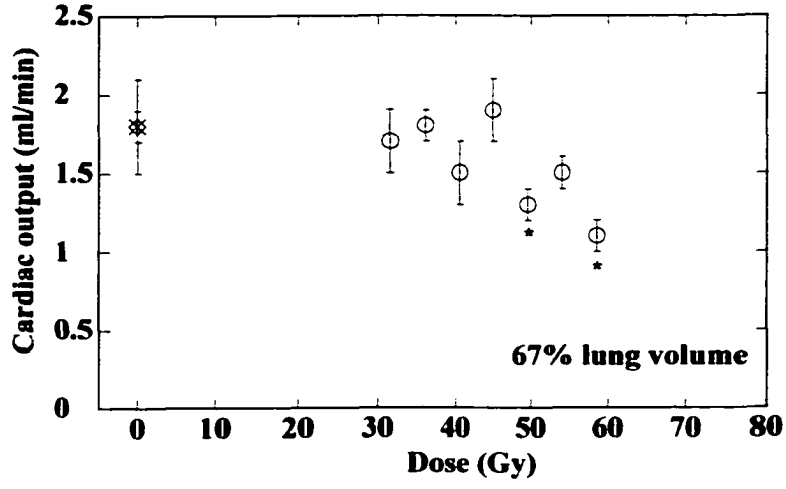

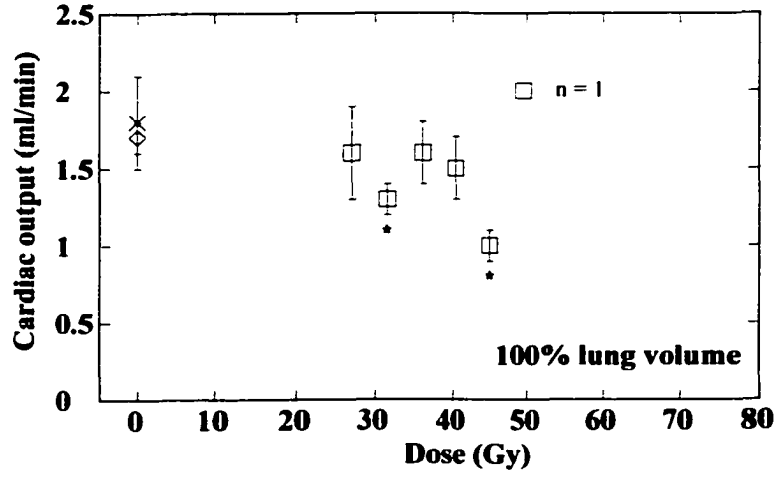

Systemic Mean Arterial Blood Pressure

There was a trend toward decreased systemic mean arterial blood pressure at the higher doses in all three lung volume groups, compared with pretreatment values (Table 14, Figure 13).

Indicator Dilution Assays

Serotonin Uptake (%)

The percentage of injected ^{14}C-labeled serotonin taken up (mean ± SEM) in pre-irradiation assays was 78.9 ± 0.6 %. Three months after irradiation there was an apparent dose related decrease in serotonin uptake for all three volume groups (Figure 14). However, significant overall decrease in serotonin uptake was observed only in dogs irradiated to 67% and 100% of their lung volume (Table 15). In the 67% lung volume irradiated group, mean serotonin uptake declined from 78% to 39% three months after irradiation for the dogs irradiated to doses of 58.5 Gy. Significant reduction started with doses as low as 45 Gy in the same group of dogs. In the dogs irradiated to 100% of their lung volume the mean pretreatment level of serotonin uptake was 79%. It declined to approximately 40%. A significant decrease in uptake was observed in this group at doses beginning with 40.5 Gy. Dogs irradiated to 33% of their lung volume did show a slight decrease in serotonin uptake, but this decrease was not significant. The probability of measured serotonin uptake values being less than 68% (pre-irradiation uptake mean less two standard deviations) three months after irradiation was significantly higher in the 67% and 100% lung volume groups than in the 33% group (Figure 15). Calculated ED_{50}

Table 14. Systemic mean arterial blood pressure (torr) and percent change three months after irradiation[§]

	Lung Volume Irradiated											
	33%				67%				100%			
Dose (Gy)	**n**	**Mean arterial BP (torr)**	**n**	**% Change**	**n**	**Mean arterial BP (torr)**	**n**	**% Change**	**n**	**Mean arterial BP (torr)**	**n**	**% Change**
Pre Tx	53	97.6 (2.1)			37	101.0 (2.4)			38	96.2 (2.2)		
Sham	—	—	—	—	—	—	—	—	5	98.4 (7.3)	5	4.3 (4.0)
27.0	—	—	—	—	—	—	—	—	4	97.0 (12.1)	4	4.5 (10.9)
31.5	4	86.3 (4.4)	4	-18.5 (6.6)	4	97.3 (7.8)	4	-5.9 (1.4)	6	**84.2 (4.0)***	6	-17.1 (5.8)
36.0	6	101.5 (6.6)	6	-0.1 (9.1)	6	99.8 (6.7)	6	-8.6 (6.3)	6	87.8 (5.7)	6	-4.0 (7.8)
40.5	6	102.3 (6.3)	6	10.7 (10.8)	6	101.2 (2.7)	6	1.6 (7.8)	5	83.5 (6.8)	5	-9.7 (8.1)
45.0	5	**85.0 (2.8)***	5	-10.7 (6.9)	5	89.2 (6.9)	5	-1.2 (15.5)	2	85.0 (18.0)	2	-3.4 (20.5)
49.5	5	**81.0 (4.1)***	5	-11.5 (4.4)	6	87.5 (8.4)	6	-10.5 (10.1)	1	71.0	1	-26.8
54.0	6	**78.3 (3.3)***	6	-21.3 (5.4)	4	86.4 (6.0)	4	-12.7 (6.4)	0	No survivors	0	—
58.5	5	84.0 (6.4)	5	-7.6 (9.7)	4	**77.3 (4.6)***	4	-18.7 (7.4)	—	—	—	—
63.0	4	94.3 (3.5)	4	-12.9 (2.7)	0	No survivors	0	—	—	—	—	—
67.5	4	72.8 (9.8)	4	-22.1 (10.7)	—	—	—	—	—	—	—	—
72.0	3	76.3 (7.8)	3	-10.1 (19.8)	—	—	—	—	—	—	—	—

[§] Mean (standard error of the mean). * Significantly different from pre-treatment values ($p \leq 0.01$).

Figure 13. Systemic mean arterial blood pressure (mmHg) three months after irradiation as a function of dose. There was a trend toward decreased systmic mean arterial blood pressure in all three lung volume groups, compared with pre-treatment values (◊) and sham-irradiated controls (♦). Error bars represent standard error of the mean. Points without error bars represent single animals.

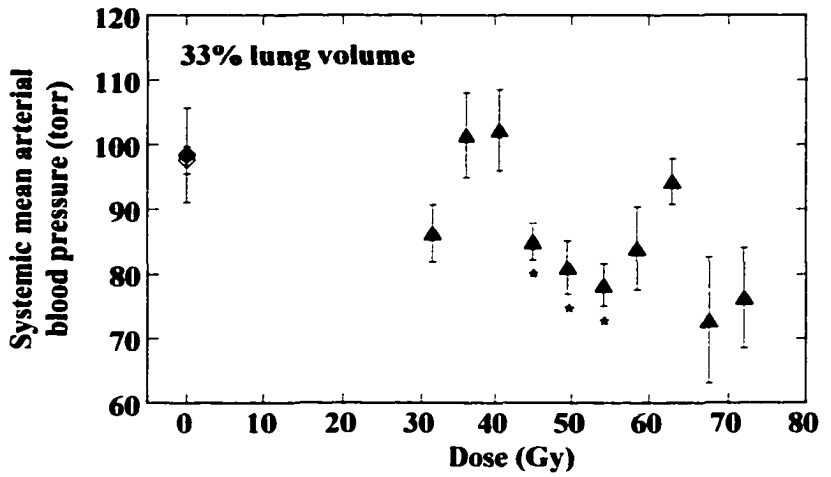

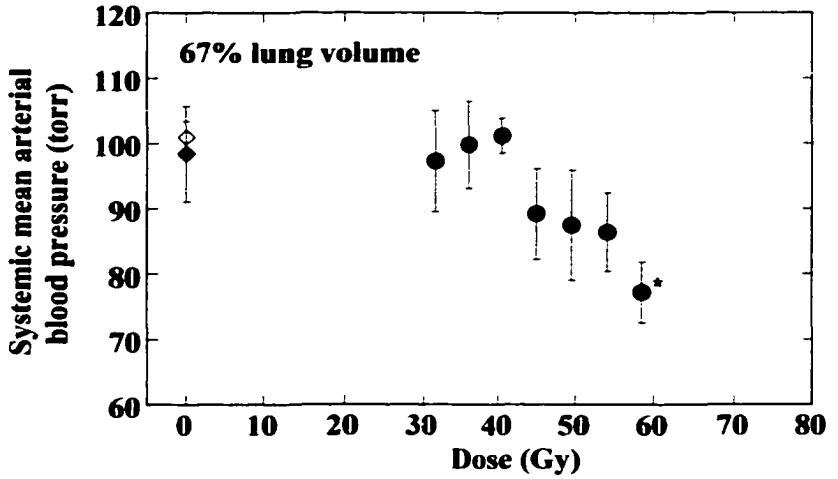

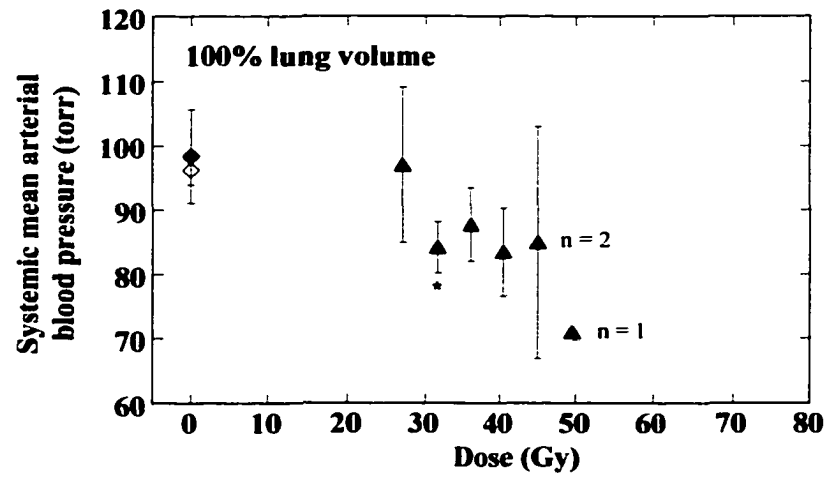

Figure 14. Serotonin uptake (%) three months after irradiation as a function of dose. There was a dose related decrease in all three volume groups. Asterisks indicate points significantly different from the pre-treatment values ($p \leq 0.05$). Error bars represent standard error of the mean. Points without error bars represent single animals.

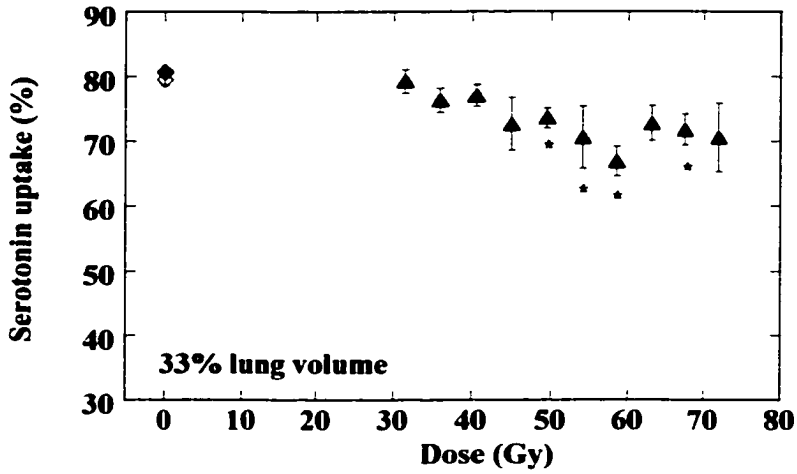

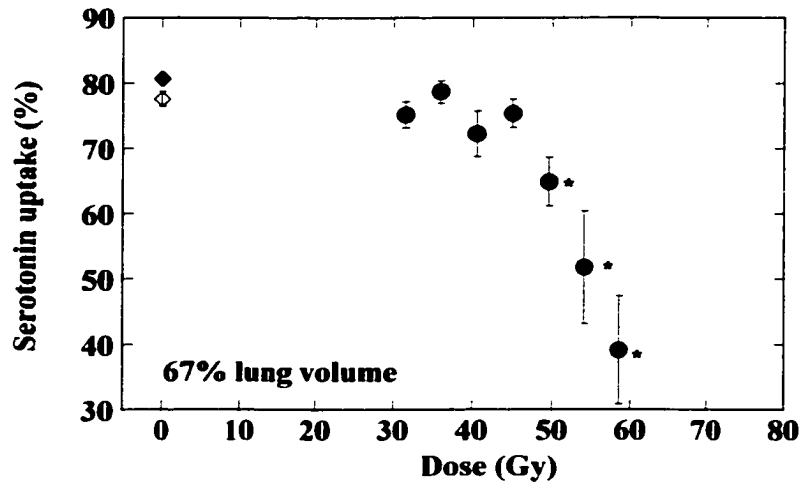

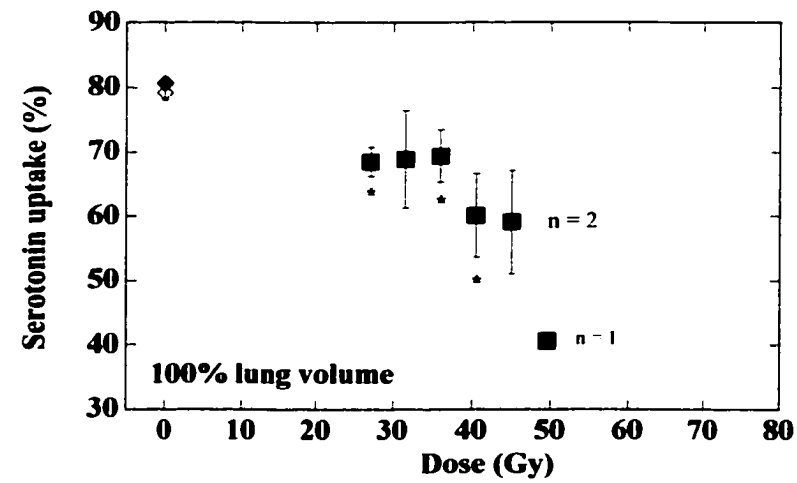

Table 15. Serotonin uptake (%) and percent change in uptake three months after irradiation[§]

	Lung Volume Irradiated											
	33%				67%				100%			
Dose (Gy)	n	Serotonin Uptake (%)	n	% Change	n	Serotonin Uptake (%)	n	% Change	n	Serotonin Uptake (%)	n	% Change
Pre Tx	53	79.5 (0.8)			36	77.6 (1.1)			37	79.2 (1.1)		
Sham	—	—	—	—	—	—	—	—	4	80.7 (0.5)	4	-0.5 (2.8)
27.0	—	—	—	—	—	—	—	—	4	**68.5 (2.3)***	4	-14.2 (5.5)
31.5	4	79.3 (1.8)	4	-2.7 (3.2)	4	75.2 (2.0)	4	-4.6 (1.9)	6	68.9 (7.6)	6	-13.6 (10.7)
36.0	6	76.4 (1.9)	6	-5.9 (2.2)	6	78.7 (1.7)	5	-1.2 (3.0)	6	**69.4 (4.1)***	6	-12.7 (5.2)
40.5	6	77.1 (1.7)	6	-3.3 (3.5)	6	72.2 (3.5)	6	-7.8 (3.4)	6	**60.1 (6.5)***	5	-31.3 (9.5)
45.0	5	72.7 (4.1)	5	-12.6 (5.8)	5	**75.4 (2.2)***	5	-5.9 (1.9)	2	59.1 (8.0)	2	-23.9 (0.3)
49.5	5	**73.6 (1.5)***	5	-7.1 (2.9)	6	**64.9 (3.7)***	6	-15.3 (3.8)	1	40.7	1	-50.5
54.0	6	**75.2 (1.7)***	5	-1.4 (7.4)	5	**51.8 (8.6)***	5	-28.7 (15.1)	0	No survivors	0	—
58.5	5	**66.9 (2.3)***	5	-11.0 (1.9)	4	**39.2 (8.3)***	4	-35.1 (9.0)	—	—	—	—
63.0	4	72.8 (2.7)	4	-6.9 (2.6)	0	No survivors	0	—	—	—	—	—
67.5	4	**71.8 (2.4)***	4	-5.6 (8.5)	—	—	—	—	—	—	—	—
72.0	3	70.6 (5.3)	3	-15.2 (5.5)	—	—	—	—	—	—	—	—

[§] Mean (standard error of the mean). * Significantly different from paired pre-treatment values ($p < 0.05$).

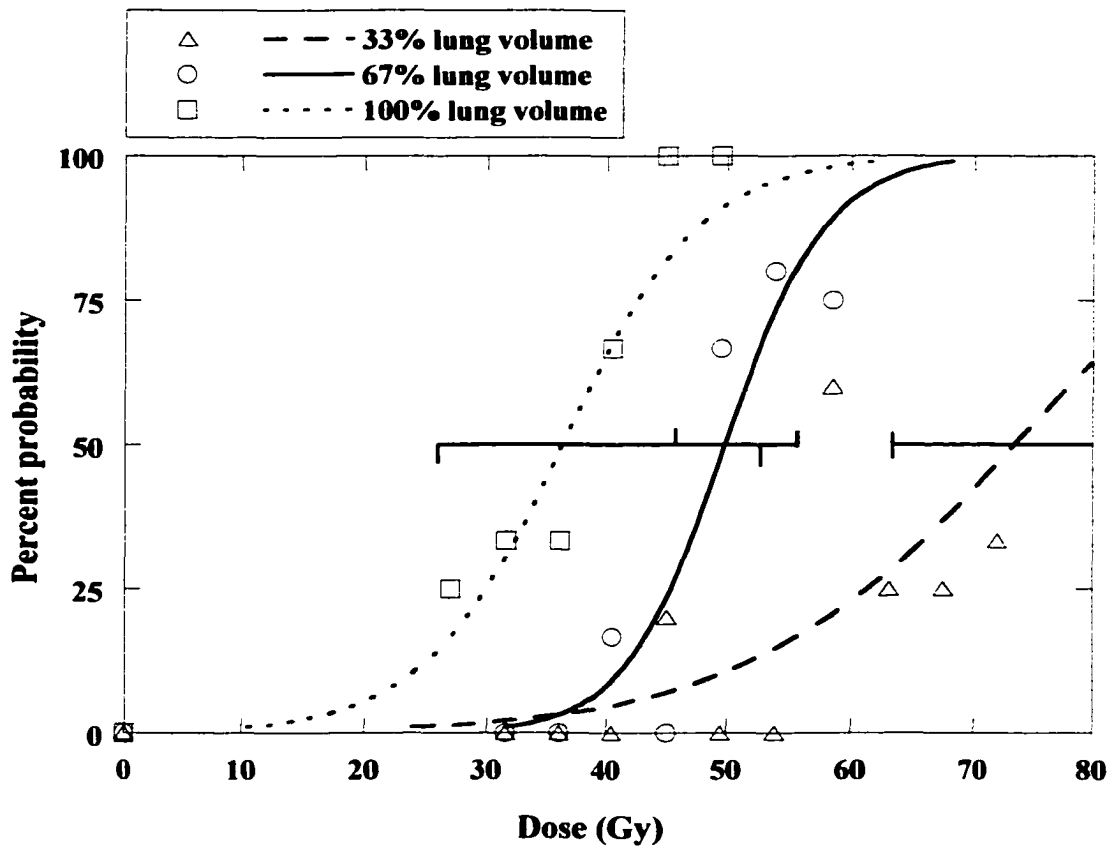

Figure 15. Dose-response curves for serotonin uptake values less than 68% of injected serotonin three months after irradiation, based on logistic fit. The ED_{50} and ED_5 (95%CI) for the 33% irradiated lung volume group were 73.5 Gy (63.3-189.0 Gy) and 41.7 Gy (0-52.5 Gy) respectively (▲ data points), significantly different from the 67% and 100% lung volume groups. The ED_{50} and ED_5 (95% CI) for the 67% volume group were 49.9 Gy (45.7-55.8 Gy) and 38.2 Gy respectively (18.1-43.3 Gy) (● data points). The ED_{50} and ED_5 (95% CI) for the 100% volume group were 36.3 Gy (26.0-52.9 Gy) and 19.8 Gy (0-28.3 Gy) respectively (■ data points). Error bars represent 95% confidence intervals.

and ED_5 values (95% CI) were 73.5 Gy (63.3-189.0 Gy) and 41.7 Gy (0-52.5 Gy) respectively for the 33% lung volume group, 49.9 Gy (45.7-55.8 Gy) and 38.2 Gy (18.1-43.3 Gy) respectively for the 67% lung volume group, and 36.3 Gy (26.0-52.9 Gy) and 19.8 Gy (0-28.3 Gy) respectively for the 100% lung volume group. Results of ^{14}C-labeled serotonin uptake assays three months after lung irradiation show a statistically significant dose-volume relationship with the greatest effect in the dogs irradiated to 100% of their lung volume.

The volume enhancement ratios (VER) comparing 33% and 67% lung volumes irradiated at the ED_{50} and ED_5 levels of effect for serotonin uptake (%) were 1.47 and 1.09, respectively. Comparing 67% and 100% lung volumes irradiated at the ED_{50} and ED_5 levels of effect for serotonin uptake (%) the VER were 1.37 and 1.93, respectively. Comparing 33% and 100% lung volumes irradiated at the ED_{50} and ED_5 levels of effect for serotonin uptake (%) the VER were 2.02 and 2.11, respectively.

Serotonin PS

Serotonin uptake corrected for permeability surface area (serotonin PS) was significantly decreased in the 33% and 67% irradiated lung volume groups (Table 16, Figure 16). Serotonin was also decreased in the 100% irradiated lung volume group, but the decreases were not significant.

Extravascular Water Volume

Extravascular water volume was not significantly increased from pre-treatment values three months after irradiation (Table 17, Figure 17).

Table 16. Serotonin PS (ml/s) and percent change three months after irradiation[§]

	Lung Volume Irradiated											
	33%				67%				100%			
Dose (Gy)	n	Serotonin PS (ml/s)	n	% Change	n	Serotonin PS (ml/s)	n	% Change	n	Serotonin PS (ml/s)	n	% Change
Pre Tx	50	35.6 (1.2)			33	35.4 (1.3)			37	34.1 (1.6)		
Sham	—	—	—	—	—	—	—	—	4	39.4 (3.6)	4	13.5 (17.1)
27.0	—	—	—	—	—	—	—	—	4	27.5 (3.4)	4	-16.0 (4.5)
31.5	4	33.6 (3.9)	4	-12.2 (14.9)	4	32.5 (5.8)	4	-10.6 (18.2)	6	25.2 (5.4)	6	-12.4 (21.4)
36.0	6	30.5 (4.2)	6	-9.6 (10.2)	6	33.1 (2.6)	5	-16.9 (3.2)	6	31.3 (4.5)	5	-15.5 (8.0)
40.5	5	28.2 (3.2)	5	-11.9 (12.8)	6	30.1 (3.5)	4	-22.3 (12.3)	5	24.9 (4.1)	5	-22.0 (20.3)
45.0	5	26.1 (4.9)	5	-39.9 (8.6)	5	34.3 (4.6)	4	-3.7 (14.6)	2	18.3 (5.6)	2	-43.8 (21.4)
49.5	5	31.4 (2.2)	4	10.3 (38.5)	6	**21.2 (1.8)***	6	-39.6 (4.0)	0	—	0	—
54.0	6	**22.4 (2.8)***	6	-34.8 (9.2)	5	**19.4 (7.0)***	5	-50.3 (17.2)	0	No survivors	0	—
58.5	5	**22.6 (0.9)***	4	-29.8 (10.6)	4	**13.9 (3.9)***	4	-45.1 (13.7)	—	—	—	—
63.0	4	**24.2 (1.7)***	3	-30.1 (9.3)	0	No survivors	0	—	—	—	—	—
67.5	4	**21.4 (3.5)***	4	-32.1 (16.0)	—	—	—	—	—	—	—	—
72.0	3	**17.7 (3.3)***	3	-39.7 (22.7)	—	—	—	—	—	—	—	—

[§] Mean (standard error of the mean). * Significantly different from pre-treatment values and sham-irradiated controls ($p \leq 0.05$).

Figure 16. Serotonin uptake (PS) three months after irradiation as a function of dose. There was a dose related decrease in all three volume groups, significant in the 33% and 67% irradiated lung volume groups. Asterisks indicate points significantly different from the pre-treatment values ($p \leq 0.05$). Error bars represent standard error of the mean. Points without error bars represent single animals.

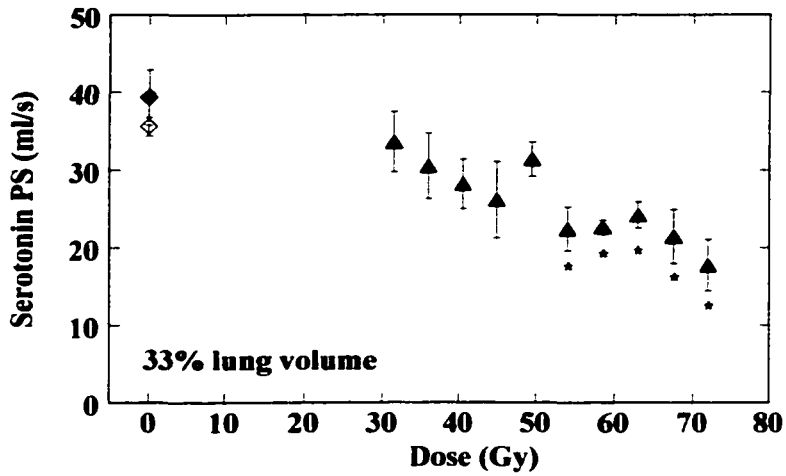

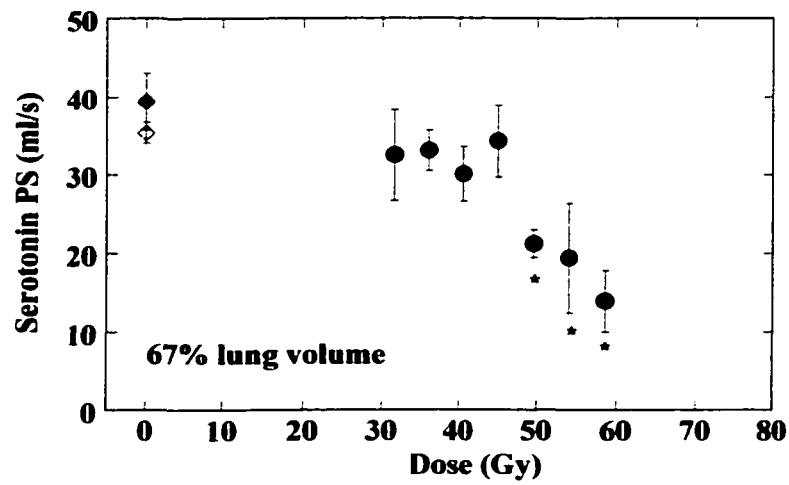

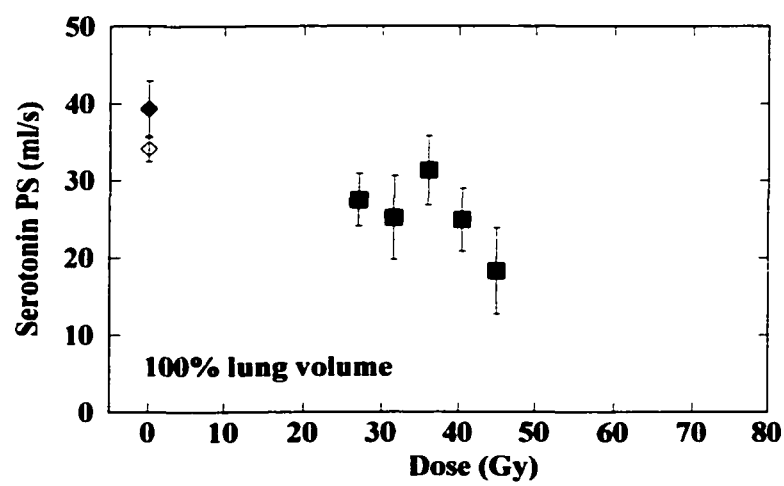

Table 17. Extravascular water (Q_{ev}) (ml) and percent change three months after irradiation[§]

	Lung Volume Irradiated											
	33%				67%				100%			
Dose (Gy)	**n**	**Extravasc. Water (Q_{ev}) (ml)**	**n**	**% Change**	**n**	**Extravasc. Water (Q_{ev}) (ml)**	**n**	**% Change**	**n**	**Extravasc. Water (Q_{ev}) (ml)**	**n**	**% Change**
Pre Tx	53	50.7 (1.6)			37	49.1 (2.1)			38	45.9 (2.0)		
Sham	—	—	—	—	—	—	—	—	5	55.4 (4.6)	5	8.3 (12.7)
27.0	—	—	—	—	—	—	—	—	4	50.1 (0.6)	4	3.6 (10.9)
31.5	4	58.2 (5.0)	4	13.6 (8.5)	4	55.6 (7.8)	4	22.9 (12.5)	5	50.7 (3.5)	5	17.4 (13.2)
36.0	6	46.6 (2.0)	6	13.7 (14.6)	6	51.6 (5.5)	6	36.9 (28.1)	6	60.9 (7.8)	6	39.6 (14.1)
40.5	6	53.6 (6.4)	6	8.3 (14.1)	6	51.8 (4.7)	6	2.8 (5.5)	5	56.0 (4.7)	5	19.0 (19.4)
45.0	5	48.6 (10.8)	5	-11.3 (12.1)	5	55.3 (5.1)	5	6.5 (9.1)	2	58.9 (7.9)	2	54.0 (55.6)
49.5	5	59.6 (6.8)	5	12.8 (21.8)	6	44.3 (4.6)	6	-9.4 (9.8)	1	102.3	1	87.7
54.0	6	**36.1 (3.2)***	6	-25.0 (10.5)	4	69.5 (15.9)	4	50.4 (45.2)	0	No survivors	0	—
58.5	5	46.7 (5.3)	5	-15.4 (13.3)	4	41.4 (6.2)	4	-2.3 (16.9)	—	—	—	—
63.0	4	43.8 (6.2)	4	3.9 (15.9)	0	No survivors	0	—	—	—	—	—
67.5	4	42.5 (6.2)	4	-9.7 (15.8)	—	—	—	—	—	—	—	—
72.0	3	41.2 (3.9)	3	-20.9 (7.9)	—	—	—	—	—	—	—	—

[§] Mean (standard error of the mean). * Significantly different from pre-treatment values ($p \leq 0.05$).

Figure 17. Extravascular water volume (ml) three months after irradiation as a function of dose. There was no significant difference in extravascular water volume three months after irradiation in comparison with pre-treatment values (◊) and sham-irradiated controls (◆). Error bars represent standard error of the mean. Points without error bars represent single animals.

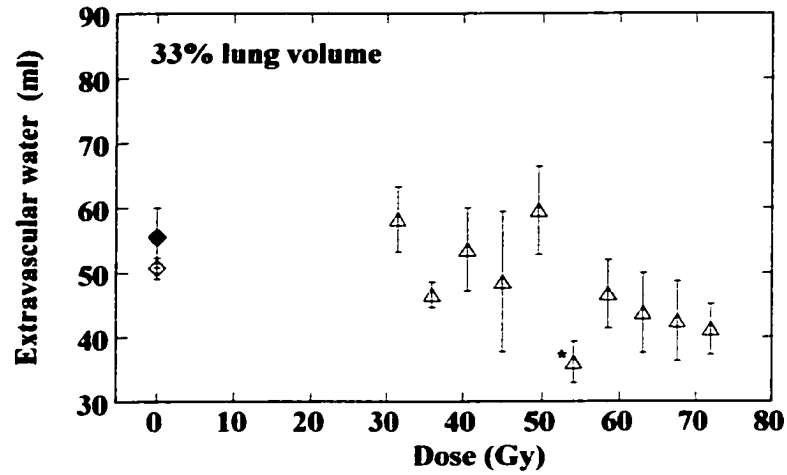

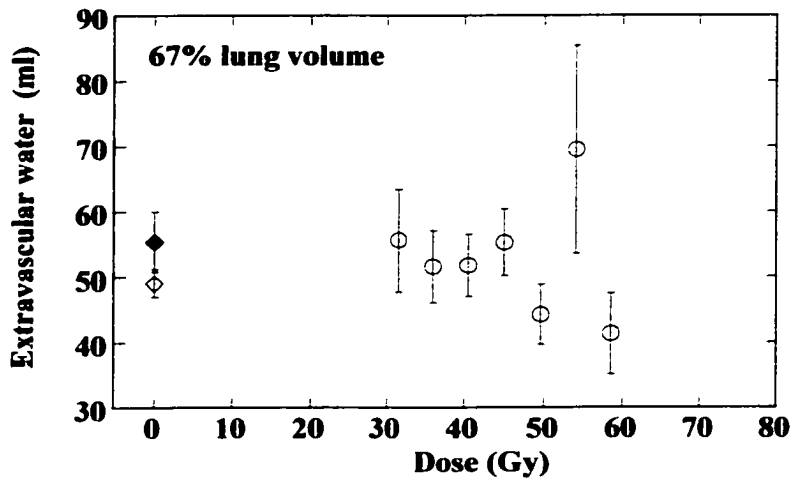

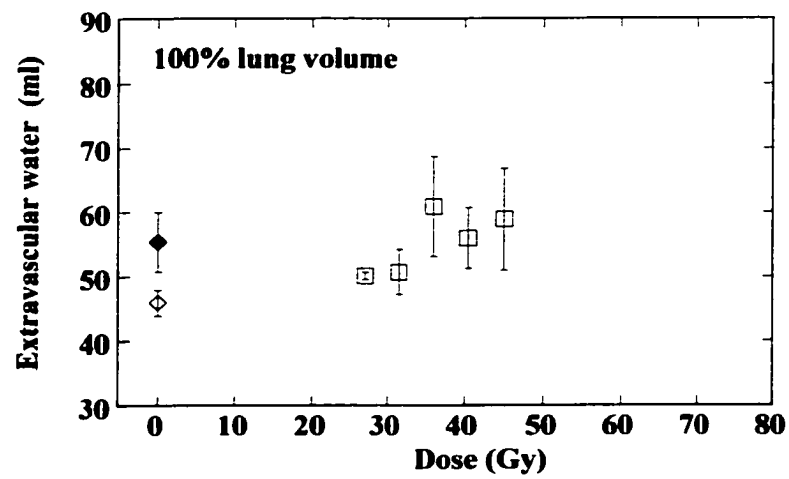

Central Blood Volume

Central blood volume was significantly decreased in all three lung volume groups throughout the range of doses (Table 18, Figure 18). However, there was no significant dose or volume effect.

Pulmonary Blood Flow

Mean pulmonary blood flow for all groups of dogs irradiated ranged from 1200 to 1500 ml/min. There was a decease in pulmonary blood flow related to the dose of radiation in all three lung volume groups (Table 19, Figure 19). However, there was no significant volume effect.

Thoracic Radiographs

Three-month follow-up radiographs of 119 irradiated dogs, and the 5 sham-irradiated dogs were evaluated. Three dogs were not radiographed because they were euthanatized shortly after irradiation ended (chylothorax, esophagitis). Follow-up radiographs of the dog humanely killed due to severe pneumonia were not included in this evaluation. Varying degrees of radiographic fissure lines were observed in 72 of the 3-month follow-up radiographs (61%). The composite radiographic grades, combining separate scores for the presence, degree, and distribution of radiographic fissure lines, decreased vascular detail and increased opacity in the treatment field are presented in Table 20.

In the 27 Gy dose group, three of four dogs receiving whole lung irradiation developed radiographic changes. Two were graded mild and one moderate changes.

Table 18. Central blood volume (ml) and percent change three months after irradiation[§]

	Lung Volume Irradiated											
	33%				67%				100%			
Dose (Gy)	**n**	**Central blood vol. (ml)**	**n**	**% Change**	**n**	**Central blood vol. (ml)**	**n**	**% Change**	**n**	**Central blood vol. (ml)**	**n**	**% Change**
Pre Tx	53	167.5 (7.5)			37	176.7 (8.7)			38	174.8 (8.9)		
Sham	—	—	—	—	—	—	—	—	5	174.0 (33.5)	5	-6.4 (14.3)
27.0	—	—	—	—	—	—	—	—	4	**136.3 (8.7)***	4	-0.9 (5.7)
31.5	4	**141.3 (5.1)***	4	-13.3 (4.4)	4	**123.3 (6.6)***	4	-21.2 (2.3)	6	**118.2 (10.7)***	6	-24.1 (8.1)
36.0	6	**130.3 (11.0)***	6	-15.8 (4.3)	6	**123.3 (10.5)***	6	-21.6 (7.4)	6	139.5 (14.7)	6	-17.5 (6.3)
40.5	6	142.2 (11.3)	6	1.7 (11.5)	6	**121.5 (10.7)***	6	-15.9 (10.4)	5	141.2 (17.4)	5	-18.1 (9.6)
45.0	5	134.4 (13.4)	5	-20.2 (5.2)	5	143.6 (23.5)	5	-21.9 (11.7)	2	157.0 (11.0)	2	-11.9 (35.6)
49.5	5	154.4 (32.4)	5	-6.9 (11.0)	6	**127.2 (8.1)***	6	-26.2 (5.2)	1	146.0	1	-30.8
54.0	6	**130.7 (13.2)***	6	-20.2 (9.1)	5	200.4 (46.1)	5	-12.7 (12.6)	0	No survivors	0	—
58.5	5	177.0 (23.8)	5	-14.4 (7.1)	4	**113.5 (13.7)***	4	-26.8 (15.2)	—	—	—	—
63.0	4	152.0 (35.0)	4	-11.9 (13.6)	0	No survivors	0	—	—	—	—	—
67.5	4	124.5 (24.4)	4	-29.0 (5.3)	—	—	—	—	—	—	—	—
72.0	3	**108.7 (15.4)***	3	-16.1 (19.8)	—	—	—	—	—	—	—	—

[§] Mean (standard error of the mean). * Significantly different from pre-treatment values ($p \leq 0.05$).

Figure 18. Central blood volume (ml) three months after irradiation as a function of dose. There were significant decreases in central blood volume in all three lung volume groups throughout the range of doses in comparison with pre-treatment values (◊) and sham-irradiated controls (◆). However, there was no significant dose or volume effect. Error bars represent standard error of the mean. Points without error bars represent single animals.

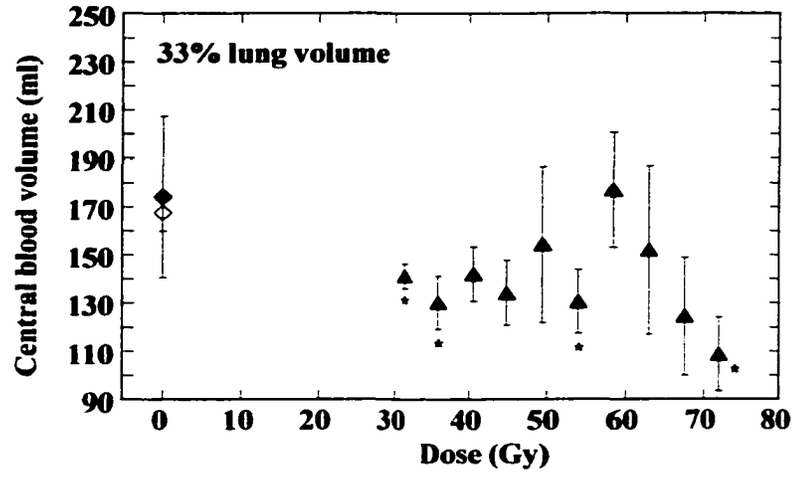

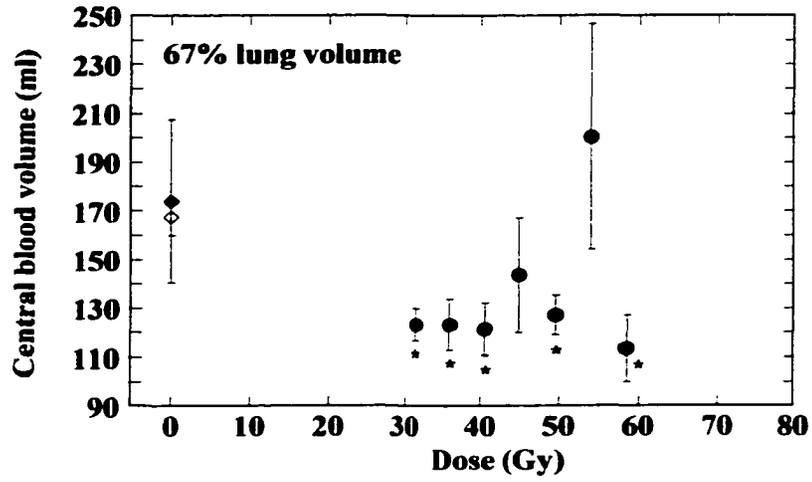

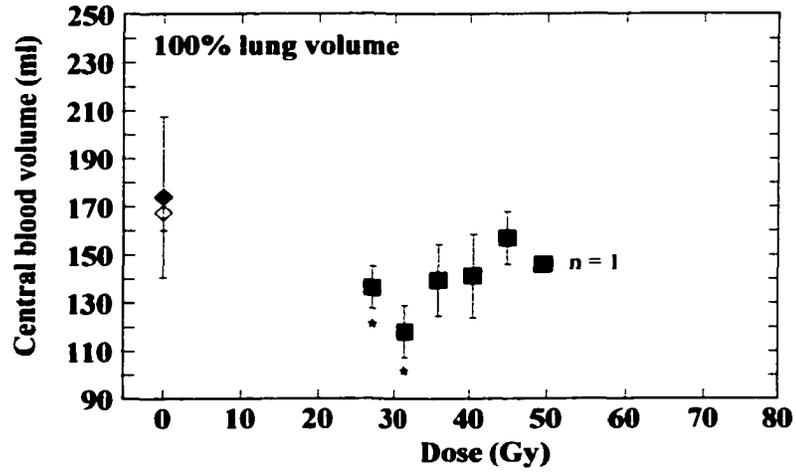

Table 19. Pulmonary blood flow (ml/min) and percent change three months after irradiation[§]

	Lung Volume Irradiated											
	33%				67%				100%			
Dose (Gy)	**n**	**Pulmonary blood flow (ml/min)**	**n**	**% Change**	**n**	**Pulmonary blood flow (ml/min)**	**n**	**% Change**	**n**	**Pulmonary blood flow (ml/min)**	**n**	**% Change**
Pre Tx	52	1370 (55)			37	1504 (68)			38	1297 (68)		
Sham	—	—	—	—	—	—	—	—	5	1397 (239)	5	9.7 (11.5)
27.0	—	—	—	—	—	—	—	—	4	1410 (119)	4	23.2 (16.0)
31.5	4	1264 (98)	4	-8.6 (7.5)	4	1395 (231)	4	-1.3 (18.5)	6	1149 (125)	6	15.7 (27.2)
36.0	6	1237 (126)	6	5.2 (13.2)	6	**1269 (66)***	6	-12.8 (4.4)	6	1570 (218)	6	33.0 (16.0)
40.5	6	1291 (171)	6	3.0 (14.1)	6	1368 (76)	6	-13.4 (8.3)	5	1347 (145)	5	1.6 (13.8)
45.0	5	1156 (118)	5	-18.2 (9.1)	5	1487 (231)	5	6.2 (14.5)	2	1183 (113)	2	0.7 (46.0)
49.5	5	1419 (118)	5	9.6 (26.8)	6	**1202 (78)***	6	-15.4 (6.7)	1	1830	1	4.5
54.0	6	1115 (175)	5	3.6 (28.3)	5	1353 (147)	5	-16.8 (9.5)	0	No survivors	0	—
58.5	5	1229 (63)	5	-19.3 (10.8)	4	**1167 (101)***	4	7.6 (9.4)	—	—	—	—
63.0	4	1136 (161)	4	-24.9 (15.3)	0	No survivors	0	—	—	—	—	—
67.5	4	1331 (116)	4	-23.2 (11.4)	—	—	—	—	—	—	—	—
72.0	3	902 (229)	3	-11.4 (31.2)	—	—	—	—	—	—	—	—

[§] Mean (standard error of the mean). * Significantly different from pre-treatment values. ($p \leq 0.05$).

Figure 19. Pulmonary blood flow (ml/min) three months after irradiation as a function of dose. There was a dose-related decrease in pulmonary blood flow in all three lung volume groups in comparison with pre-treatment values (◊) and sham-irradiated controls (♦). There was no significant volume effect. Error bars represent standard error of the mean. Points without error bars represent single animals.

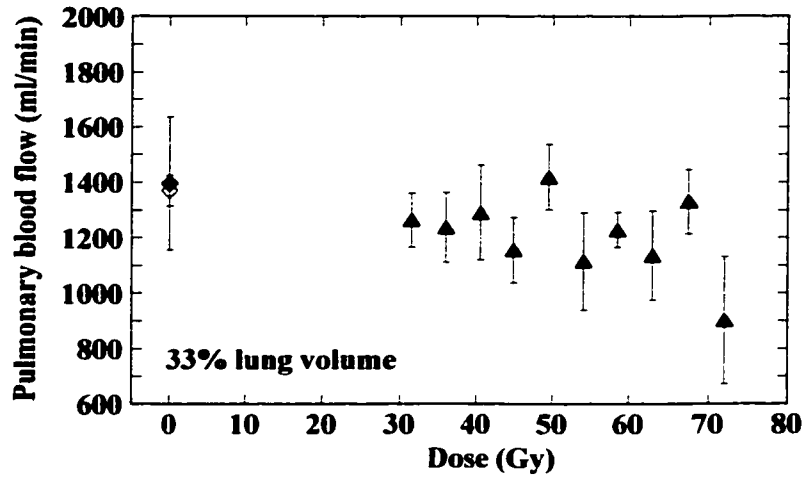

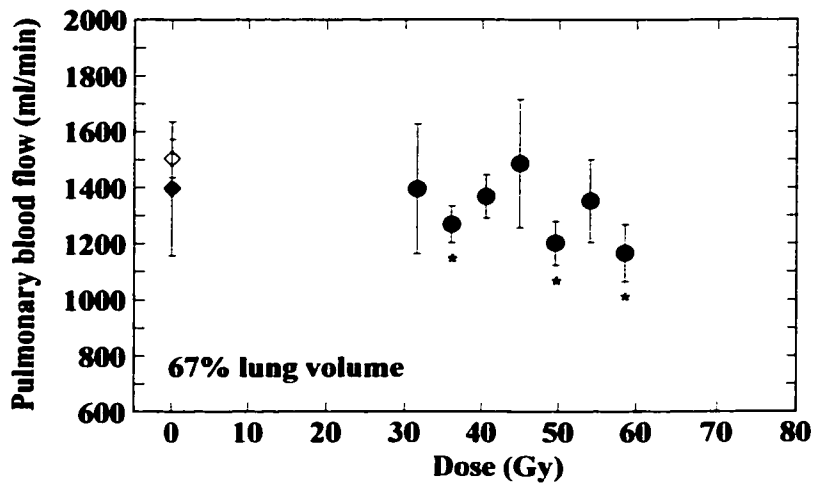

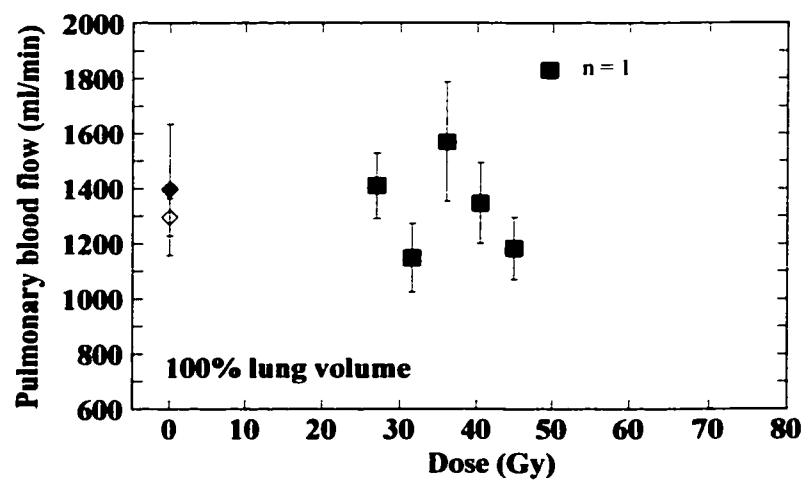

Table 20. Composite grade, radiographic changes three months after irradiation (number of dogs with respective grade/number of dogs evaluated)

	NO CHANGE OR MILD			MODERATE			SEVERE		
Dose (Gy)	**33%**	**67%**	**100%**	**33%**	**67%**	**100%**	**33%**	**67%**	**100%**
0.0			(5/5) nc			(0/5)			(0/5)
27.0			1/4 nc 2/4 mild			1/4			(0/4)
31.5	1/4 nc 3/4 mild	0/4 nc 4/4 mild	0/6 nc 4/6 mild	(0/4)	(0/4)	2/6	(0/4)	(0/4)	(0/6)
36.0	1/6 nc 5/6 mild	1/6 nc 4/6 mild	0/6 nc 4/6 mild	(0/6)	1/6	2/6	(0/6)	(0/6)	(0/6)
40.5	2/6 nc 4/6 mild	0/6 nc 6/6 mild	0/8 nc 2/8 mild	(0/6)	(0/6)	6/8	(0/6)	(0/6)	(0/8)
45.0	0/5 nc 4/5 mild	0/5 nc 2/5 mild	0/4 nc 1/4 mild	1/5	3/5	1/4	(0/5)	(0/5)	2/4
49.5	1/5 nc 4/5 mild	0/6 nc 3/6 mild	(0/1)	(0/5)	3/6	1/1	(0/5)	(0/6)	(0/1)
54.0	0/7 nc 5/7 mild	0/5 nc 1/5 mild	(0/1)	2/7	2/5	1/1	(0/7)	2/5	(0/1)
58.5	0/5 nc 3/5 mild	0/4		2/5	3/4		(0/5)	1/4	
63.0	0/4 nc 2/4 mild	(0/1)		2/4	(0/1)		(0/4)	1/1	
67.5	0/4 nc 2/4 mild			1/4			1/4		
72.0	0/3 nc 1/3 mild			1/3			1/3		

Dogs receiving 31.5 Gy had mild radiographic changes which appeared to be volume dependent. With further dose escalation there was a trend toward a dose-volume effect, showing a higher incidence of moderate and severe radiographic changes at higher doses and larger volumes.

The probability for moderate to severe radiographic lung changes three months after irradiation was significantly higher in the 67% and 100% lung volume groups than in the 33% group (Figure 20). Calculated ED_{50} and ED_5 values (95% CI) were 68.1 Gy (60.5-94.6 Gy) and 38.7 Gy (0-48.8 Gy) respectively for the 33% lung volume group, 47.3 Gy (42.8-52.4 Gy) and 34.6 Gy (15.2-40.1 Gy) respectively for the 67% lung volume group, and 36.4 Gy (28.8-43.7 Gy) and 19.6 Gy (0-27.8 Gy) respectively for the 100% lung volume group. Grading of thoracic radiographs three months after lung irradiation show a statistically significant dose-volume relationship with the greatest effect in the dogs irradiated to 100% of their lung volume.

The volume enhancement ratios (VER) comparing 33% and 67% lung volumes irradiated at the ED_{50} and ED_5 levels of effect for moderate to severe thoracic radiograph changes were 1.44 and 1.12, respectively. Comparing 67% and 100% lung volumes irradiated at the ED_{50} and ED_5 levels of effect for serotonin uptake (%) the VER were 1.30 and 1.77, respectively. Comparing 33% and 100% lung volumes irradiated at the ED_{50} and ED_5 levels of effect for serotonin uptake (%) the VER were 1.87 and 1.97, respectively.

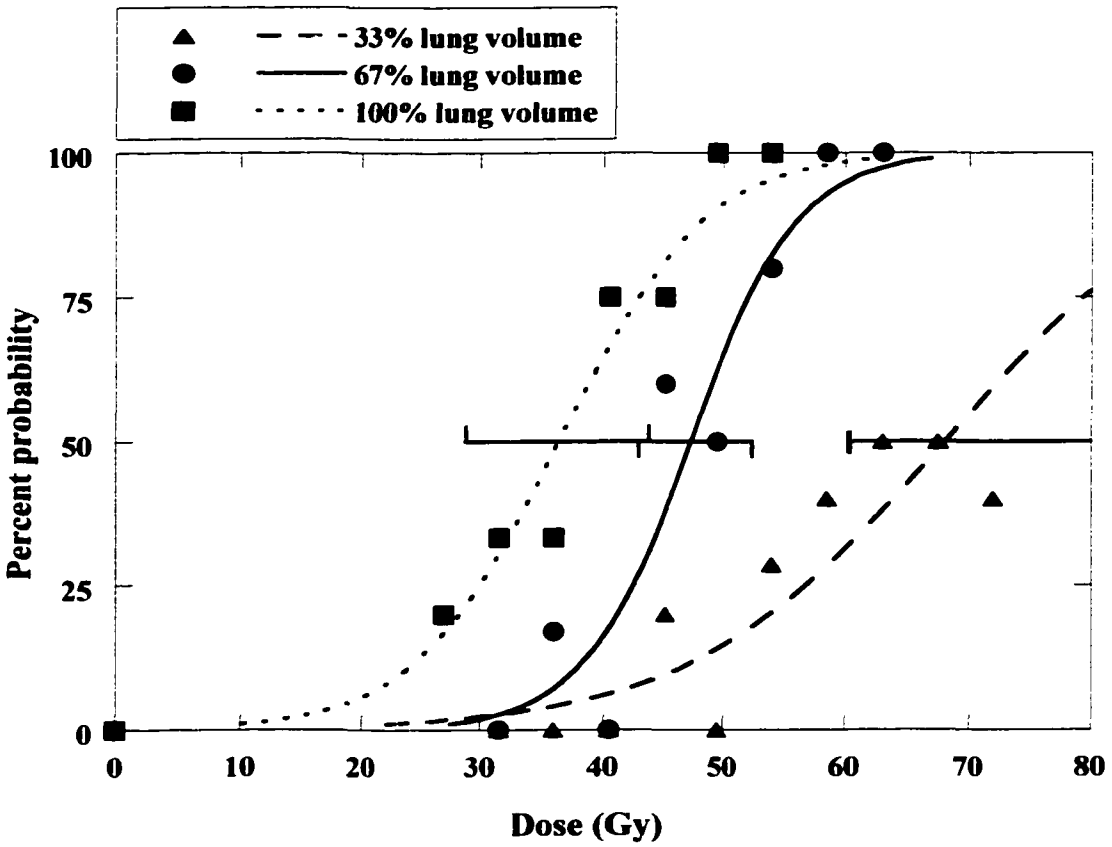

Figure 20. Dose-response curves for thoracic radiograph grades of moderate and severe three months after irradiation, based on logistic fit. The ED_{50} and ED_5 (95% CI) for the 33% irradiated lung volume group were 68.1 Gy (60.5-94.6 Gy) and 38.7 Gy (0-48.8 Gy) respectively (▲ data points), significantly different from the 67% and 100% lung volume groups. The ED_{50} and ED_5 (95% CI) for the 67% irradiated lung volume group were 47.3 Gy (42.8-52.4 Gy) and 34.6 Gy (15.2-40.1 Gy) respectively (● data points). The ED_{50} and ED_5 (95% CI) for the 100% irradiated lung volume group were 36.4 Gy (28.8-43.7 Gy) and 19.6 Gy (0-27.8 Gy) respectively (■ data points). Error bars represent 95% confidence intervals.

Perfusion SPECT Lung Imaging

The volume of perfused lung within the irradiation fields, as assessed by drawing regions of interest on pre-treatment SPECT studies based on portal film images, averaged 27% (0.02%, n=4) for the 33% lung volume group. The volume of perfused lung within the irradiation fields averaged 49% (0.01%, n=3) for the 67% lung volume group, based on perfusion SPECT data.

Histomorphometric Analysis

Qualitative changes

The 12 dogs that developed severe symptomatic pneumonitis had similar histopathologic changes within the irradiated portions of the lung fields. In most dogs there was a surprisingly sharp line of demarcation between the irradiated and non-irradiated portions of the lung lobes. The portion of lung outside the irradiated field was normal or had very minor alveolar edema. The portions of lung within the irradiated field had numerous abnormalities consistent with radiation pneumonitis. All dogs had some degree of alveolar edema, interstitial fibrosis, type II pneumocyte hyperplasia and hypertrophy, and increased numbers of alveolar macrophages. These changes were either diffuse and confluent or at times more multifocal and patchy in nature. In 6 of the 12 dogs the reaction tended to be more severe in peripheral, subpleural portions of the irradiated lung. Most dogs also had some fibrin exudate within airways and small focal accumulations of lymphocytes and plasma cells. No dogs had appreciable accumulations of neutrophils. Areas of squamous metaplasia alternating with epithelial hyperplasia

were present, affecting the epithelium of medium and large bronchioles and bronchi. The pleura within the radiation field was thickened with fibrous tissue and the pleural surface was covered by hypertrophied and hyperplastic mesothelial cells. Many small and large pulmonary arterioles and arteries had intimal proliferations of loose connective tissue and enlarged endothelial cells, sometimes resulting in near occlusion of the vessel lumen. Frequently the most severe changes in the pulmonary parenchyma were located around these affected vessels. Most vessels also had appreciable perivascular fibrosis of varying degrees.

Dogs Killed Humanely Due to Development of Severe Symptomatic Pneumonitis

Using image analysis, the percentage of air space within irradiated portions of the lung ranged from 10.88 to 27.65% (Table 21). There was no detectable difference in the percentage of air space related to either dose, volume, or latency of severe symptomatic pneumonitis. There was no difference detectable in the lung lobes involved, as the lobe with the lowest percentage of air space was the cranial lobes five times, the middle lobes one time, the caudal lobes four times and the accessory lobe two times. Alternatively, the lobe with the highest percentage of air space was the cranial lobes two times, the middle lobes three times, the caudal lobes four times and the accessory lobe two times (Table 21).

Using point count techniques the percentage of air space ranged from 7.60 to 21.81% (Table 21). There was no detectable difference in the percentage of air space related to either dose, volume, or latency of severe symptomatic pneumonitis. There was

Table 21. Histomorphometry: Dogs humanely killed due to development of severe symptomatic pneumonitis

Dose (Gy)	Lung Volume Irradiated	Survival Time (wks)	% Air Space		Avg % Edema	Avg% Fibrin	Avg % Type II Cells	Avg % Macro-phages	Avg % Fibrosis
			Point Count	Image Analysis					
49.5	67	15	10.47	20.04	12.75	0.77	10.52	3.69	59.38
54	67	14	11.48	19.63	11.15	2.12	13.79	4.42	55.81
58.5	67	12	16.95	14.54	2.20	19.49	13.41	5.65	40.42
58.5	67	15	8.13	10.88	21.45	5.58	9.79	5.14	48.97
58.5	67	17	7.60	14.37	15.54	0.38	10.29	3.08	55.03
63	67	11	13.54	22.40	5.33	1.23	10.19	5.61	61.46
40.5	100	7	10.67	19.04	12.41	2.02	26.84	7.83	38.98
45	100	8	13.51	17.64	18.79	0.10	18.22	11.75	36.54
45	100	9	17.73	14.64	2.26	10.39	9.56	9.42	47.69
45	100	9	11.31	13.18	0.24	16.80	15.03	3.28	51.37
49.5	100	9	17.40	21.39	13.07	1.16	18.84	5.77	41.49
54	100	9	21.81	27.65	0.44	0.24	8.91	6.67	55.60

no difference detectable in the lung lobes involved as the lobe with the lowest percentage of air space was the cranial lobes nine times and the caudal lobes three times. Alternatively the lobe with the highest percentage of air space was the cranial lobes six times and the caudal lobes six times (Table 21). The percentage of edema ranged from 0.24 to 21.45% and the percentage of fibrin exudate ranged from 0.10 to 19.49% (Table 21). There was no detectable difference in the percentage of edema or fibrin related to either dose, volume, or latency of severe symptomatic pneumonitis. The percentage of type II cells ranged from 8.91 to 26.84% and the percentage of alveolar macrophages ranged from 3.08 to 11.75 % (Table 21). There was no detectable difference in the percentage of alveolar macrophages or type II cells with relation to dose or volume. The percentage of these cell types were more numerous in dogs examined at 9 weeks or less after irradiation compared to those examined at 11 weeks or greater after irradiation, but the differences were not statistically significant. For dogs examined at 9 weeks or less after irradiation, the mean percentage of type II cells was 16.23% compared to 11.33% in dogs examined at 11 weeks or greater after irradiation ($p \leq 0.14$). Similarly, for dogs examined at 9 weeks or less after irradiation, the mean percentage of macrophages was 7.45% compared to 4.60% in dogs examined at 11 weeks or greater after irradiation ($p \leq 0.06$). The percentage of interstitial fibrosis ranged from 36.54 to 61.46% (Table 21). There was no detectable difference in the percentage of interstitial fibrosis with relation to dose or volume. The percentage of fibrosis was less in dogs examined at 9 weeks or less after irradiation compared to those examined at 11 weeks or greater after irradiation,

but the difference was not statistically significant. For dogs examined at 9 weeks or less after irradiation, the mean percentage of interstitial fibrosis was 45.28% compared to 53.51% in dogs examined at 11 weeks or greater after irradiation ($p \leq 0.09$). None of the differences between the dogs examined at 9 weeks or less after irradiation and the dogs examined at 11 weeks or greater after irradiation were significantly different at the $p \leq 0.05$ level.

Dogs Killed Humanely Due to Causes Other Than Pneumonitis

Using image analysis, the percentage of air space within irradiated portions of the lung ranged from 24.15 to 73.42% (Table 22). There was no detectable difference in the percentage of air space related to either dose or volume or time from irradiation to death. There was no difference detectable in the lung lobes involved as the lobe with the lowest percentage of air space was the cranial lobes seven times, the caudal lobes seven times and the accessory lobe one time. Alternatively the lobe with the highest percentage of air space was the cranial lobes four times, the middle lobes three times, the caudal lobes three times and the accessory lobe five times (Table 22).

Using point count techniques the percentage of air space ranged from 9.70 to 56.51% (Table 22). There was no detectable difference in the percentage of air space related to either dose or volume or time from irradiation to death. The cranial lung lobes appeared to be less severely affected, as the lobe with the lowest percentage of air space was the cranial lobes four times and the caudal lobes eleven times. Alternatively the lobe with the highest percentage of air space was the cranial lobes eleven times and the

Table 22. Histomorphometry: Dogs humanely killed due to causes other than pneumonitis

Dose (Gy)	Lung Volume Irradiated	Surv. Time (wks)	% Air Space		Avg % Edema	Avg% Fibrin	Avg % Type II Cells	Avg % Macro-phages	Avg % Fibrosis	Cause
			Point Count	Image Analysis						
45	33	5	55.32	73.42	0	0	10.25	2.79	6.11	chylothorax
54	33	9	42.84	31.52	0.67	7.30	9.70	3.65	23.87	liver complications
54	33	32	9.70	24.15	9.70	0	13.73	2.50	69.85	died, undetermined
63	33	1	43.24	46.31	0	3.05	15.02	7.37	9.34	esophagitis
72	33	2	56.51	57.79	0.53	0	8.70	2.82	3.55	esophagitis
72	33	3	37.76	29.35	0.64	0	18.69	7.85	16.23	esophagitis
72	33	13	13.94	28.14	30.11	0.15	6.99	4.12	33.98	heart complications
49.5	67	57	25.60	53.87	0.05	0	6.33	0.77	63.09	meningitis
54	67	73	27.01	34.87	1.01	0	5.49	3.56	58.02	chylothx, fibrosis
36	100	87	24.34	32.78	13.23	0	12.10	2.65	40.08	pneumothorax
40.5	100	58	30.07	31.39	0.05	0	10.06	2.75	52.93	pneumothorax
40.5	100	25	25.21	28.27	0	19.10	11.20	4.60	30.93	pulm. hypertension
40.5	100	11	39.26	51.20	0	0	16.01	3.84	28.09	pulm. hypertension.
45	100	13	22.79	31.19	2.68	0	25.04	4.69	40.69	pulm. hypertension
49.5	100	4	50.68	45.77	5.51	0	1.50	0.68	15.85	liver complications

caudal lobes four times (Table 22). The percentage of edema ranged from 0.0 to 30.11% and the percentage of fibrin exudate ranged from 0.0 to 19.10%. There was no detectable difference in the percentage of edema or fibrin related to either dose or volume or time from irradiation to death. The percentage of type II cells ranged from 1.50 to 25.04% and the percentage of alveolar macrophages ranged from 0.68 to 7.85% (Table 22). There was no detectable difference in the percentage of alveolar macrophages or type II cells with relation to dose or volume, or time from irradiation to death. The percentage of interstitial fibrosis ranged from 6.11 to 69.85% (Table 22). There was no detectable difference in the percentage of interstitial fibrosis with relation to dose or volume. However the percentage of fibrosis was less in dogs examined at 9 weeks or less after irradiation compared to those examined at 11 weeks or greater after irradiation. For dogs examined at 9 weeks or less after irradiation, the mean percentage of interstitial fibrosis was 12.49% compared to 46.41% in dogs examined at 11 weeks or greater after irradiation ($p \leq 0.00008$).

Sham Irradiated Dogs

Using image analysis, the percentage of air space within irradiated portions of the lung ranged from 74.38 to 79.90% (Table 23). Using point count techniques the percentage of air space ranged from 65.26 to 70.25%. The percentage of edema was 0.0% and the percentage of fibrin exudate was 0.0%. The percentage of type II cells ranged from 0.20 to 0.35% and the percentage of alveolar macrophages ranged from 0.10 to 0.25%. The percentage of interstitial fibrosis ranged from 0.40 to 0.69% (Table 23).

Table 23. Histomorphometry: Sham-irradiated controls, 104 weeks after irradiation

Dose (Gy)	Lung Volume Irradiated	Survival Time (wks)	% Air Space		Avg % Edema	Avg% Fibrin	Avg % Type II Cells	Avg % Macro-phages	Avg % Fibrosis
			Point Count	Image Analysis					
0	—	104	70.25	79.90	0	0	0.35	0.20	0.40
0	—	104	68.83	74.38	0	0	0.20	0.10	0.69
0	—	104	65.26	78.16	0	0	0.25	0.25	0.55

Summary of Histomorphometric Results

In both the pneumonitis and non-pneumonitis groups the percentage of air space within irradiated portions of the lung was significantly lower than in the sham-irradiated control group by both point count and image analysis ($p \leq 0.000001$) (Figure 21A). The percentage of air space within irradiated portions of the lung was significantly lower in the pneumonitis group than in the non-pneumonitis group by both point count and imag analysis ($p \leq 0.0001$) (Figure 21A). The average percentage of fibrosis in both groups was significantly greater than in the sham-irradiated control group ($p \leq 0.0001$) (Figure 21B). The average percentage of fibrosis in the pneumonitis group was significantly greater than in the non-pneumonitis group ($p \leq 0.02$) (Figure 21B).

The average percentage of type II cells in both the pneumonitis and the non-pneumonitis groups was significantly greater than in the sham-irradiated controls ($p \leq 0.00001$), but not significantly different from each other (pneumonitis compared with non-pneumonitis) ($p \leq 0.27$) (Figure 22A). The average percentage of alveolar macrophages in both the pneumonitis and the non-pneumonitis groups was significantly greater than in the sham-irradiated controls ($p \leq 0.00001$). The average percentage of alveolar macrophages in the pneumonitis group was significantly greater than in the non-pneumonitis group ($p \leq 0.02$) (Figure 22A).

The average percentages of edema and fibrin in the pneumonitis group were significantly greater than the sham-irradiated controls (edema, $p \leq 0.001$; fibrin, $p \leq 0.03$) (Figure 22B). The average percentages of edema and fibrin in the non-pneumonitis

Figure 21. Histomorphometrically measured percentage of air space (A. Point count method, cross-hatched bar; image analysis method, solid bar) and average percentage of fibrosis (B.) in dogs humanely killed from 1 to 87 weeks post-irradiation due to development of severe symptomatic pneumonitis or causes other than pneumonitis (non-pneumonitis). Sham-irradiated controls were evaluated 104 weeks post sham-irradiation. Asterisks indicate points significantly different from the sham-irradiated controls and each other (pneumonitis vs. non-pneumonitis), ($p \leq 0.05$). Error bars represent standard error of the mean.

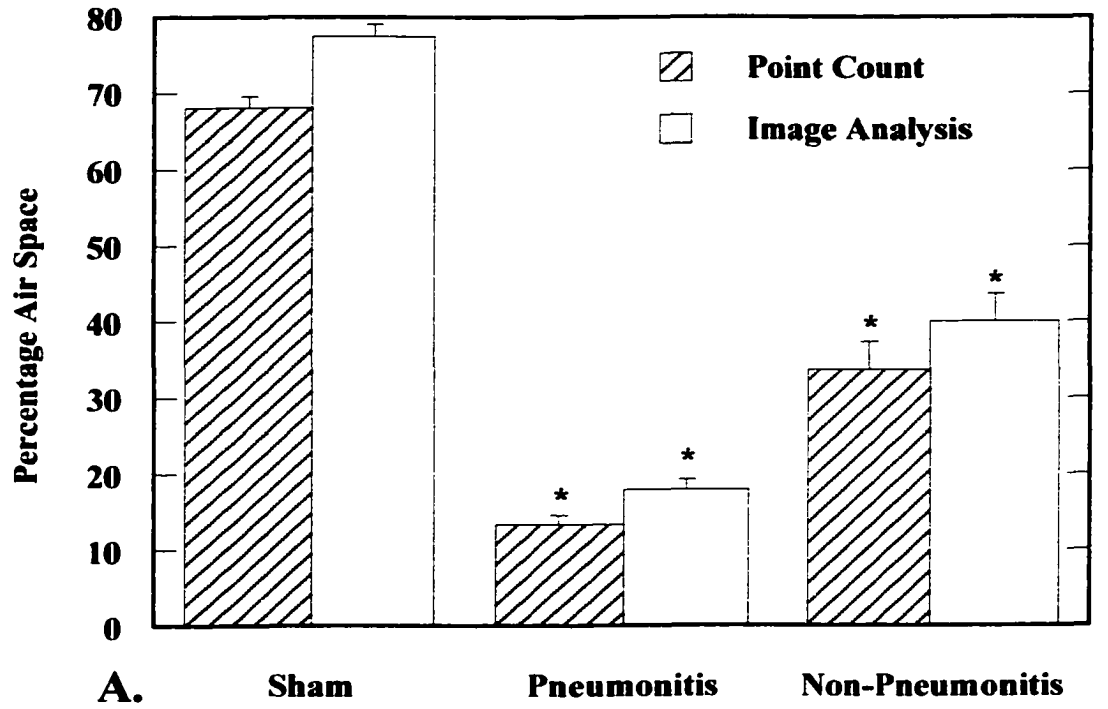

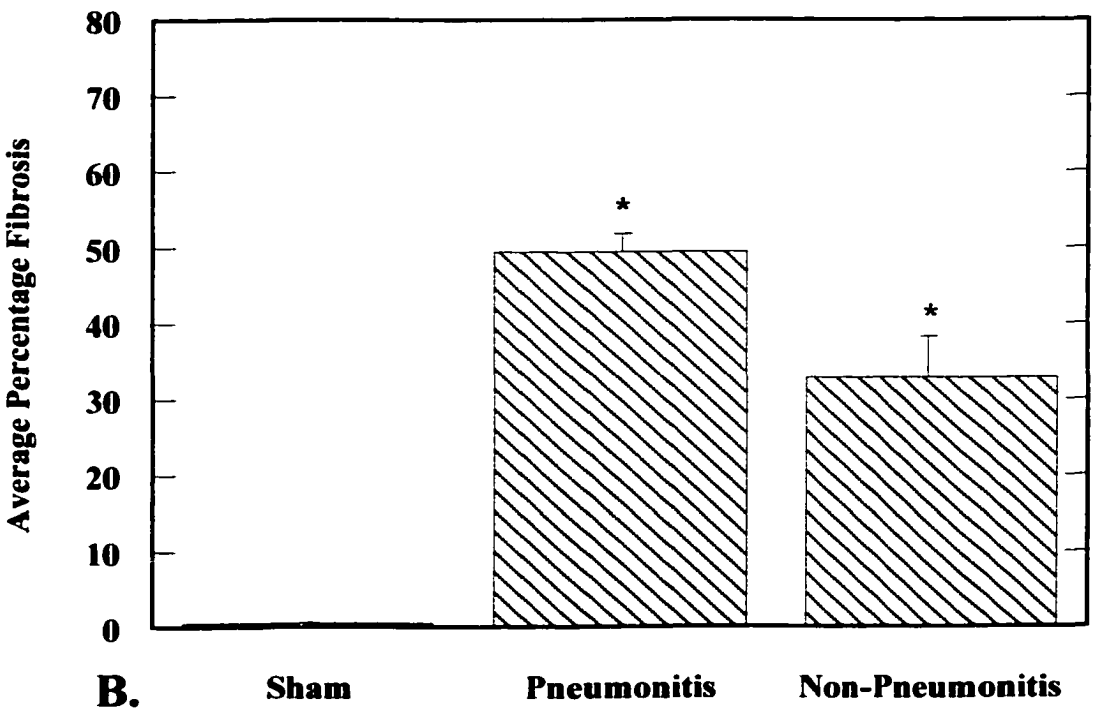

Figure 22. Histomorphometrically measured average percentages of Type II cells (A. solid bar), macrophages (A. cross-hatched bar), edema (B. dotted bar) and fibrin (B. dark bar) in dogs humanely killed from 1 to 87 weeks post-irradiation due to development of severe symptomatic pneumonitis or causes other than pneumonitis (non-pneumonitis). Sham-irradiated controls were evaluated 104 weeks post sham-irradiation. Asterisks indicate points significantly different from the sham-irradiated controls and each other (pneumonitis vs. non-pneumonitis), ($p \leq 0.05$). Error bars represent standard error of the mean.

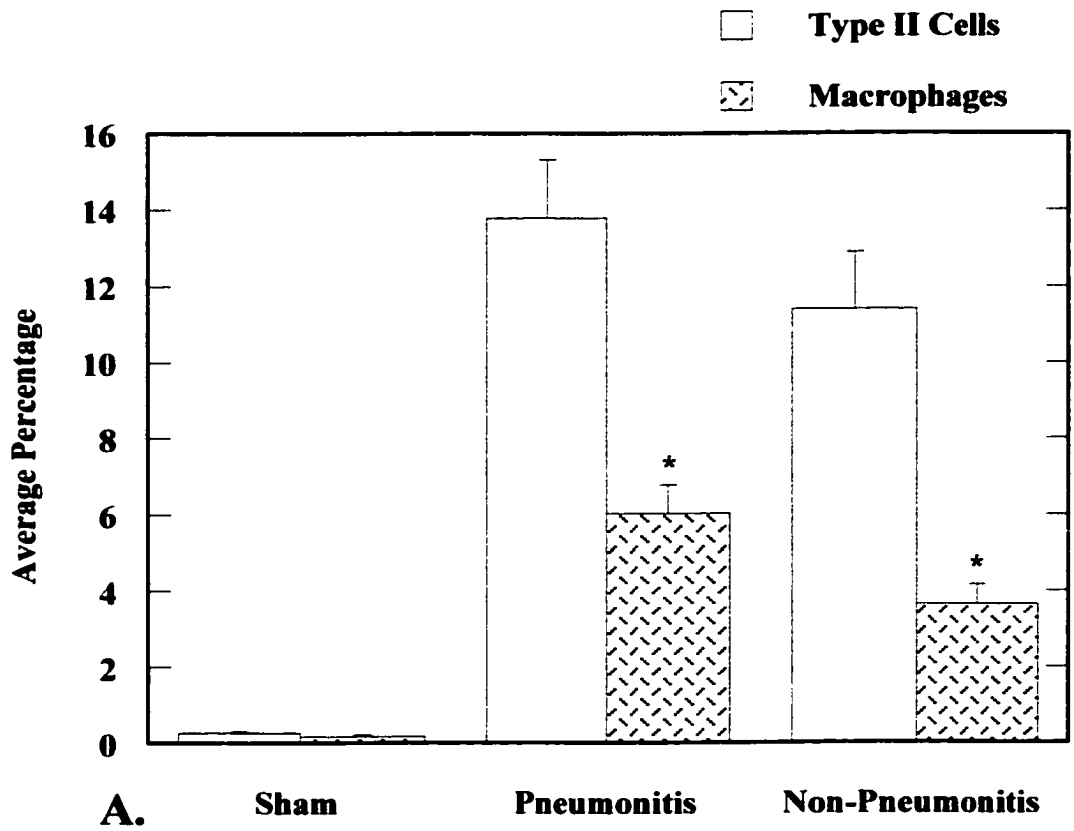

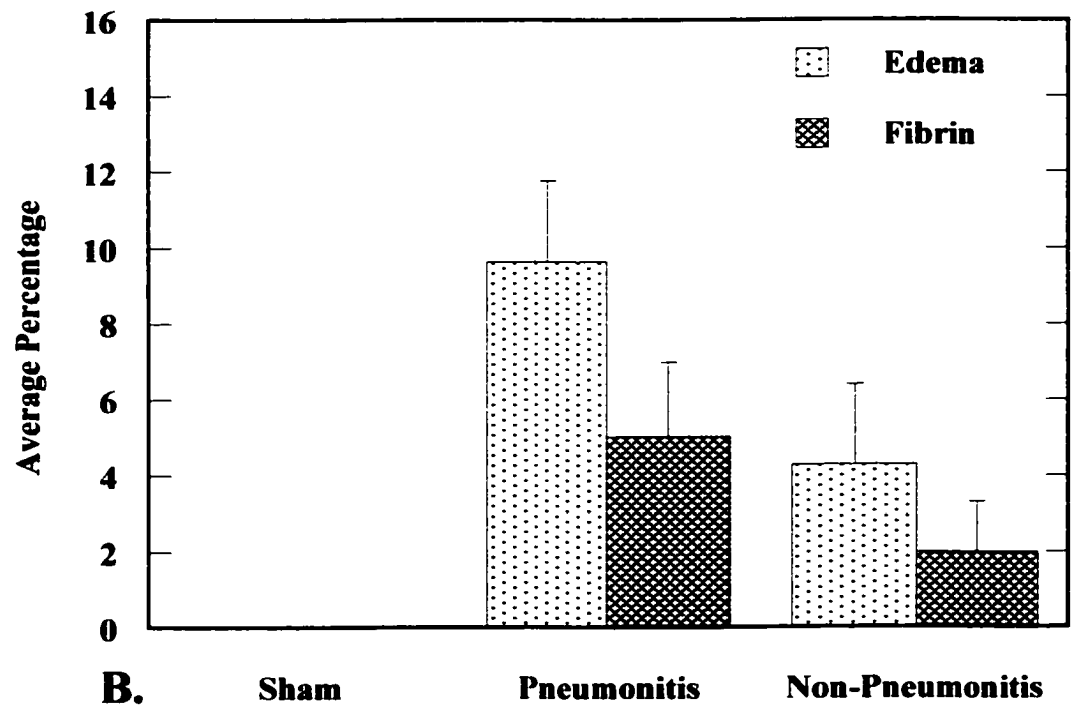

group were not significantly different from the sham-irradiated controls or the pneumonitis group (Figure 22B).

DISCUSSION

The objective of the present study was to evaluate volume and tolerance-dose relationships for lung in normal beagle dogs. Evaluation of the influence of volume on functional capacity of the lung is of clinical importance. Radiation therapy plays an important and ever-increasing role in the treatment of lung cancer, breast cancer, Hodgkin's disease and other malignancies involving the thorax. Lung volume irradiated is the most important limiting factor when planning radiation treatment of structures in the chest, but the maximum allowable volume has not been adequately quantified. The guidelines presently in use are based on clinical experience in the absence of quantitative data. This study clearly demonstrates that in the application of thoracic radiotherapy, lung is one of the most critical volume-limiting normal tissues. Although lung is often classified as a late responding tissue, early effects of lung irradiation are of extreme importance. Severe radiation pneumonitis during the first six months after irradiation may be life threatening. In patients who survive this pneumonitis phase, the type and severity of the early radiation response may have bearing on the type and severity of the ensuing late response. The influence of volume on radiation tolerance of the lung is not well understood. The dog was used as a model in these experiments to allow a meaningful range of volumes to be used. Large animal studies allow the use of clinically relevant physiologic studies similar to those used clinically in humans. Extrapolation of

dose-volume tolerances from animals to humans must be done cautiously and carefully, but the relative changes in effect are likely to be the same for dogs and humans. The radiation response of canine lung appears to be very similar to that of human lung, so guidelines can be provided by these animal studies.

Morbidity related to pneumonitis was increased with increasing volume of lung irradiated (Table 4). However, other measures of pulmonary function and morbidity did not uniformly demonstrate a volume effect. The dose-volume relationship for lung appears to depend on the endpoint used to assess lung injury. Severe symptomatic pneumonitis (Figure 2), serotonin uptake (Figures 15, 16) and thoracic radiograph changes (Figure 20) proved to be the most informative volume effect endpoints evaluated in this study. A number of the other studies, covering a panel of endpoints related to lung pathophysiology and overall lung function, showed marked changes at the highest doses in the 67% and 100% lung volume groups. However, at the lower doses in all three volume groups the changes were not significant, likely due to the enormous capacity of the nonirradiated lung to compensate for loss of function in the irradiated volume.

Overall Survival

When three different lung volumes were irradiated to total doses ranging from 27 to 72 Gy, the overall severe morbidity rate during the first six months after irradiation was approximately 20%. Only 9% of all dogs in this study had to be humanely killed due to causes other than severe symptomatic radiation pneumonitis (Table 2). This clearly

demonstrates that pulmonary tissue is one of the most critical limiting normal tissues involved in thoracic radiotherapy.

Three Month Follow-Up Studies

Three months was chosen as the first follow up time point because we felt this would be in the window of the pneumonitis phase of lung injury. However, the first signs of early lung injury are seen almost immediately after irradiation, and may persist as long as 8 months after irradiation [58]. Six dogs were not evaluated for changes lung mechanics, hemodynamics, or indicator dilution assays before they were humanely killed due to the development of severe symptomatic pneumonitis prior to 3 months post-irradiation. Eight of eleven dogs humanely killed due to other causes were euthanatized prior to 3 months post-irradiation and were not evaluated for changes in lung mechanics, hemodynamics, or indicator dilution assays post-irradiation (Table 3). These were dogs that would likely have been responders for many of the pulmonary endpoints evaluated; especially the dogs euthanatized due to severe lung toxicity. We clearly missed evaluating 14 dogs that would have added important information to the high dose, large volume end of the dose-response curves. By the same token, it is likely that not all dogs that were evaluated were evaluated at the peak of their response. Based on the latency of morbidity related to pneumonitis during the first 6 months after irradiation (Table 4) it would have been ideal to have evaluated the physiological endpoints at 2 months, 3 months and 4 months. Unfortunately, resources were not unlimited and we chose the timepoint in the middle of this range, hoping to measure the changes as near the peak of

the response as possible. Considering this deficit in the high dose, large volume end of the dose response curves, the volumes effects we did observe are that much more appreciable.

Severe Symptomatic Pneumonitis

Severe pneumonitis appeared to be a valuable and clinically relevant endpoint of pulmonary toxicity. Based on the endpoint of severe symptomatic pneumonitis results, it was possible to calculate 50% and 5% effective doses (ED_{50} and ED_5) for dogs irradiated to 67 and 100% of their total lung volume (Figure 15). In the 33% volume group no pneumonitis-related morbidity was observed, showing the clinical importance of the volume effect on the overall lung response after thoracic irradiation.

Earlier studies in mice and rats have primarily used lethality (LD_{50}) as an endpoint of radiation-induced lung injury. Most of these earlier studies used whole lung, single dose [61, 171] or a few large doses of fractionated irradiation [175, 179, 180]. These results are difficult to extrapolate to the clinic. Furthermore, the LD_{50} endpoints in these studies were hampered by the development of pleural effusion, resulting in early deaths prior to the development of significant lung damage. Although respiratory failure due to pneumonitis was frequently used as the endpoint in rodents to measure different aspects of lung irradiation, only the recent study in mice, by Liao *et al.* [87], used respiratory mortality together with respiratory rate to assess the dose-volume relationships after irradiation. Eight fractional volumes ranging from 100% to 17% of both lungs combined were irradiated with single doses ranging from 12 to 20 Gy,

depending on the volume irradiated. In that study, the calculated LD_{50} for the whole lung was 12.6 Gy. The LD_{50} after irradiation of 70% of total lung volume including the base region was 15.5 Gy. The LD_{50} after irradiation of 75% of the apex region was not reached. This suggests a difference in radiation sensitivity between the base and apex regions of the lung. In the present study, the ED_{50} values were significantly higher than the LD_{50} values reported by Liao, *et al.* [87]. These differences can be accounted for by the difference in fractionation between the two studies. Species differences and differences in the size and shape of the radiation field may also have been factors. The present study used mediastinal fields of increasing width to encompass the prescribed volume. The group studying mice used changes in cranial and caudal positioning and length of the fields [87].

Increased breathing rates as a measure of functional lung damage were evaluated in pigs irradiated to 25% (lower half of right lung) or 50% (whole right lung) of their total lung volume [66]. ED_{50} values for increased breathing frequency with 25% or 50% irradiated lung volume were > 31 Gy and 26.8 Gy respectively. Doses ranged from 14.3 Gy to 38.0 Gy and were given in 5 equal fractions.

$TD_{5/5}$ (the probability of 5% complication within five years from treatment) and $TD_{50/5}$ (the probability of 50% complication within five years from treatment) values for the development of radiation-induced pneumonitis have been estimated based on information from human patients treated with 1.8 to 2.0 Gy per day, 5 days per week, and clinical observations [45]. The estimated $TD_{5/5}$ values for clinical pneumonitis in that

work were 45 Gy, 30 Gy and 17.5 Gy for 33, 67 and 100% irradiated volumes, respectively. The estimated $TD_{50/5}$ values were 65 Gy, 40 Gy and 24.5 Gy for 33, 67 and 100% irradiated volumes, respectively. Our ED_5 and ED_{50} values for severe symptomatic pneumonitis are markedly higher than these estimates. While the fractionation schemes were similar, the endpoints are not equivalent so the doses cannot be compared directly. The pneumonitis endpoint in the dogs was severe enough to require humane killing of the animals, although with intensive therapy and supportive care some of the animals may have survived. Still, there were no cases of severe symptomatic pneumonitis in the dogs with 33% of their lung volume irradiated to total doses of up to 72 Gy, suggesting that the Emami *et al.* [45] estimates may be low.

Several normal tissue complication probability (NTCP) models have used Emami's dose estimates to correlate calculated NTCP value to observed incidence of radiation pneumonitis. Comparisons of calculated NTCP values with the observed incidence of radiation pneumonitis suggest that there may be a correlation [4, 54, 109, 126]. However, more biological data are needed to validate these models. Kwa, *et al.* [81] found that the mean lung dose, NTD_{mean}, was a useful predictor of the risk of radiation pneumonitis. Lung may not fit the general volume effect model of Schultheiss, *et al.* [155] because morbidity may increase due to the same effect in a larger volume of tissue. Volume models incorporating organ-specific biological parameters likely must be developed for lung, spinal cord, skin, kidney, and other organs of interest.

Arterial Blood Gases

There was a trend toward decreased arterial oxygen tension at the higher doses in all three lung volume groups while the dogs were anesthetized and breathing 100% oxygen (Table 6, Figure 5) and while they were awake and breathing room air (Table 5, Figure 4). The large standard error resulted in p values greater than 0.05 in all but the highest dose groups. The four primary causes of a reduced PO_2 in arterial blood are hypoventilation, diffusion impairment, shunt, and ventilation-perfusion inequality.

Hypoxemia due to hypoventilation is easily eliminated by increasing the inspired PO_2. Although anesthetized animals may still be underventilated, the inspired PO_2, and correspondingly the arterial PO_2, are increased by several hundred mm Hg during the administration of 100% oxygen. Another hallmark feature of hypoventilation is that it always causes a rise in PCO_2. A PCO_2 value of around 40 mm Hg is normal. The mean $PaCO_2$ in the dogs while awake and breathing room air was 35 mm Hg both prior to and three months after treatment. This is in the normal range, so the hypoxemia seen in the dogs while breathing room air was not likely due to hypoventilation. The mean $PaCO_2$ in the dogs while anesthetized and breathing 100% oxygen was 49 mm Hg both prior to and three months after treatment. This suggests that the dogs were, on average, mildly underventilated while they were anesthetized. However, since they were breathing 100% oxygen, hypoxemia due purely to hypoventilation was eliminated.

Diffusion through tissues is described by Fick's law, which states that the rate of transfer of a gas through a sheet of tissue is proportional to the tissue area and the

difference in gas partial pressure between the two sides, and inversely proportional to the tissue thickness [191]. Diffusion impairment results when equilibration does not occur between the PO_2 in the pulmonary capillary blood and alveolar gas. The normal lung has a great reserve capacity for equilibration time. Even during strenuous exercise, equilibration normally occurs. When the blood-gas barrier is thickened, diffusion may be so slowed that equilibration is incomplete. Since diffusion in the lung is also a function of the total area available for gas exchange, diffusion is likely a function of lung volume and might be expected to show a volume effect. Alveolar edema and interstitial fibrosis are two situations in which diffusion impairment may contribute to hypoxemia. Both alveolar edema and diffuse interstitial fibrosis were observed histologically in the dogs in this study that were euthanatized due to lung toxicity. Hypoxemia caused by diffusion impairment is corrected with the administration of supplemental oxygen. The increased diffusion resistance of the thickened alveolar membrane is readily overcome by the large increase in alveolar PO_2 of several hundred mm Hg. Hence, hypoxemia caused by diffusion impairment would be clinically evident in dogs breathing room air, but would be eliminated in anesthetized dogs breathing 100% oxygen.

A shunt occurs when some blood reaches the arterial system without passing through ventilated regions of the lung. A large, completely unventilated but perfused area of lung constitutes an intrapulmonary shunt. The mixture of shunted blood with equilibrated arterial blood results in decreased oxygen content. True pulmonary shunt is completely unresponsive to supplemental oxygen. The $PaCO_2$ is not increased as a result

of a shunt. Arterial PCO_2 may even be below normal due to hypoxemic stimulation of ventilation. If pulmonary shut were the major mechanism of hypoxemia in these dogs, no response to supplemental oxygen administration would be expected.

When ventilation and blood flow are mismatched in various regions of the lung (ventilation-perfusion inequality) all gas transfer becomes inefficient. This is the most common mechanism of hypoxemia. The decreased arterial oxygen tension seen in chronic obstructive pulmonary disease, interstitial pulmonary fibrosis and pulmonary embolism is for the most part attributable to this mechanism. Ventilation-perfusion inequality is usually distinguished from hypoventilation, diffusion impairment and shunt by ruling out these other causes of hypoxemia. Shunt may be described as one extreme end of the ventilation-perfusion inequality spectrum, but the characteristic pattern of gas exchange of shunt is unique (limited increase in PaO_2, no increase in $PaCO_2$). Transfer of all gases is inefficient in ventilation-perfusion inequality, and CO_2 retention may result in elevated $PaCO_2$. Ventilation-perfusion inequality is responsive to supplemental oxygen. The magnitude of the response to supplemental oxygen depends on the magnitude of the ventilation-perfusion inequality.

In most cases, hypoxemia is caused by a mixture of mechanisms, often impossible to single out and define. The administration of pure oxygen results in the correction of hypoxemia due to hypoventilation and diffusion impairment. Remaining decreases in arterial oxygen tension are the result of shunt or ventilation-perfusion mismatch, or both. The trend toward decreased arterial oxygen tension values at the higher doses in all three

lung volume groups while the dogs were awake and breathing room air (Table 5, Figure 4) persisted when measured while the dogs were anesthetized and breathing 100% oxygen (Table 6, Figure 5), but the hypoxemia was completely eliminated with the administration of supplemental oxygen. The fact that the PaO_2 was >400 mmHg while breathing 100% oxygen virtually eliminates shunt as a major mechanism of hypoxemia in these dogs. This suggests that the lung that was lost was no longer being ventilated or perfused. The most likely mechanism of hypoxemia in these dogs was diffusion impairment due to loss of total area of lung available for diffusion. This is a predictable volume effect.

Lung Mechanics

Tidal volume was significantly decreased at the higher doses in the 67% irradiated lung volume group and throughout the range of doses in the 100% irradiated lung volume group (Table 8, Figure 7). Tidal volume is passively measured during normal breathing, in this study while the dogs were anesthetized. When airways become obstructed or collapse, less of the lung is ventilated and the tidal volume is decreased. Dynamic compliance was significantly decreased at the higher doses in both the 67% and 100% irradiated lung volume groups (Table 9, Figure 8). Alveolar edema decreases compliance by preventing the inflation of some alveoli. Interstitial fibrosis of the lung also causes decreased compliance. There was no significant change in functional residual capacity in any of the lung volume groups (Table 7, Figure 6). Lung mechanics in dogs are necessarily passive studies and are not as sensitive to changes in pulmonary function as

active tests done in humans. Human studies are very dynamic in that the subjects are not anesthetized and actively participate in the study. Human subjects are asked to breathe deeply, exhale forcibly and hold their breath at various times during the evaluation of their pulmonary function. In the present studies, we evaluated tidal breathing in anesthetized dogs and saw decreases in tidal volume and dynamic compliance. It is possible that the functional residual capacity studies done in anesthetized dogs may not be dynamic enough to demonstrate a conclusive dose-volume effect. A more marked effect might be expected using these endpoints to evaluate pulmonary function two years after irradiation, when the pulmonary changes would be expected to be characteristic of late radiation changes, primarily fibrosis. The animals may be less able to compensate for these later changes in function, allowing the changes to be more easily discerned. Evaluation of the two-year data is beyond the scope of this dissertation and will be presented elsewhere.

Hemodynamics

There were marked elevations in right ventricular systolic pressures (Table 10, Figure 9) and mean pulmonary artery pressures at the higher doses in the 100% irradiated lung volume group (Table 11, Figure 10). However, few animals survived to be evaluated in this group, and the differences were not significant. There were no significant changes in pulmonary artery wedge pressures 3 months after irradiation (Table 12, Figure 11). Trends toward decreased cardiac output (Table 13, Figure 12) and decreased systemic mean arterial blood pressure (Table 14, Figure 13) were noted in all three lung volume groups, but the differences between the groups were not significant.

The hemodynamic endpoints showed clear cut changes only at the highest doses in the 67% and 100% lung volume groups, where there were several dogs missing because they were humanely killed early due to severe lung morbidity. This suggests a threshold for the ability to compensate for lung injury affecting these endpoints. Below this threshold the animals are able to function without measurable changes in hemodynamic function. Above the threshold, the capacity of the lung to compensate for decreases in function is exceeded and the degree of functional decrease is fatal. These endpoints may not be sensitive enough to detect volume effects in these dogs. The differences may be there, but are undetected. It is also possible that these endpoints are not volume dependent. The mediastinum was included in the radiation field of each dog, and some changes may be related to effects on the large vessels and airways located in the hilar region, resulting in changes downstream in the lung regardless of the volume irradiated.

Indicator Dilution Assays

The pulmonary vascular endothelium, a metabolically active tissue, acts as a target site for many types of lung injury, including radiation [148]. Normally, seventy to ninety percent of injected serotonin has been shown to be removed in one passage through the pulmonary circulation by pulmonary endothelial cells [192]. Removal of serotonin from the circulation represents one of the metabolic functions of the pulmonary endothelial cells that is reduced early during the course of lung injury [31, 64].

Experimental evidence from this study, as well as others [10, 24, 31, 35, 36, 49, 101], shows that measurement of serotonin uptake using an indicator dilution assay appears to be a more sensitive, volume-dependent measure of acute radiation-induced lung injury than more conventional diagnostic tests such as radiographs, pulmonary

function tests, and arterial blood gases. There was clearly a volume effect for decreased serotonin uptake at the ED_{50} level (Figure 15). When the serotonin uptake was corrected for blood flow (permeability surface area) there was a dose related decrease in all three volume groups, significant in the 33% and 67% lung volume groups (Table 16, Figure 16). The dose-response curve (serotonin uptake %, Figure 15) for the 33% lung volume group may be artificially shifted to the left at the lower doses, owing to a lack of data at doses higher than 72 Gy (the maximum in our range of doses). The ED_5 values for the 33% and 67% volume groups were not significantly different (41.7 Gy and 38.2 Gy respectively), while the ED_{50} values were well separated (73.5 Gy and 49.9 Gy respectively). This is consistent with the probability model [155], a commonly used model for volume effects in tissues. A characteristic of this model is that the slope of the dose-response curve decreases with decreasing volume of irradiated tissue. This decreasing slope makes it difficult to detect differences at low probability levels, even though a volume effect may exist at high probabilities if injury. There is a significant volume effect for serotonin uptake at the 50% level of probability of injury, but this volume effect is undetectable at the ED_5 level of probability typical of treatment regimens used in the clinic [134]. This should be considered when making comparisons using the ED_5 for serotonin uptake, or in any clinical situation in which the ED_5/TD_5 is the basis for treatment planning and decisions.

Decreased serotonin uptake by the pulmonary endothelium can lead to increased concentrations of serotonin in the pulmonary vasculature. Serotonin is a potent

vasoconstrictor. Alterations in metabolism of vasoactive amines resulting in prolonged circulation times may contribute to the pathogenesis of radiation-induced, non volume-dependent pulmonary injury and pulmonary hypertension. Endothelial cell injury may result in an inflammatory reaction leading to the activation of a cytokine cascade, including activation of transforming growth factor β (TGFβ) leading to subsequent fibrosis [148].

Based on the results of this study, serotonin uptake is a method that may allow clinicians to identify pulmonary endothelial cell damage earlier and perhaps more sensitively than by more conventional diagnostic tests such as radiographs, pulmonary function tests, and arterial blood gases. Measurement of serotonin uptake may be a way to evaluate radiation injury clinically during the course of radiation therapy to identify patients who may be at risk for serious side effects, or who may benefit from dose escalation.

Extravascular water volume was not significantly increased 3 months after irradiation (Table 17, Figure 17). No volume effect was observed in central blood volume (Table 18, Figure 18) or pulmonary blood flow (Table 19, Figure 19). This suggests that these endpoints are also either not sensitive enough to detect differences in the dogs in this study, or, more likely, that these endpoints are not volume dependent. Normal pulmonary vascular resistance is extremely low. An increase in pulmonary arterial or venous pressure causes pulmonary vascular resistance to fall. Normally, some capillaries are either closed, or open but with no flow. As the pressure rises, blood is

conducted through these vessels in a process termed recruitment, and overall resistance is lowered. At higher vascular pressures the individual capillary segments become wider (distension). Distension is evidently the predominant mechanism for the decrease in pulmonary vascular resistance at relatively high vascular pressures. Vascular recruitment and distension are mechanisms that allow the lung to compensate for increased pulmonary arterial or venous pressure, to a point. At some point the loss of vasculature can no longer be accomodated and pulmonary hypertension results. Loss of vasculature in the lung therefore behaves more like a threshold effect than a volume effect.

The functional subunit (FSU) model [193] describes a system of functional subunits in normal tissues which are arranged either in serial alignment (e.g. ureter) or in parallel (e.g. kidney). Lung is a complex organ with FSUs spatially arranged both serially and in parallel. The large airways and vessels can be thought of as serial FSUs that deliver oxygen and blood to FSUs downstream. The respiratory airways and alveoli are FSUs arranged in parallel and at the terminal end of the serial arrangement of FSUs upstream. Irradiating the same volume of lung in the mediastinal region and in a distal, peripheral region are likely not equivalent. The mediastinal lung contains large vessels and airways, upon which all distal portions of lung are dependent. Injury to the more proximal areas of lung is likely to affect not only the irradiated lung but may also have a profound effect on the function of the lung "downstream".

Complete surgical removal of a lung lobe is possible, demonstrating that there is considerable reserve capacity to the lung. One possible consequence of lung irradiation

might be that if a portion of the lung were damaged to the extent that gas exchange in the injured volume was impaired or eliminated, yet it still received some of the pulmonary blood flow the result would be venous admixture of the blood going back out into the systemic circulation. This would result in hypoxemia, which is a contributor to pulmonary hypertension. The end result may be greater loss of function than if that volume of lung were actually removed. The injured lung causes the functional lung to receive less flow of oxygenated blood, decreasing the compensatory capacity of the still functional lung. It would be better to have removed the volume completely than to have it interfering with the efficient distribution of oxygenated blood to the rest of the lung. While irradiation of a larger volume of lung may increase the probability for such a shunting process to occur, the resulting physiologic changes from this chain of events would not necessarily be volume dependent.

The fact that the hypoxemia in these dogs was readily corrected with the administration of supplemental oxygen suggests that shunting and ventilation-perfusion inequality were not major factors in the changes seen in these dogs. More likely, alveoli and pulmonary vessels are both injured and eliminated within the radiation field, resulting in the volume effect seen in the decreased serotonin uptake and decreased tidal volume results.

Thoracic Radiographs

There was a volume effect for moderate to severe radiographic changes at the ED_{50} level (Table 20, Figure 20). The radiographic changes seen three months after

irradiation included fissure lines, indicative of pleural effusion or fibrosis, decreased vascular detail and increased opacity in the irradiated region. The changes had a sharp edge and were confined to the treatment field.

The dose-response curve for the 33% lung volume group may be artificially shifted to the left at the lower doses, owing to a lack of data at doses higher than 72 Gy (the maximum in our range of doses). The ED_5 values for the 33% and 67% volume groups were not significantly different (38.7 Gy and 34.6 Gy respectively), while the ED_{50} values were well separated (68.1 Gy and 47.3 Gy respectively). As with the serotonin uptake results, these results are consistent with the probability model [155]. The decreasing slope of the dose-response curve predicted by this model results in similar ED_5 values, even when the ED_{50} values for different volumes are significantly different. The volume effect that exists at the higher probability levels is undetectable and perhaps non-existent at the low probabilities of injury typical of the clinic [134]. This possibility should be considered when making comparisons using the ED_5 for radiographic changes.

In a study of lung volume effects in pigs, Hermann, *et al.* [66] found that early structural lung damage as assessed by chest radiographs was not dependent on the irradiated lung volume. The dog study was done over a wider range of doses and lung volumes, which may have been the reason a volume effect was observed in the dogs but not in the pigs.

Sensitivity of thoracic radiograph changes may be limited by considerable intra- and interobserver variability. Optical densitometry has been used in an effort to more

quantitatively evaluate radiographic density changes in irradiated lung [9], but was not used in this study.

Perfusion SPECT Lung Imaging

Based on regions of interest drawn on perfusion SPECT scans to represent the irradiated lung volume and nonirradiated lung volume, the volume of perfused lung irradiated was estimated to be the percentage of functional lung volume in the "irradiated" region of interest. Perfused lung volume irradiated in the 33% volume group averaged 27% (0.02%, n=4), which was quite similar to the 33% we planned to irradiate. Perfused lung volume irradiated in the 67% volume group averaged 49% (0.01%, n=3). Likely much of the mediastinal field is heterogeneous, containing large vessels and airways medially which do not contribute to gas exchange. The three-dimensional treatment plans were designed to omit as many large vessels and airways as possible. It is possible that in the 67% lung volume fields these large airways and vessels were decreasing in size as the field was widened away from the mediastinum to encompass a greater lung volume, making them more difficult to exclude them. These structures do not contribute to gas exchange, but do take up significant space. This may account for the difference between the estimated volume of perfused lung in the irradiated field (49%) and the planned treatment volume (67%).

Histomorphometric Analysis

Histologic changes observed in the dogs that were euthanatized due to lung toxicity during the first six months of this study were consistent with radiation

pneumonitis. Alveolar edema, interstitial fibrosis, type II pneumocyte hyperplasia and hypertrophy, and increased numbers of alveolar macrophages were seen in all 12 of the dogs euthanatized for severe symptomatic pneumonitis (Table 21, Figures 21, 22). These changes were evident only in irradiated lung, and were not related to total dose, lung volume irradiated, or time from irradiation to death. The only differences were the volume of lung in which these changes were present. This is consistent with a model of the lung as a parallel architecture structure consisting of functional subunits and exhibiting a critical volume phenomenon, where increased morbidity is the result of the same effect in a larger volume of tissue [87, 194]. These histologic lung changes were significantly greater in the dogs humanely killed due to symptomatic lung toxicity than in the dogs euthanatized for other reasons.

Future Directions

These data add to the sparse biological dose-volume relationship data previously available with which to test existing volume models and develop new models. They will be used to test selected existing volume models by our research group, and made available to others for testing and development of new models as well.

Measurement of serotonin uptake proved to be a sensitive method to measure endothelial cell injury and volume effects in the lung. The technique used in this study was based on the fraction of serotonin extracted on a single passage through the lung. This technique requires multiple arterial blood samples and does not provide information on spatial distribution of the localized lung injury. Nuclear medicine techniques have

already been developed using a ^{11}C -labelled form of cyanoimprimine to measure uptake in the lungs and brain of healthy human volunteers by positron emission tomography. Cyanoimiprimine has a high affinity for the serotonin transporter. The lung may function as a reservoir for antidepressants with high affinity to the serotonin transporter, and the investigators were interested in ways to block lung uptake in order to increase brain uptake of the drugs [163]. Radioiodinated (^{131}I) metaiodobenzylguanadine (MIBG) has been shown to have uptake properties similar to those of biogenic amines in rat lung and may be useful as a marker of pulmonary endothelial cell function [158]. Further studies in sheep and humans indicate that changes in first transit pulmonary extraction of ^{123}I-labelled MIBG can easily be monitored externally using conventional gamma camera computer systems. These techniques allow for not only evaluation of pulmonary endothelial cell function, but also spatial information about the lung injury.

Non-invasive techniques to evaluate pulmonary endothelial cell function and spatial distribution of lung injury could be used clinically to assess lung toxicity during the course of radiation therapy. After an initial dose, e.g. 60 Gy, has been given, serotonin uptake could be evaluated to identify patients who may be at risk for serious pulmonary complications, or patients who might be candidates for dose escalation.

SUMMARY

In the present study, when the volume of lung irradiated was increased from 67% to the whole lung, the volume enhancement ratio (VER) at the ED_{50} level for developing severe symptomatic pneumonitis was 1.27. (Table 24, Figure 23). The volume enhancement ratios for decreased serotonin uptake (percent) and moderate to severe radiographic changes at the ED_{50} level of effect for the same change in irradiated lung volume were 1.37 and 1.30 respectively (Table 24, Figure 23). This is due to the effect of compensatory increases in pulmonary function in nonirradiated lung in partial-volume lung irradiation. Therefore, the volume enhancement ratio for a smaller partial-volume to a larger partial-volume may be lower than the volume enhancement ratio for the same smaller partial volume to whole lung. This is demonstrated when comparing decreased serotonin uptake and radiographic changes at the ED_5 level of effect in 33% and 67% irradiated lung volumes where the VERs are 1.09 and 1.12 respectively (Figure 23, Table 24). However, these ED_5 values for the 33% lung volume group may be artificially low, due to the lack of data in this group for doses greater than 72 Gy (the maximum dose in our range). At the ED_{50} level of effect for decreased serotonin uptake, the VER is higher when comparing 33%:67% than when comparing 67%:100% (1.47 and 1.37 respectively) At the ED_{50} level of effect for radiographic changes, the VER is also higher when comparing 33%:67% than when comparing 67%:100% (1.44 and 1.30, respectively)

Table 24. Volume enhancement ratios for severe symptomatic pneumonitis, serotonin uptake (%) and thoracic radiograph changes

Endpoint (Gy)	Lung Volume Irradiated			Volume Enhancement Ratios		
	33%	67%	100%	33%:67%	67%:100%	33%:100 %
Severe symptomatic pneumonitis ED_{50}	NR*	56.0	44.1	—	1.27	—
Severe symptomatic pneumonitis ED_5	NR*	48.1	39.1	—	1.23	—
Serotonin uptake (%) ED_{50}	73.5	49.9	36.3	1.47	1.37	2.02
Serotonin uptake (%) ED_5	41.7	38.2	19.8	1.09	1.93	2.11
Thoracic radiographs changes ED_{50}	68.1	47.3	36.4	1.44	1.30	1.87
Thoracic radiographs changes ED_5	38.7	34.6	19.6	1.12	1.77	1.97

* Not reached.

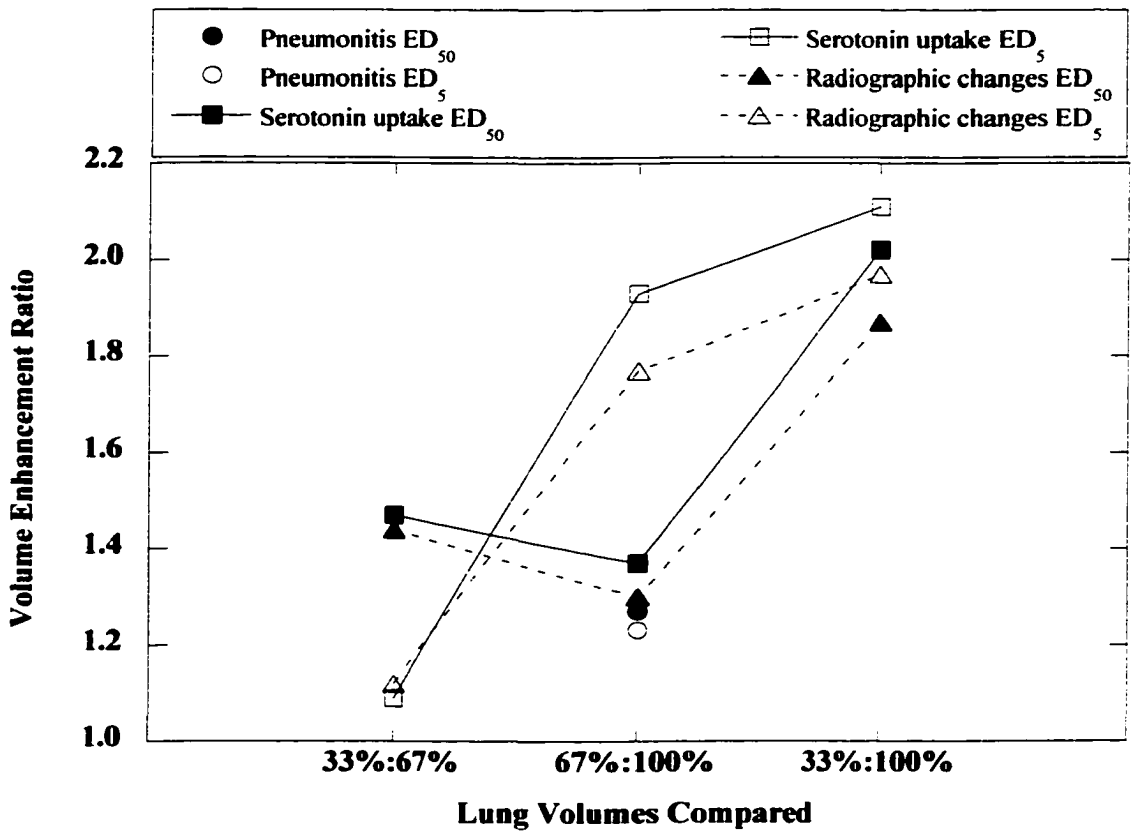

Figure 23. Line plot of the volume enhancement ratio (VER) for the development of severe symptomatic pneumonitis (ED_{50} ●, ED_5 ○), decreased serotonin uptake (%) (ED_{50} ■, ED_5 □) and moderate to severe radiographic changes (ED_{50} ▲, ED_5 △) 3 months after irradiation. Comparisons between 33% and 67%, 67% and 100% and 33% and 100% lung volume irradiated are made.

(Table 24, Figure 23). This suggests a great capacity for compensation by the non-irradiated normal lung when only 33% of the lung volume is irradiated. This capacity for compensation is markedly decreased when 67% of the lung volume is irradiated.

The volume enhancement ratio will also depend on the pre-treatment pulmonary function. Less compensation by nonirradiated lung will be possible in patients with poor pulmonary function at the start of treatment. In patients with underlying conditions such as smoking, emphysema, and space-occupying tumor volume, partial lung volume irradiation might have the same detrimental effect on post-therapy pulmonary function as whole lung irradiation and the volume enhancement ratio might be increased.

Combined radiotherapy and chemotherapy regimens are used increasingly in the treatment of thoracic tumors. Radiation therapy combined with pneumotoxic chemotherapy agents might further reduce the ability of nonirradiated lung to compensate for radiation injury, resulting in even greater morbidity when larger partial volumes of lung are in the treatment field.

Published radiation dose-volume tolerance estimates for human lung [45], and experimental animal models [66, 87] cannot be compared directly with each other or with the data from the present study, owing to differences in fractionation and treatment schedules, endpoints evaluated and species. However, bearing those difference in mind, some careful observations can be made. TD_{50} (probabililty of 50% complication) and TD_5 (probability of 5% complication) values for clinical pneumonitis in human patients [45], breathing rate and lethap pneumonitis in mice (ED_{50} only) [87], breathing rate and

radiographic changes in pigs [66], and severe symptomatic pneumonitis, serotonin uptake, and radiographic changes in normal beagle dogs (present study) are presented in Tables 25 and 26. Equivalent tolerance doses were calculated for each endpoint using 2.0 Gy as the standardized fraction size and an α/β ratio of 3 Gy for lung. Equivalent TD_{50}s for pneumonitis in humans and serotonin uptake and radiographic changes in normal beagle dogs when 1/3 of the lung volume was irradiated were very similar (65 Gy, 66.2 Gy and 61.3 Gy respectively) (Table 25). A TD_{50} for severe symptomatic pneumonitis was not reached in the 1/3 lung volume group of beagle dogs. Equivalent TD_{50}s for breathing rate and lethal pneumonits in mice, and severe pneumonitis in beagle dogs were considerably higher than the human estimates when 2/3 or the whole lung volume was irradiated. These endpoints in the animal models included pneumonitis severe enough to require sacrifice for humane reasons, which was much more severe than in the human patients. Still, there were no cases of severe symptomatic pneumonitis in the dogs with 1/3 or their lung volume irradiated to total doses of up to 72 Gy, suggesting that the Emami *et al.* [45] estimates might be too conservative. Equivalent TD_{50}s for serotonin uptake and radiographic changes in the beagle dogs when 2/3 or the whole lung volume was irradiated were closer to the human estimates, but still considerably higher (Table 26). These endpoints are more clinically relevant and can be more directly compared with the human pneumonitis estimates. These data also suggest that the human estimates may be low. The equivalent TD_5s for serotonin uptake and radiographic changes in the normal beagle dogs irradiated to 2/3 and 3/3 total lung volume are very similar to the

Table 25. Comparison of radiation tolerance dose estimates and data: Probability of 50% complication*

	TD 50 (Gy) Lung Volume Irradiated										
Study	**1/4**	**1/4§**	**1/3**	**1/3§**	**1/2**	**1/2§**	**2/3**	**2/3§**	**3/3**	**3/3§**	**Endpoint / Species**
Emami, *et al.* (1991) 1.8-2.0 Gy fractions	—	—	65	65	—	—	40	40	24.5	24.5	TD_{50} pneumonitis / human
Liao, *et al.* (1995) Single doses Apex (A) or base (B)	—	—	NR	NR	15.7 A 19.5 B	58.7 87.8	14.7 B	52.0	12.5	38.8	ED_{50} pneumonitis (BR, 22 wks) / C3Hf/Kam mouse
Liao, *et al.* (1995) Single doses Apex (A) or base (B)	—	—	NR	NR	NR A 18.7 B	81.2	NR A 15.5B	57.4	12.6	39.3	LD_{50} pneumonitis (28 wks) / C3Hf/Kam mouse
Herrman, *et al.* (1997) 5 equal fractions Rt. base (RB) or rt. (R)	>31 RB	>57	—	—	26.8 R	44.8	—	—	—	—	ED_{50} pneumonitis (BR, ≤ 8 wks) / pig
Herrman, *et al.* (1997) 5 equal fractions Rt. base (RB) or rt. (R)	21.1 RB	30.5	—	—	21.7 R	31.9	—	—	—	—	ED_{50} pneumonitis (radiographic, ≤ 8 wks) / pig
Normal Beagle Dogs 1.5 Gy fractions Mediastinal field	—	—	NR	NR	—	—	56.0	50.4	44.1	39.7	ED_{50} severe pneumonitis (≤ 6 m) / dog
Normal Beagle Dogs 1.5 Gy fractions Mediastinal field	—	—	73.5	66.2	—	—	49.9	44.9	36.3	32.7	ED_{50} serotonin uptake (3 m) / dog
Normal Beagle Dogs 1.5 Gy fractions Mediastinal field	—	—	68.1	61.3	—	—	47.3	42.6	36.4	32.8	ED_{50} pneumonitis (radiographic, 3 m) / dog

* Abbreviations: TD = tolerance dose, ED = effective dose, LD = lethal dose, BR = breathing rate, NR = not reached

§ Equivalent dose in 2.0 Gy fractions (α/β = 3 Gy)

Table 26. Comparison of radiation tolerance dose estimates and data: Probability of 5% complication*

Study	TD 5 (Gy) Lung Volume Irradiated										Endpoint / Species
	1/4	1/4§	1/3	1/3§	1/2	1/2§	2/3	2/3§	3/3	3/3§	
Emami, *et al.* (1991) 1.8–2.0 Gy fractions	—	—	45	45	—	—	30	30	17.5	17.5	TD_5 pneumonitis / human
Herrman, *et al.* (1997) 5 equal fractions (2 Gy) Right lung	—	—	—	—	10	10	—	—	—	—	ED_5 pneumonitis (BR, ≤ 8 wks) / pig
Herrman, *et al.* (1997) 5 equal fractions (2.8 Gy) Right lung	—	—	—	—	14	16.2	—	—	—	—	ED_5 pneumonitis (radiographic, ≤ 8 wks) / pig
Normal Beagle Dogs 1.5 Gy fractions Mediastinal field	—	—	NR	NR	—	—	48.1	43.3	39.1	35.2	ED_5 severe pneumonitis (≤ 6 m) / dog
Normal Beagle Dogs 1.5 Gy fractions Mediastinal field	—	—	41.7	37.5	—	—	38.2	34.4	19.8	17.8	ED_5 serotonin uptake (3 m) / dog
Normal Beagle Dogs 1.5 Gy fractions Mediastinal field	—	—	38.7	34.8	—	—	34.6	31.1	19.6	17.6	ED_{50} pneumonitis (radiographic, 3 m) / dog

* Abbreviations: TD = tolerance dose, ED = effective dose, LD = lethal dose, BR = breathing rate, NR = not reached

§ Equivalent dose in 2.0 Gy fractions (α/β = 3 Gy)

human pneumonitis estimates. The equivalent TD_5s for these endpoints are lower in the beagle dog than for the human pneumonitis estimates, but these tolerance doses in the dogs in the 1/3 lung volume group may be artificially decreased at the lower doses, owing to a lack of data at doses higher than 72 Gy (the maximum in our range of doses). Considering these data and the fact that human radiation therapy prescriptions are based on a 5% probability/risk for complications, perhaps the human pneumonitis estimates are not far off after all. However, considering that no severe pulmonary toxicity was observed in the dogs when 33% of their lung volume was irradiated to doses up to 72 Gy, there is likely still room for dose escalation in lung volumes of 1/3 or less. It seems likely that when small volumes of lung are irradiated, the dose-limiting complications are not radiation-induced pulmonary effects, but other complications such as hemorrhage and fistula formation.

As the volume of lung irradiated increases, the probability for clinical signs of pulmonary injury increases. This is an important consideration not only from the perspective of tumor control and treatment planning, but quality of life for the patient after therapy has been completed. Loss of pulmonary function beyond the patient's capacity to compensate will have a dramatic effect on their day to day activities after their cancer has been controlled. The question whether it is better to give a "lot to a little or a little to a lot" [173] is very important to the 32 year old breast cancer patient with a 3 year old toddler at home to keep up with. In other patients, the functional reserve of the nonirradiated lung may be reduced by preexisting disease (emphysema, tumor volume),

age, smoking habits, or concurrent chemotherapy, decreasing the compensation term of the equation to start with. The ultimate goal of using all of these assays and endpoints is to sort out how best to deliver the radiotherapy with the greatest probability of tumor control while affecting the patient's normal pulmonary function as little as possible.

Withers and Thames [194] stressed the importance if making distinctions between increased effect per unit dose with increasing volume, representing an increased radiosensitivity; an increased probability for the same effect with an increased amount of tissue at risk, and increased morbidity due to the same effect in a larger volume of tissue. The histological lung changes we observed in this study differed only by the volume of lung in which the changes were present. This is consistent with increased morbidity due to the same effect in a larger volume of tissue. Others have made similar observations in mice [87] and pigs [66].

There is a significant relationship between the volume irradiated and functional lung damage, e.g. severe symptomatic pneumonitis and serotonin uptake. This underscores the message that when considering the effects of volume in the lung, the relationship depends on the endpoint being evaluated. Some endpoints, such as serotonin uptake and development of severe symptomatic pneumonitis, demonstrate a clear volume effect. Other endpoints, such as lung mechanics or hemodynamics assessments, may be either independent of volume irradiated, or not sensitive enough to sort out the differences in irradiated volume. The great compensatory capacity of the lung makes these distinctions even more difficult.

CONCLUSIONS

In conclusion, this study clearly demonstrates that the extreme radiation sensitivity of the lung makes the total volume of lung irradiated the critical dose-limiting factor involved in thoracic radiotherapy. Severe pneumonitis proved to be a very informative volume-effect endpoint. ED_{50} values for severe symptomatic pneumonitis, serotonin uptake and radiographic changes in this study were significantly higher than Emami's TD_{50} estimates for clinical pneumonitis, suggesting that the human tolerance dose estimates for lung may be too conservative. Volume effects in lung are dependent on the compensatory capacity of the nonirradiated lung. Evaluation of pre-treatment pulmonary function should be an important consideration in the design of an appropriate treatment strategy. Underlying pathophysiology of irradiated tissue, as well as decreased compensatory capacity of nonirradiated tissue may have a strong effect on the dose-volume response.

Dose-volume relationships in lung are critically dependent on the endpoint being considered. Functional endpoints such as the development of severe symptomatic pneumonitis and decreased serotonin uptake seem to depend on the volume of lung irradiated. Other functional endpoints, such as functional residual capacity, mean pulmonary artery pressure may be either not sensitive enough to demonstrate a volume

effect, or be independent of volume irradiated. Most likely, there is a threshold effect in which a certain level of impairment must be exceeded before measurable changes occur.

Structural endpoints evaluated in this study as assessed by histological evaluation were independent of irradiated lung volume, and therefore must be considered separately when discussing volume effects in lung.

No pulmonary toxicity was observed after irradiation of 33% of the lung volume to doses up to 72 Gy. When small volumes of lung are irradiated the dose limiting toxicity may not be decreased pulmonary function, but complications resulting from structural damage to the vasculature and airways leading to hemorrhage and fistulae formation.

REFERENCES

1. American Cancer Society Website. http://www.cancer.org, 2001.
2. Abratt, R. P. and Willcox, P. A. The effect of irradiation on lung function and perfusion in patients with lung cancer. Int J Radiat Oncol Biol Phys **31**(4): 915-919, 1995.
3. Anscher, M. S., Peters, W. P., Reisenbichler, H., Petros, W. P. and Jirtle, R. L. Transforming growth factor beta as a predictor of liver and lung fibrosis after autologous bone marrow transplantation for advanced breast cancer. N Engl J Med **328**(22): 1592-1598, 1993.
4. Armstrong, J., Raben, A., Zelefsky, M., Burt, M., Leibel, S., Burman, C., Kutcher, G., Harrison, L., Hahn, C., Ginsberg, R., Rusch, V., Kris, M. and Fuks, Z. Promising survival with three-dimensional conformal radiation therapy for non-small cell lung cancer. Radiother Oncol **44**(1): 17-22, 1997.
5. Arriagada, R., Le Chevalier, T., Quoix, E., Ruffie, P., de Cremoux, H., Douillard, J. Y., Tarayre, M., Pignon, J. P. and Laplanche, A. ASTRO (American Society for Therapeutic Radiology and Oncology) plenary: Effect of chemotherapy on locally advanced non-small cell lung carcinoma: a randomized study of 353 patients. GETCB (Groupe d'Etude et Traitement des Cancers Bronchiques), FNCLCC (Federation Nationale des Centres de Lutte contre le Cancer) and the CEBI trialists [see comments]. Int J Radiat Oncol Biol Phys **20**(6): 1183-1190, 1991.
6. Barcellos-Hoff, M. H. Radiation-induced transforming growth factor beta and subsequent extracellular matrix reorganization in murine mammary gland. Cancer Res **53**(17): 3880-3886, 1993.
7. Bastin, K. T. and Curley, R. Non-small-cell lung carcinoma. Current and future therapeutic management. Drugs **49**(3): 362-375, 1995.
8. Bell, J., McGivern, D., Bullimore, J., Hill, J., Davies, E. R. and Goddard, P. Diagnostic imaging of post-irradiation changes in the chest. Clin Radiol **39**: 109-119, 1988.
9. Bentzen, S. M., Skoczylas, J. Z., Overgaard, M., Overgaard, J., Nielsen, O. G. and Madsen, E. H. Quantitative assessment of radiation-induced lung changes by computerized optical densitometry of routine chest x-rays. Int J Radiat Oncol Biol Phys **34**(2): 421-427, 1996.

10. Block, E. R. Early metabolic changes in response to lung injury: extrapolation from animals to humans. J Toxicol Environ Health **13**(2-3): 369-386, 1984.

11. Boersma, L. J. Lung function and radiotherapy--An analysis of local and overall radiation effects. Dissertation, University of Amsterdam, April, 1995.

12. Boersma, L. J., Damen, E. M., de Boer, R. W., Muller, S. H., Roos, C. M., Valdes Olmos, R. A., van Zandwijk, N. and Lebesque, J. V. Dose-effect relations for local functional and structural changes of the lung after irradiation for malignant lymphoma. Radiother Oncol **32**(3): 201-209, 1994.

13. Boersma, L. J., Damen, E. M., de Boer, R. W., Muller, S. H., Valdes Olmos, R. A., Hoefnagel, C. A., Roos, C. M., van Zandwijk, N. and Lebesque, J. V. A new method to determine dose-effect relations for local lung-function changes using correlated SPECT and CT data. Radiother Oncol **29**(2): 110-116, 1993.

14. Boersma, L. J., Damen, E. M., de Boer, R. W., Muller, S. H., Valdes Olmos, R. A., van Zandwijk, N. and Lebesque, J. V. Estimation of overall pulmonary function after irradiation using dose- effect relations for local functional injury [see comments]. Radiother Oncol **36**(1): 15-23, 1995.

15. Border, W. A. and Noble, N. A. Transforming growth factor beta in tissue fibrosis. N Engl J Med **331**(19): 1286-1292, 1994.

16. Botterman, J., Tasson, J., Schelstraete, K., Pauwels, R., Van der Straeten, M. and De Schryver, A. Scintigraphic, spirometric, and roentgenologic effects of radiotherapy on normal lung tissue. Short-term observations in 14 consecutive patients with breast cancer. Chest **97**(1): 97-102, 1990.

17. Byhardt, R. W. The evolution of Radiation Therapy Oncology Group (RTOG) protocols for nonsmall cell lung cancer. Int J Radiat Oncol Biol Phys **32**(5): 1513-1525, 1995.

18. Byhardt, R. W., Scott, C., Sause, W. T., Emami, B., Komaki, R., Fisher, B., Lee, J. S. and Lawton, C. Response, toxicity, failure patterns, and survival in five Radiation Therapy Oncology Group (RTOG) trials of sequential and/or concurrent chemotherapy and radiotherapy for locally advanced non-small-cell carcinoma of the lung. Int J Radiat Oncol Biol Phys **42**(3): 469-478, 1998.

19. Canney, P. A. and Dean, S. Transforming growth factor beta: a promotor of late connective tissue injury following radiotherapy? Br J Radiol **63**(752): 620-623, 1990.

20. Chinard, F. P. Estimation of extravascular lung water by indicator-dilution techniques. Circ Res **37**(2): 137-145, 1975.

21. Choi, N. C. Cancer of the Intrathorax. Clinical Radiation Oncology. C. C. Wang (Ed.^Eds.) PSG Publishing Co., Littleton, MA: 196-236, 1988.

22. Choi, N. C. and Kanarek, D. J. Toxicity of thoracic radiotherapy on pulmonary function in lung cancer. Lung Cancer **10 Suppl 1**: S219-230, 1994.

23. Choi, N. C., Kanarek, D. J. and Kazemi, H. Physiologic changes in pulmonary function after thoracic radiotherapy for patients with lung cancer and role of regional pulmonary function studies in predicting postradiotherapy pulmonary function before radiotherapy. Cancer Treatment Symposia **2**: 119-130, 1985.

24. Coates, G., Firnau, G., Meyer, G. J. and Gratz, K. F. Noninvasive measurement of lung carbon-11-serotonin extraction in man. J Nucl Med **32**(4): 729-732, 1991.

25. Coggle, J. E., Lambert, B. E. and Moores, S. R. Radiation effects in the lung. Environ Health Perspect **70**: 261-291, 1986.

26. Collis, C. H., Down, J. D., Pearson, A. E. and Steel, G. G. Bleomycin and radiation-induced lung damage in mice. Br J Radiol **56**(661): 21-26, 1983.

27. Collis, C. H. and Steel, G. G. Lung damage in mice from cyclophosphamide and thoracic irradiation: the effect of timing. Int J Radiat Oncol Biol Phys **9**(5): 685-689, 1983.

28. Coutard, H. Roentgen therapy of epitheliomas of the tonsillar region, hypopharynx and larynx from 1920 to 1926. J.Am.Roentgen Ray Society **28**(3): 313-331, 1931.

29. Cox, J. D., Azarnia, N., Byhardt, R. W., Shin, K. H., Emami, B. and Pajak, T. F. A randomized phase I/II trial of hyperfractionated radiation therapy with total doses of 60.0 Gy to 79.2 Gy: possible survival benefit with greater than or equal to 69.6 Gy in favorable patients with Radiation Therapy Oncology Group stage III non-small-cell lung carcinoma: report of Radiation Therapy Oncology Group 83-11. J Clin Oncol **8**(9): 1543-1555, 1990.

30. Cromack, D. T., Sporn, M. B., Roberts, A. B., Merino, M. J., Dart, L. L. and Norton, J. A. Transforming growth factor beta levels in rat wound chambers. J Surg Res **42**(6): 622-628, 1987.

31. Cronau, L. H., Kerstein, M. D., Mandel, S. and Gillis, C. N. 5-Hydroxytryptamine extraction by the lung. Surg Gynecol Obstet **143**(1): 51-55, 1976.

32. Curran, W. J., Jr., Moldofsky, P. J. and Solin, L. J. Observations on the predictive value of perfusion lung scans on post- irradiation pulmonary function among 210 patients with bronchogenic carcinoma [see comments]. Int J Radiat Oncol Biol Phys **24**(1): 31-36, 1992.

33. Damen, E. M., Muller, S. H., Boersma, L. J., de Boer, R. W. and Lebesque, J. V. Quantifying local lung perfusion and ventilation using correlated SPECT and CT data. J Nucl Med **35**(5): 784-792, 1994.

34. Davis, S. D., Yankelevitz, D. F. and Henschke, C. I. Radiation effects on the lung: clinical features, pathology, and imaging findings. AJR Am J Roentgenol **159**(6): 1157-1164, 1992.

35. Dawson, C. A., Christensen, C. W., Rickaby, D. A., Linehan, J. H. and Johnston, M. R. Lung damage and pulmonary uptake of serotonin in intact dogs. J Appl Physiol **58**(6): 1761-1766, 1985.

36. Dawson, C. A., Linehan, J. H., Rickaby, D. A. and Bronikowski, T. A. Kinetics of serotonin uptake in the intact lung. Ann Biomed Eng **15**(2): 217-227, 1987.

37. Depledge, M. H., Collis, C. H. and Barrett, A. A technique for measuring carbon monoxide uptake in mice. Int J Radiat Oncol Biol Phys **7**(4): 485-489, 1981.

38. Deuel, T. F. and Senior, R. M. Growth factors in fibrotic diseases [editorial]. N Engl J Med **317**(4): 236-237, 1987.

39. Dobuler, K. J., Catravas, J. D. and Gillis, C. N. Early detection of oxygen-induced lung injury in conscious rabbits. Reduced in vivo activity of angiotensin converting enzyme and removal of 5-hydroxytryptamine. Am Rev Respir Dis **126**(3): 534-539, 1982.

40. Down, J. D. The nature and relevance of late lung pathology following localized irradiation of the thorax in mice and rats. Br J Cancer **53**: 330-332, 1986.

41. Down, J. D., Easton, D. F. and Steel, G. G. Repair in the mouse lung during low dose-rate irradiation. Radiother Oncol **6**(1): 29-42, 1986.

42. Down, J. D., Nicholas, D. and Steel, G. G. Lung damage after hemithoracic irradiation: dependence on mouse strain. Radiother Oncol **6**(1): 43-50, 1986.

43. Down, J. D. and Steel, G. G. The expression of early and late damage after thoracic irradiation: a comparison between CBA and C57B1 mice. Radiat Res **96**(3): 603-610, 1983.

44. Dritschilo, A., Chaffey, J. T., Bloomer, W. D. and Marck, A. The complication probability factor: a method for selection of radiation treatment plans. Br J Radiol **51**(605): 370-374, 1978.

45. Emami, B., Lyman, J., Brown, A., Coia, L., Goitein, M., Munzenrider, J. E., Shank, B., Solin, L. J. and Wesson, M. Tolerance of normal tissue to therapeutic irradiation. Int J Radiat Oncol Biol Phys **21**(1): 109-122, 1991.

46. Fajardo, L. F. (In) Pathology of Radiation Injury. Masson Publishing USA, Inc., New York, New York, 1982.

47. Franko, A. J. and Sharplin, J. Assessment of radiation-induced lung injury in mice using carbon monoxide uptake: correlation with histologically visible damage. Radiat Res **133**(2): 245-251, 1993.

48. Geist, B. J. and Trott, K. R. Radiographic and function changes after partial lung irradiation in the rat. Strahlenther Onkol **168**(3): 168-173, 1992.

49. Gillette, S. M., Dawson, C. A., Rickaby, D. A., Johnston, M. R. and Gillette, E. L. Late response to whole-lung irradiation alone and with whole-body hyperthermia in dogs. Radiat Res **147**(2): 257-262, 1997.

50. Gillette, S. M., Gillette, E. L., Shida, T., Boon, J., Miller, C. W. and Powers, B. E. Late radiation response of canine mediastinal tissues. Radiother Oncol **23**(1): 41-52, 1992.

51. Gillette, S. M., Powers, B. E., Orton, E. C. and Gillette, E. L. Early radiation response of the canine heart and lung. Radiat Res **125**(1): 34-40, 1991.

52. Glatstein, E. Alterations in rubidium-86 extraction in normal mouse tissues after irradiation. An estimate of long-term blood flow changes in kidney, lung, liver, skin and muscle. Radiat Res **53**(1): 88-101, 1973.

53. Gordon, G. S. and Vokes, E. E. Chemoradiation for locally advanced, unresectable NSCLC. New standard of care, emerging strategies. Oncology (Huntingt) **13**(8): 1075-1088; discussion 1088, 1091-1074, 1999.

54. Graham, M. V., Dryzmala, R. E., Jain, N. L. and Purdy, J. P. Confirmation of dose-volume histograms and normal tissue complication probability calculations to predict pulmonary complications after radiotherapy for lung cancer (abstract). 1994.

55. Graham, M. V., Matthews, J. W., Harms, W. B., Sr., Emami, B., Glazer, H. S. and Purdy, J. A. Three-dimensional radiation treatment planning study for patients with carcinoma of the lung. Int J Radiat Oncol Biol Phys **29**(5): 1105-1117, 1994.

56. Graham, M. V., Purdy, J. A., Emami, B., Matthews, J. W. and Harms, W. B. Preliminary results of a prospective trial using three dimensional radiotherapy for lung cancer. Int J Radiat Oncol Biol Phys **33**(5): 993-1000, 1995.

57. Groover, e. a. Observations on the use of the copper filter in the roentgen therapy of deep seated malignancies. South Med J **15**: 440-444, 1922.

58. Gross, N. J. Pulmonary effects of radiation therapy. Ann Intern Med **86**(1): 81-92, 1977.

59. Gross, N. J. Experimental radiation pneumonitis. IV. Leakage of circulatory proteins onto the alveolar surface. J Lab Clin Med **95**(1): 19-31, 1980.

60. Gross, N. J. The pathogenesis of radiation-induced lung damage. Lung **159**(3): 115-125, 1981.

61. Gross, N. J. and Narine, K. R. Experimental radiation pneumonitis. Corticosteroids increase the replicative activity of alveolar type 2 cells. Radiat Res **115**(3): 543-549, 1988.

62. Groth, S., Zaric, A., Sorensen, P. B., Larsen, J., Sorensen, P. G. and Rossing, N. Regional lung function impairment following post-operative radiotherapy for breast cancer using direct or tangential field techniques. Br J Radiol **59**(701): 445-451, 1986.

63. Hardman, P. D., Tweeddale, P. M., Kerr, G. R., Anderson, E. D. and Rodger, A. The effect of pulmonary function of local and loco-regional irradiation for breast cancer. Radiother Oncol **30**(1): 33-42, 1994.

64. Hart, C. M. and Block, E. R. Lung serotonin metabolism. Clin Chest Med **10**(1): 59-70, 1989.

65. Hassink, E. A., Souren, T. S., Boersma, L. J., Peerboom, P. F., Melkert, R., van Zandwijk, N., Lebesque, J. V. and Bruning, P. F. Pulmonary morbidity 10-18 years after irradiation for Hodgkin's disease. Eur J Cancer **3**: 343-347, 1993.

66. Herrmann, T., Baumann, M., Voigtmann, L. and Knorr, A. Effect of irradiated volume on lung damage in pigs. Radiother Oncol **44**(1): 35-40, 1997.

67. Hines. Fibrosis of the lung following roentgen-ray treatment for tumor. JAMA **79**: 720-722, 1922.

68. Hopewell, J. W. The volume effect in radiotherapy--its biological significance. Br J Radiol **70 Spec No**: S32-40, 1997.

69. Horning, S. J., Adhikari, A., Rizk, N., Hoppe, R. T. and Olshen, R. A. Effect of treatment for Hodgkin's disease on pulmonary function: results of a prospective study. J Clin Oncol **12**(2): 297-305, 1994.

70. Jackson, A., Kutcher, G. J. and Yorke, E. D. Probability of radiation-induced complications for normal tissues with parallel architecture subject to non-uniform irradiation. Med Phys **20**(3): 613-625, 1993.

71. Johns, H. E. and Cunningham, J. R. (In) The Physics of Radiology. Charles C. Thomas, Springfield, Illinois, 1983.

72. Källman, P., Ågren, A. and Brahme, A. Tumour and normal tissue responses to fractionated non-uniform dose delivery. Int.J.Radiat.Biol. **62**: 249-262, 1992.

73. Kaplan, E. L. and Meier, P. Nonparametric estimation from incomplete observations. J Am Stat Assoc **53**: 457-481, 1958.

74. Katzenstein, A. A. and Askin, F. B. (In) Surgical pathology of non-neoplastic lung disease. W. B. Saunders, Philadelphia, 1990.

75. Kimsey, F. C., Mendenhall, N. P., Ewald, L. M., Coons, T. S. and Layon, A. J. Is radiation treatment volume a predictor for acute or late effect on pulmonary function? A prospective study of patients treated with breast- conserving surgery and postoperative irradiation. Cancer **73**(10): 2549-2555, 1994.

76. King, S. C., Acker, J. C., Kussin, P. S., Marks, L. B., Weeks, K. J. and Leopold, K. A. High-dose, hyperfractionated, accelerated radiotherapy using a concurrent boost for the treatment of nonsmall cell lung cancer: unusual toxicity and promising early results [see comments]. Int J Radiat Oncol Biol Phys **36**(3): 593-599, 1996.

77. Klumper, A. and Zwijnenburg, A. Dual isotope (81Krm and 99Tcm) SPECT in lung function diagnosis. Phys Med Biol **31**(7): 751-761, 1986.

78. Komaki, R., Scott, C. B., Byhardt, R., Emami, B., Asbell, S. O., Russell, A. H., Roach, M., Parliament, M. B. and Gaspar, L. E. Failure patterns by prognostic group determined by recursive partitioning analysis (RPA) of 1547 patients on four radiation therapy oncology group (RTOG) studies in inoperable nonsmall-cell lung cancer (NSCLC). Int J Radiat Oncol Biol Phys **42**(2): 263-267, 1998.

79. Kutcher, G. J. and Burman, C. Calculation of complication probability factors for non-uniform normal tissue irradiation: the effective volume method [see comments]. Int J Radiat Oncol Biol Phys **16**(6): 1623-1630, 1989.

80. Kutcher, G. J., Burman, C., Brewster, L., Goitein, M. and Mohan, R. Histogram reduction method for calculating complication probabilities for three-dimensional treatment planning evaluations. Int J Radiat Oncol Biol Phys **21**(1): 137-146, 1991.

81. Kwa, S. L., Lebesque, J. V., Theuws, J. C., Marks, L. B., Munley, M. T., Bentel, G., Oetzel, D., Spahn, U., Graham, M. V., Drzymala, R. E., Purdy, J. A., Lichter, A. S., Martel, M. K. and Ten Haken, R. K. Radiation pneumonitis as a function of mean lung dose: an analysis of pooled data of 540 patients. Int J Radiat Oncol Biol Phys **42**(1): 1-9, 1998.

82. Langendijk, H. A., Lamers, R. J. S., ten Velde, G. P. M., Sanders, D. G. M., de Jong, J. M. A., Kessels, F. and Wouters, E. F. M. Is the chest radiograph a reliable tool in the assessment of tumor response after radiotherapy in nonsmall cell lung carcinoma? Int j radiat oncol Biol Phys **41**(5): 1037-1065, 1998.

83. Law, M. P. Vascular permeability and late radiation fibrosis in mouse lung. Rad Res **103**: 60-76, 1985.

84. Law, M. P. Vascular and epithelial damage in the lung of the mouse after X rays or neutrons. Rad Res **117**: 128-144, 1989.

85. Le Chevalier, T., Arriagada, R., Quoix, E., Ruffie, P., Martin, M., Tarayre, M., Lacombe-Terrier, M. J., Douillard, J. Y. and Laplanche, A. Radiotherapy alone versus combined chemotherapy and radiotherapy in nonresectable non-small-cell lung cancer: first analysis of a randomized trial in 353 patients [see comments]. J Natl Cancer Inst **83**(6): 417-423, 1991.

86. Levinson, B., Marks, L. B., Munley, M. T., Poulson, J., Hollis, D., Jaszczak, R. and Coleman, R. E. Regional dose response to pulmonary irradiation using a manual method. Radiother Oncol **48**(1): 53-60, 1998.

87. Liao, Z. X., Travis, E. L. and Tucker, S. L. Damage and morbidity from pneumonitis after irradiation of partial volumes of mouse lung [see comments]. Int J Radiat Oncol Biol Phys **32**(5): 1359-1370, 1995.

88. Libshitz, H. I. and Shuman, L. S. Radiation induced pulmonary change: CT findings. J Comput Assist Tomogr **8**: 15-19, 1984.

89. Lingos, T. I., Recht, A., Vicini, F., Abner, A., Silver, B. and Harris, J. R. Radiation pneumonitis in breast cancer patients treated with conservative surgery and radation therapy. Int J Radiat Oncol Biol Phys **21**: 355-360, 1991.

90. Lochrin, C., Goss, G., Stewart, D. J., Cross, P., Agboola, O., Dahrouge, S., Tomiak, E. and Evans, W. K. Concurrent chemotherapy with hyperfractionated accelerated thoracic irradiation in stage III non-small cell lung cancer. Lung Cancer **23**(1): 19-30, 1999.

91. Lockhart, S. P., Down, J. D. and Steel, G. G. The effect of low dose-rate and cyclophosphamide on the radiation tolerance of the mouse lung. Int J Radiat Oncol Biol Phys **12**(8): 1437-1440, 1986.

92. Lockhart, S. P., Down, J. D. and Steel, G. G. Mouse hemithoracic irradiation and its interaction with cytotoxic drugs. Radiother Oncol **24**(3): 177-185, 1992.

93. Lund, L. R., Riccio, A., Andreasen, P. A., Nielsen, L. S., Kristensen, P., Laiho, M., Saksela, O., Blasi, F. and Dano, K. Transforming growth factor-beta is a strong and fast acting positive regulator of the level of type-1 plasminogen activator inhibitor mRNA in WI-38 human lung fibroblasts. Embo J **6**(5): 1281-1286, 1987.

94. Lund, M. B., Myhre, K. I., Melsom, H. and Johansen, B. The effect on pulmonary function of tangential field technique in radiotherapy for carcinoma of the breast [see comments]. Br J Radiol **64**(762): 520-523, 1991.

95. Lyman, J. T. Complication probability as assessed from dose-volume histograms. Radiat Res Suppl **8**(9): S13-19, 1985.

96. Lyman, J. T. and Wolbarst, A. B. Optimization of radiation therapy, III: A method of assessing complication probabilities from dose-volume histograms. Int J Radiat Oncol Biol Phys **13**(1): 103-109, 1987.

97. Lyman, J. T. and Wolbarst, A. B. Optimization of radiation therapy, IV: A dose-volume histogram reduction algorithm. Int J Radiat Oncol Biol Phys **17**(2): 433-436, 1989.

98. Maasilta, P. Deterioration in lung function following hemithorax irradiation for pleural mesothelioma. Int J Radiat Oncol Biol Phys **20**: 433-438, 1991.

99. Mah, K. and Van Dyk, J. Quantitative measurement of changes in human lung density following irradiation. Radiother Oncol **11**(2): 169-179, 1988.

100. Mah, K., Van Dyk, J., Keane, T. and Poon, P. Y. Acute radiation-induced pulmonary damage: A clinical study on the response to fractionated radiation therapy. Int J Radiat Oncol Biol Phys **13**: 179-188, 1987.

101. Malcorps, C. M., Dawson, C. A., Linehan, J. H., Bronikowski, T. A., Rickaby, D. A., Herman, A. G. and Will, J. A. Lung serotonin uptake kinetics from indicator-dilution and constant- infusion methods. J Appl Physiol **57**(3): 720-730, 1984.

102. Malcorps, C. M., Will, J. A. and Herman, A. G. Kinetics of serotonin uptake in the isolated dog lung. Arch Int Pharmacodyn Ther **262**(2): 319-321, 1983.

103. Mantel, N. Evaluation of survival data and two new rank order statistics arising in its consideration. Cancer Chem Rep **5**: 1623-1630, 1966.

104. Marks, L. B. The pulmonary effects of thoracic irradiation. Oncology (Huntingt) **8**(6): 89-106; discussion 100, 103-104, 1994.

105. Marks, L. B., Munley, M. T., Bentel, G. C., Zhou, S. M., Hollis, D., Scarfone, C., Sibley, G. S., Kong, F. M., Jirtle, R., Jaszczak, R., Coleman, R. E., Tapson, V. and Anscher, M. Physical and biological predictors of changes in whole-lung function following thoracic irradiation [see comments]. Int J Radiat Oncol Biol Phys **39**(3): 563-570, 1997.

106. Marks, L. B., Munley, M. T., Spencer, D. P., Sherouse, G. W., Bentel, G. C., Hoppenworth, J., Chew, M., Jaszczak, R. J., Coleman, R. E. and Prosnitz, L. R. Quantification of radiation-induced regional lung injury with perfusion imaging. Int J Radiat Oncol Biol Phys **38**(2): 399-409, 1997.

107. Marks, L. B., Spencer, D. P., Bentel, G. C., Ray, S. K., Sherouse, G. W., Sontag, M. R., Coleman, R. E., Jaszczak, R. J., Turkington, T. G., Tapson, V. and et al. The utility of SPECT lung perfusion scans in minimizing and assessing the physiologic consequences of thoracic irradiation. Int J Radiat Oncol Biol Phys **26**(4): 659-668, 1993.

108. Martel, M. K., Strawderman, M., Hazuka, M. B., Turrisi, A. T., Fraass, B. A. and Lichter, A. S. Volume and dose parameters for survival of non-small cell lung cancer patients. Radiother Oncol **44**(1): 23-29, 1997.

109. Martel, M. K., Ten Haken, R. K., Hazuka, M. B., Turrisi, A. T., Fraass, B. A. and Lichter, A. S. Dose-volume histogram and 3-D treatment planning evaluation of patients with pneumonitis [see comments]. Int J Radiat Oncol Biol Phys **28**(3): 575-581, 1994.

110. Martin, M., Lefaix, J. L., Pinton, P., Crechet, F. and Daburon, F. Temporal modulation of TGF-beta 1 and beta-actin gene expression in pig skin and muscular fibrosis after ionizing radiation. Radiat Res **134**(1): 63-70, 1993.

111. Mauderly, J. L., Muggenburg, B. A., Hahn, F. F. and Boecker, B. B. The effects of inhaled 144Ce on cardiopulmonary function and histopathology of the dog. Radiat Res **84**(2): 307-324, 1980.

112. Mayneord, W. V. The measurement of radiation for medical purposes. Proc Phys Soc **54**: 405, 1942.

113. McChesney Gillette, S., Dawson, C. A., Scott, R. J., Rickaby, D. A., Powers, B. E., Johnston, M. R., Chen, C. and Gillette, E. L. Whole-body hyperthermia combined with hyperfractionated irradiation of the thorax in dog: acute physiological response. Int J Hyperthermia **9**(3): 369-382, 1993.

114. McChesney, S. L. Radiation response of the canine heart and lung. Dissertation, Colorado State University, Spring, 1988.

115. McChesney, S. L., Gillette, E. L. and Orton, E. C. Canine cardiomyopathy after whole heart and partial lung irradiation. Int J Radiat Oncol Biol Phys **14**(6): 1169-1174, 1988.

116. McChesney, S. L., Gillette, E. L. and Powers, B. E. Response of the canine lung to fractionated irradiation: pathologic changes and isoeffect curves. Int J Radiat Oncol Biol Phys **16**(1): 125-132, 1989.

117. McDonald, S., Rubin, P., Phillips, T. L. and Marks, L. B. Injury to the lung from cancer therapy: clinical syndromes, measurable endpoints, and potential scoring systems. Int J Radiat Oncol Biol Phys **31**(5): 1187-1203, 1995.

118. McEntee, M. C., Page, R. L., Cline, J. M. and Thrall, D. E. Radiation pneumonitis in three dogs. Veterinary Radiology & Ultrasound **33**(4): 190-197, 1992.

119. Miller, G. G., Dawson, D. T. and Battista, J. J. Computed tomographic assessment of radiation induced damage in the lung of normal and WR 2721 protected LAF1 mice. Int J Radiat Oncol Biol Phys **12**(11): 1971-1975, 1986.

120. Moosavi, H., McDonald, S., Rubin, P., Cooper, R., Stuard, D. and Penney, D. Early radiation dose-response in lung: An ultrastructural study. Int J Radiat Oncol Biol Phys **2**: 921-931, 1977.

121. Morton, R. F., Jett, J. R., McGinnis, W. L., Earle, J. D., Therneau, T. M., Krook, J. E., Elliott, T. E., Mailliard, J. A., Nelimark, R. A., Maksymiuk, A. W. and et al. Thoracic radiation therapy alone compared with combined chemoradiotherapy for locally unresectable non-small cell lung cancer. A randomized, phase III trial [see comments]. Ann Intern Med **115**(9): 681-686, 1991.

122. Mustoe, T. A., Pierce, G. F., Thomason, A., Gramates, P., Sporn, M. B. and Deuel, T. F. Accelerated healing of incisional wounds in rats induced by transforming growth factor-beta. Science **237**(4820): 1333-1336, 1987.

123. Nicholas, D. and Down, J. D. The assessment of early and late radiation injury to the mouse lung using X-ray computerised tomography. Radiother Oncol **4**(3): 253-263, 1985.

124. Niemierko, A. and Goitein, M. Modeling of normal tissue response to radiation: the critical volume model [see comments]. Int.J.Radiat.Oncol.Biol.Phys. **25**: 135-145, 1993.

125. Niemierko, A. and Goitein, M. Dose-volume distributions: a new approach to dose-volume histograms in three-dimensional treatment planning. Med Phys **21**(1): 3-11, 1994.

126. Oetzel, D., Schraube, P., Hensley, F., Sroka-Perez, G., Menke, M. and Flentje, M. Estimation of pneumonitis risk in three-dimensional treatment planning using dose-volume histogram analysis. Int J Radiat Oncol Biol Phys **33**(2): 455-460, 1995.

127. Penney, D. P., Siemann, D. W., Rubin, P., Shapiro, D. L., Finkelstein, J. and Cooper, R. A. Morphologic changes reflecting early and late effects of irradiation of the distal lung of the mouse. Review. Scan Electron Microsc **I**: 413-425, 1982.

128. Perez, C. A., Bauer, M., Edelstein, S., Gillespie, B. W. and Birch, R. Impact of tumor control on survival in carcinoma of the lung treated with irradiation [published erratum appears in Int J Radiat Oncol Biol Phys 1986 Nov;12(11):2057]. Int J Radiat Oncol Biol Phys **12**(4): 539-547, 1986.

129. Perez, C. A., Pajak, T. F., Rubin, P., Simpson, J. R., Mohiuddin, M., Brady, L. W., Perez-Tamayo, R. and Rotman, M. Long-term observations of the patterns of failure in patients with unresectable non-oat cell carcinoma of the lung treated with definitive radiotherapy. Report by the Radiation Therapy Oncology Group. Cancer **59**(11): 1874-1881, 1987.

130. Phillips, T. L., Wharam, M. D. and Margolis, L. W. Modification of radiation injury to normal tissues by chemotherapeutic agents. Cancer **35**(6): 1678-1684, 1975.

131. Pigott, K. H. and Saunders, M. I. The long-term outcome after radical radiotherapy for advanced localized non-small cell carcinoma of the lung. Clin Oncol **5**(6): 350-354, 1993.

132. Polansky, S. M., Ravin, C. E. and Prosnitz, L. R. Pulmonary changes after primary radiation for early breast carcinoma. Am J Radiol **134**: 101-105, 1980.

133. Postlethwaite, A. E., Keski-Oja, J., Moses, H. L. and Kang, A. H. Stimulation of the chemotactic migration of human fibroblasts by transforming growth factor beta. J Exp Med **165**(1): 251-256, 1987.

134. Powers, B. E., Thames, H. D., Gillette, S. M., Smith, C., Beck, E. R. and Gillette, E. L. Volume effects in the irradiated canine spinal cord: do they exist when the probability of injury is low? [see comments]. Radiother Oncol **46**(3): 297-306, 1998.

135. Price, A., Jack, W. J., Kerr, G. R. and Rodger, A. Acute radiation pneumonitis after postmastectomy irradiation: effect of fraction size. Clin Oncol R Coll Radiology **2**: 224-229, 1990.

136. Randall, K. and Coggle, J. E. Expression of transforming growth factor-beta 1 in mouse skin during the acute phase of radiation damage. Int J Radiat Biol **68**(3): 301-309, 1995.

137. Rappaport, D. S., Niewoehner, D. E., Kim, T. H., Song, C. W. and Levitt, S. H. Uptake of carbon monoxide by C3H mice following X irradiation of lung only or total-body irradiation with 60Co. Radiat Res **93**(2): 254-261, 1983.

138. Rezvani, M., Heryet, J. C. and Hopewell, J. W. E. Effects of single dose of gamma radiation on pig lung. Radiother Oncol **14**: 133-142, 1989.

139. Rickaby, D. A., Dawson, C. A. and Linehan, J. H. Kinetics of serotonin uptake by the dog lung is pH independent in the physiological range. Proc Soc Exp Biol Med **175**(3): 361-365, 1984.

140. Rickaby, D. A., Dawson, C. A. and Maron, M. B. Pulmonary inactivation of serotonin and site of serotonin pulmonary vasoconstriction. J Appl Physiol **48**(4): 606-612, 1980.

141. Rickaby, D. A., Fehring, J. F., Johnston, M. R. and Dawson, C. A. Tolerance of the isolated perfused lung to hyperthermia. J Thorac Cardiovasc Surg **101**(4): 732-739, 1991.

142. Rickaby, D. A., Linehan, J. H., Bronikowski, T. A. and Dawson, C. A. Kinetics of serotonin uptake in the dog lung. J Appl Physiol **51**(2): 405-414, 1981.

143. Roberts, A. B. and Sporn, M. B. Regulation of endothelial cell growth, architecture, and matrix synthesis by TGF-beta. Am Rev Respir Dis **140**(4): 1126-1128, 1989.

144. Roberts, A. B., Sporn, M. B., Assoian, R. K., Smith, J. M., Roche, N. S., Wakefield, L. M., Heine, U. I., Liotta, L. A., Falanga, V., Kehrl, J. H. and et al. Transforming growth factor type beta: rapid induction of fibrosis and angiogenesis in vivo and stimulation of collagen formation in vitro. Proc Natl Acad Sci U S A **83**(12): 4167-4171, 1986.

145. Rosiello, R. A. and Merrill, W. W. Radiation-induced lung injury. Clinics in Chest Medicine **11**: 65-71, 1990.

146. Roswit, B. and White, D. C. Severe radiation injuries of the lung. AJR Am J Roentgenol **129**(1): 127-136, 1977.

147. Rubin, P. and Casarett, G. W. (In) Clinical radiation pathology. W. B. Saunders, Philadelphia, 1968.

148. Rubin, P., Johnston, C. J., Williams, J. P., McDonald, S. and Finkelstein, J. N. A perpetual cascade of cytokines postirradiation leads to pulmonary fibrosis [see comments]. Int J Radiat Oncol Biol Phys **33**(1): 99-109, 1995.

149. Rubin, P., Shapiro, D. L., Finklestein, J. N. and Penney, D. P. The early release of surfactant following lung irradiation of alveolar type II cells. Int J Radiat Oncol Biol Phys **6**(1): 75-77, 1980.

150. Rubin, P., Siemann, D. W., Shapiro, D. L., Finkelstein, J. N. and Penney, D. P. Surfactant release as an early measure of radiation pneumonitis. Int J Radiat Oncol Biol Phys **9**(11): 1669-1673, 1983.

151. Saunders, M., Dische, S., Barrett, A., Harvey, A., Gibson, D. and Parmar, M. Continuous hyperfractionated accelerated radiotherapy (CHART) versus conventional radiotherapy in non-small-cell lung cancer: a randomised multicentre trial. CHART Steering Committee [see comments]. Lancet **350**(9072): 161-165, 1997.

152. Sause, W. T., Scott, C., Taylor, S., Johnson, D., Livingston, R., Komaki, R., Emami, B., Curran, W. J., Byhardt, R. W., Turrisi, A. T. and et al. Radiation Therapy Oncology Group (RTOG) 88-08 and Eastern Cooperative Oncology Group (ECOG) 4588: preliminary results of a phase III trial in regionally advanced, unresectable non-small-cell lung cancer. J Natl Cancer Inst **87**(3): 198-205, 1995.

153. Schaake-Koning, C., Schuster-Uitterhoeve, L., Hart, G. and Gonzalez Gonzalez, D. Prognostic factors of inoperable localized lung cancer treated by high dose radiotherapy. Int J Radiat Oncol Biol Phys **9**(7): 1023-1028, 1983.

154. Schaake-Koning, C., van den Bogaert, W., Dalesio, O., Festen, J., Hoogenhout, J., van Houtte, P., Kirkpatrick, A., Koolen, M., Maat, B., Nijs, A. and et al. Effects of concomitant cisplatin and radiotherapy on inoperable non- small-cell lung cancer [see comments]. N Engl J Med **326**(8): 524-530, 1992.

155. Schultheiss, T. E., Orton, C. G. and Peck, R. A. Models in radiotherapy: Volume effects. Med.Phys. **10**: 410-415, 1983.

156. Sibley, G. S., Mundt, A. J., Shapiro, C., Jacobs, R., Chen, G., Weichselbaum, R. and Vijayakumar, S. The treatment of stage III nonsmall cell lung cancer using

high dose conformal radiotherapy. Int J Radiat Oncol Biol Phys **33**(5): 1001-1007, 1995.

157. Slanina, J., Musshoff, K., Rahner, T. and Stiasny, R. Long-term side effects in irradiated patients with Hodgkin's disease. Int j Radiat Oncol Biol Phys **2**: 1-19, 1977.

158. Slosman, D. O., Davidson, D., Brill, A. B. and Alderson, P. O. ^{131}I-metaiodobenzylguanadine uptake in the isolated rat lung: a potential marker of endothelial cell function. Eur J Nucl Med **13**(10): 543-547, 1988.

159. Slosman, D. O., Morel, D. R. and Alderson, P. O. A new imaging approach to quantitative evaluation of pulmonary vascular endothelial metabolism. J Thorac Imaging **3**(1): 49-52, 1988.

160. Sporn, M. B., Roberts, A. B., Shull, J. H., Smith, J. M., Ward, J. M. and Sodek, J. Polypeptide transforming growth factors isolated from bovine sources and used for wound healing in vivo. Science **219**(4590): 1329-1331, 1983.

161. Stewart, L. A. and Pignon, J. P. Chemotherapy in non-small cell lung cancer: A meta-analysis using updated data on individual patients from 52 randomised clinical trials. Non-small Cell Lung Cancer Group. Br Med J **311**: 899-909, 1995.

162. Strum, J. M. and Junod, A. F. Radioautographic demonstration of 5-hydroxytryptamine- 3 H uptake by pulmonary endothelial cells. J Cell Biol **54**(3): 456-467, 1972.

163. Suhara, T., Sudo, Y., Yoshida, K., Okubo, Y., Fukuda, H., Obata, T., Yoshikawa, K., Suzuki, K. and Sasaki, Y. Lung as reservoir for antidepressants in pharmacokinetic drug interactions. Lancet **351**(9099): 332-335., 1998.

164. Theuws, J. C., Kwa, S. L., Wagenaar, A. C., Seppenwoolde, Y., Boersma, L. J., Damen, E. M., Muller, S. H., Baas, P. and Lebesque, J. V. Prediction of overall pulmonary function loss in relation to the 3-D dose distribution for patients with breast cancer and malignant lymphoma [see comments]. Radiother Oncol **49**(3): 233-243, 1998.

165. Thornton, S. C., Robbins, J. M., Penny, R. and Breit, S. N. Fibroblast growth factors in connective tissue disease associated interstitial lung disease. Clin Exp Immunol **90**(3): 447-452, 1992.

166. Toivonen, H. J., Makari, N. and Catravas, J. D. Monitoring of pulmonary endothelial enzyme function: an animal model for a simplified clinically applicable procedure. Anesthesiology **68**(1): 44-52, 1988.

167. Travis, E. L. Early indicators of radiation injury in the lung: are they useful predictors for late changes? Int J Radiat Oncol Biol Phys **6**(9): 1267-1269, 1980.

168. Travis, E. L. The sequence of histological changes in mouse lungs after single doses of x-rays. Int J Radiat Oncol Biol Phys **6**(3): 345-347, 1980.

169. Travis, E. L. Relative Radiosensitivity of the Human Lung. Advances in Radiation Biology. J. T. Lett (Ed.^Eds.) Academic Press, Orlando, Florida, **12:** 205-236, 1987.

170. Travis, E. L. and Down, J. D. Repair in mouse lung after split doses of X rays. Radiat Res **87**(1): 166-174, 1981.

171. Travis, E. L., Down, J. D., Holmes, S. J. and Hobson, B. Radiation pneumonitis and fibrosis in mouse lung assayed by respiratory frequency and histology. Radiat Res **84**(1): 133-143, 1980.

172. Travis, E. L., Harley, R. A., Fenn, J. O., Klobukowski, C. J. and Hargrove, H. B. Pathologic changes in the lung following single and multi-fraction irradiation. Int J Radiat Oncol Biol Phys **2**(5-6): 475-490, 1977.

173. Travis, E. L., Liao, Z. X. and Tucker, S. L. Spatial heterogeneity of the volume effect for radiation pneumonitis in mouse lung. Int J Radiat Oncol Biol Phys **38**(5): 1045-1054, 1997.

174. Travis, E. L., Parkins, C. S., Down, J. D., Fowler, J. F. and Thames, H. D., Jr. Repair in mouse lung between multiple small doses of X rays. Radiat Res **94**(2): 326-339, 1983.

175. Travis, E. L. and Tucker, S. L. Isoeffect models and fractionated radiation therapy. Int J Radiat Oncol Biol Phys **13**(2): 283-287, 1987.

176. Travis, E. L., Vojnovic, B., Davies, E. E. and Hirst, D. G. A plethysmographic method for measuring function in locally irradiated mouse lung. Br J Radiol **52**(613): 67-74, 1979.

177. van der Kogel, A. J. Dose-volume effects in the spinal cord. Radiother Oncol **29**: 105-109, 1993.

178. van der Kogel, A. J. Radiobiological and clinical data on dose/volume effect relationships in normal tissues. Radiother Oncol **29**: 127-128, 1993.

179. van Rongen, E., Tan, C. H. and Durham, S. K. Late functional, biochemical and histological changes in the rat lung after fractionated irradiation to the whole thorax. Radiother Oncol **10**(3): 231-246, 1987.

180. Vegesna, V., Withers, H. R., Thames, H. D., Jr. and Mason, K. Multifraction radiation response of mouse lung. Int J Radiat Biol Relat Stud Phys Chem Med **47**(4): 413-422, 1985.

181. Vigneswaran, W. T., Stanbrook, H. S., Doctor, R., McCormick, S., Schwappach, J. and Johnston, M. R. 5-Hydroxytryptamine uptake in oxygen radical-mediated acute lung injury. Am Rev Respir Dis **139**(2): 382-386, 1989.

182. Vijayakumar, S., Myrianthopoulos, L. C., Rosenberg, I., Halpern, H. J., Low, N. and Chen, G. T. Optimization of radical radiotherapy with beam's eye view techniques for non-small cell lung cancer. Int J Radiat Oncol Biol Phys **21**(3): 779-788, 1991.

183. von der Maase, H., Overgaard, J. and Vaeth, M. Effect of cancer chemotherapeutic drugs on radiation-induced lung damage in mice. Radiother Oncol **5**(3): 245-257, 1986.

184. Vujaskovic, Z., Down, J. D., van t' Veld, A. A., Mooyaart, E. L., Meertens, H., Piers, D. A., Szabo, B. G. and Konings, A. W. Radiological and functional assessment of radiation-induced lung injury in the rat. Exp Lung Res **24**(2): 137-148, 1998.

185. Ward, W. F. Radiation-induced pulmonary arterial perfusion defects: modification by D-penicillamine. Radiology **139**(1): 201-204, 1981.

186. Ward, W. F., Lin, P. J., Wong, P. S., Behnia, R. and Jalali, N. Radiation pneumonitis in rats and its modification by the angiotensin- converting enzyme inhibitor captopril evaluated by high-resolution computed tomography. Radiat Res **135**(1): 81-87, 1993.

187. Ward, W. F., Molteni, A., Solliday, N. H. and Jones, G. E. The relationship between endothelial dysfunction and collagen accumulation in irradiated rat lung. Int J Radiat Oncol Biol Phys **11**(11): 1985-1990, 1985.

188. Ward, W. F., Shih-Hoellwarth, A., Port, C. D. and Kim, Y. T. Modification of radiation-induced pulmonary fibrosis in rats. Radiology **131**(3): 751-758, 1979.

189. Webb, S. (In) The Physics of Three-Dimensional Radiation Therapy. Institute of Physics Publishing, London, 1993.

190. Weichselbaum, R. R. and Awan, A. M. Principles of radiation oncology. Lung cancer--A comprehensive treatise. J. D. Bitran, H. M. Golomb, A. G. Little and R. R. Weichselbaum (Ed.^Eds.) Grune and Stratton, Orlando: 61-70, 1987.

191. West, J. B. (In) Respiratory Physiology -- The essentials. Williams & Wilkins, Baltimore, 1995.

192. White, M. K., Hechtman, H. B. and Shepro, D. Canine lung uptake of plasma and platelet serotonin. Microvasc Res **9**(2): 230-241, 1975.

193. Withers, H. R., Taylor, J. M. and Maciejewski, B. Treatment volume and tissue tolerance. Int J Radiat Oncol Biol Phys **14**(4): 751-759, 1988.

194. Withers, H. R. and Thames, H. D. Dose fractionation and volume effects in normal tissues and tumors. Am J Clin Oncol **11**(3): 313-329, 1988.

195. Wolbarst, A. B., Sternick, E. S., Curran, B. H. and Dritschilo, A. Optimized radiotherapy treatment planning using the complication probability factor (CPF). Int J Radiat Oncol Biol Phys **6**(6): 723-728, 1980.

196. Yaes, R. J. and Kalend, A. Local stem cell depletion model for radiation myelitis. Int J Radiat Oncol Biol Phys **14**(6): 1247-1259, 1988.

197. Yorke, E. D., Kutcher, G. J., Jackson, A. and Ling, C. C. Probability of radiation-induced complications in normal tissues with parallel architecture under conditions of uniform whole or partial organ irradiation. Radiother Oncol **26**(3): 226-237, 1993.

APPENDIX A

Appendix A. Beagle Census and Schedule

Prefix	Ear Number	Dose (Gy)	Volume (%)	Sex	Date of Birth	Date Start XRT	Age at XRT (Months)	Date End XRT
L1	80065	54.0	33	F	10/28/89	06/22/92	32.3	07/31/92
L2	80008	49.5	67	F	07/05/89	07/13/92	36.8	08/21/92
L3	80034	45.0	100	CM	08/01/89	07/13/92	35.9	08/21/92
L4	80036	58.5	33	CM	09/20/89	07/20/92	34.5	08/28/92
L5	80042	54.0	67	CM	07/05/89	07/20/92	37.0	08/28/92
L6	80048	0.0	0	F	08/16/89	08/03/92	36.1	09/11/92
L7	80066	63.0	33	F	10/27/89	08/10/92	33.9	09/18/92
L8	80070	58.5	67	F	11/02/89	08/17/92	34.0	09/25/92
L9	80084	49.5	100	CM	10/22/89	08/24/92	34.6	10/02/92
L10	80085	67.5	33	CM	10/22/89	08/31/92	34.8	10/09/92
L11	80086	63.0	67	CM	10/23/89	08/31/92	34.8	10/09/92
L12	80087	54.0	100	CM	10/24/89	09/14/92	35.2	10/23/92
L13	80089	54.0	33	CM	10/28/89	09/14/92	35.1	10/23/92
L14	80090	49.5	67	CM	10/29/89	09/28/92	35.5	11/06/92
L15	80082	40.5	100	CM	10/19/89	11/09/92	37.2	12/18/92
L16	80095	58.5	33	CM	11/17/89	10/05/92	35.1	11/13/92
L17	80096	54.0	67	CM	11/17/89	10/19/92	35.6	11/27/92
L18	80100	0.0	0	CM	11/10/89	10/12/92	35.6	11/20/92
L19	80101	63.0	33	CM	04/07/90	10/26/92	31.1	12/04/92
L20	80105	58.5	67	CM	10/20/89	10/26/92	36.7	12/04/92
L21	80118	40.5	100	CM	08/20/91	11/23/92	15.4	01/01/93
L22	80117	67.5	33	CM	07/13/91	11/30/92	16.9	01/08/93
L23	80116	49.5	67	CM	07/05/91	12/07/92	17.4	01/15/93
L24	80109	45.0	100	F	07/22/91	12/14/92	17.0	01/22/93
L25	80120	54.0	33	CM	08/31/91	12/28/92	16.2	02/05/93

Prefix	Ear Number	Dose (Gy)	Volume (%)	Sex	Date of Birth	Date Start XRT	Age at XRT (Months)	Date End XRT
L26	80121	40.5	67	CM	09/09/91	01/04/93	16.1	02/12/93
L27	80122	36.0	100	CM	09/13/91	01/11/93	16.2	02/19/93
L28	80123	49.5	33	CM	09/13/91	01/18/93	16.4	02/26/93
L29	80115	45.0	67	F	09/29/91	01/25/93	16.1	03/05/93
L30	80150	36.0	100	F	10/07/91	02/01/93	16.1	03/12/93
L31	80160	45.0	33	CM	12/05/91	02/08/93	14.4	03/19/93
L32	80148	40.5	67	F	12/14/91	02/15/93	14.3	03/26/93
L33	80181	45.0	100	CM	01/21/92	02/22/93	13.3	04/02/93
L34	80142	58.5	33	F	02/13/92	03/01/93	12.7	04/09/93
L35	80138	45.0	67	F	02/15/92	03/08/93	12.9	04/16/93
L36	80166	49.5	100	CM	03/03/92	03/22/93	12.8	04/30/93
L37	80146	49.5	33	F	03/29/92	03/29/93	12.2	05/07/93
L38	80140	40.5	67	F	03/24/92	04/05/93	12.6	05/14/93
L39	80144	31.5	100	F	03/30/92	04/12/93	12.6	05/21/93
L40	80184	45.0	33	CM	11/22/91	04/26/93	17.4	06/04/93
L41	80183	45.0	67	CM	03/25/92	05/10/93	13.7	06/18/93
L42	80136	40.5	100	F	04/25/92	05/17/93	12.9	06/25/93
L43	80179	49.5	33	CM	03/06/92	06/14/93	15.5	07/23/93
L44	80134	49.5	67	F	04/27/92	06/21/93	14.0	07/30/93
L45	80177	36.0	100	CM	03/12/92	06/28/93	15.8	08/06/93
L46	80132	54.0	33	F	04/25/92	07/05/93	14.5	08/13/93
L47	80174	54.0	67	CM	03/17/92	07/11/93	16.0	08/20/93
L48	80130	36.0	100	F	04/29/92	07/19/93	14.9	08/27/93
L49	80172	58.5	33	CM	03/12/92	07/26/93	16.7	09/03/93
L50	80128	54.0	67	F	04/27/92	08/02/93	15.4	09/10/93
L51	2122791	45.0	100	F	12/28/92	08/23/93	7.9	10/01/93

Prefix	Ear Number	Dose (Gy)	Volume (%)	Sex	Date of Birth	Date Start XRT	Age at XRT (Months)	Date End XRT
L52	2117401	40.5	33	CM	12/18/92	08/09/93	7.8	09/17/93
L53	2117355	40.5	67	CM	12/18/92	08/30/93	8.5	10/08/93
L54	2121611	40.5	100	F	12/27/92	09/13/93	8.7	10/22/93
L55	2121115	72.0	33	F	12/27/92	09/13/93	8.7	10/22/93
L56	2117827	45.0	67	CM	12/20/92	09/20/93	9.1	10/29/93
L57	2119838	31.5	100	F	12/24/92	09/20/93	9.0	10/29/93
L58	2115565	40.5	33	CM	12/16/92	10/04/93	9.7	11/12/93
L59	2121921	49.5	67	F	12/26/92	09/27/93	9.2	11/05/93
L60	2116260	40.5	100	CM	12/20/92	10/18/93	10.1	11/26/93
L61	2120798	40.5	33	CM	12/25/92	10/18/93	9.9	11/26/93
L62	2122022	40.5	67	CM	12/26/92	11/01/93	10.3	12/10/93
L63	2117789	27.0	100	CM	12/20/92	11/01/93	10.5	12/10/93
L64	2122634	45.0	33	F	12/28/92	11/08/93	10.5	12/17/93
L65	2118114	36.0	67	CM	12/18/92	11/08/93	10.8	12/17/93
L66	2118483	40.5	100	CM	12/19/92	11/22/93	11.3	12/31/93
L67	2119021	40.5	33	CM	12/21/92	11/22/93	11.2	12/31/93
L68	2168626	49.5	67	CM	03/23/93	12/13/93	8.8	01/21/94
L69	2169126	0.0	0	F	03/24/93	12/13/93	8.8	01/21/94
L70	2168715	36.0	33	CM	03/23/93	12/13/93	8.8	01/21/94
L71	2169355	54.0	67	F	03/23/93	12/20/93	9.1	01/28/94
L72	2169002	45.0	100	CM	03/23/93	12/20/93	9.1	01/28/94
L73	2170159	45.0	33	F	03/26/93	12/20/93	9.0	01/28/94
L74	2169754	36.0	67	CM	03/25/93	01/03/94	9.5	02/11/94
L75	2170230	27.0	100	F	03/26/93	01/10/94	9.7	02/18/94
L76	2170621	36.0	33	CM	03/25/93	01/10/94	9.7	02/18/94
L77	2170353	36.0	67	F	03/26/93	01/24/94	10.1	03/05/94

Prefix	Ear Number	Dose (Gy)	Volume (%)	Sex	Date of Birth	Date Start XRT	Age at XRT (Months)	Date End XRT
L78	2170647	31.5	100	CM	03/25/93	01/31/94	10.4	03/11/94
L79	2170370	40.5	33	F	03/26/93	02/07/94	10.6	03/18/94
L80	2213788	36.0	67	F	06/13/93	02/14/94	8.2	03/25/94
L81	2214245	27.0	100	F	06/13/93	02/28/94	8.7	04/08/94
L82	2214571	49.5	33	CM	06/13/93	02/28/94	8.7	04/08/94
L83	2214857	0.0	0	CM	06/14/93	03/07/94	8.9	04/15/94
L84	2216221	36.0	33	F	06/16/93	03/07/94	8.8	04/15/94
L86	2217261	54.0	33	CM	06/18/93	03/21/94	9.2	04/29/94
L87	2220245	36.0	100	F	06/23/93	03/21/94	9.0	04/29/94
L88	2220750	63.0	33	F	06/24/93	03/28/94	9.2	05/06/94
L89	2219557	58.5	67	CM	06/22/93	04/04/94	9.5	05/13/94
L90	2242419	27.0	100	CM	07/25/93	04/11/94	8.7	05/20/94
L91	2190265	67.5	33	F	05/05/93	04/11/94	11.4	05/20/94
L92	2188881	31.5	67	CM	05/01/93	06/06/94	13.4	07/15/94
L93	2191130	63.0	33	F	05/06/93	05/23/94	12.7	07/01/94
L94	2190257	0.0	0	CM	05/05/93	05/23/94	12.8	07/01/94
L95	2205718	31.5	100	CM	05/30/93	06/06/94	12.4	07/15/94
L96	2192071	67.5	33	CM	05/08/93	06/06/94	13.1	07/15/94
L97	2196573	36.0	33	F	05/16/93	05/30/94	12.6	07/08/94
L98	2194856	40.5	33	CM	05/14/93	06/13/94	13.2	07/22/94
L99	2199467	36.0	100	F	05/21/93	06/13/94	12.9	07/22/94
L100	2200023	36.0	67	CM	05/22/93	06/13/94	12.9	07/22/94
L101	2201682	45.0	33	F	05/23/93	06/20/94	13.1	07/29/94
L102	2202298	40.5	67	CM	05/23/93	06/20/94	13.1	07/29/94
L103	2204274	27.0	100	F	05/27/93	06/27/94	13.2	08/05/94
L104	2204924	58.5	33	CM	05/28/93	07/04/94	13.4	08/12/94

Prefix	Ear Number	Dose (Gy)	Volume (%)	Sex	Date of Birth	Date Start XRT	Age at XRT (Months)	Date End XRT
L105	2205581	45.0	67	F	05/30/93	07/04/94	13.3	08/12/94
L106	2204932	31.5	100	CM	05/28/93	07/11/94	13.6	08/19/94
L107	2206561	31.5	33	F	05/31/93	07/11/94	13.5	08/19/94
L108	2212056	31.5	67	CM	06/09/93	07/18/94	13.5	08/26/94
L109	2222361	31.5	100	F	06/28/93	07/18/94	12.8	08/26/94
L110	2212196	31.5	33	CM	06/10/93	07/25/94	13.7	09/02/94
L111	2224828	36.0	33	F	06/30/93	07/25/94	13.0	09/02/94
L112	2212960	36.0	67	CM	06/11/93	08/01/94	13.9	09/09/94
L113	2227291	31.5	33	F	07/05/93	08/01/94	13.1	09/09/94
L114	2214164	31.5	67	CM	06/13/93	08/01/94	13.8	09/09/94
L115	2229927	40.5	100	F	07/09/93	08/08/94	13.2	09/16/94
L116	2214598	45.0	33	CM	06/13/93	08/08/94	14.0	09/16/94
L117	2243598	36.0	33	F	07/26/93	08/15/94	12.8	09/23/94
L118	2215705	31.5	33	CM	06/16/93	08/15/94	14.2	09/23/94
L119	2244128	31.5	67	F	07/27/93	08/22/94	13.0	09/30/94
L120	2218674	49.5	33	CM	06/21/93	08/22/94	14.2	09/30/94
L121	2245302	63.0	33	F	07/29/93	08/29/94	13.2	10/07/94
L122	2249464	54.0	33	F	08/05/93	08/29/94	13.0	10/07/94
L123	2249529	72.0	33	CM	08/05/93	08/29/94	13.0	10/07/94
L124	2249502	72.0	33	F	08/05/93	08/29/94	13.0	10/07/94
L125	2249952	40.5	100	CM	08/06/93	08/29/94	12.9	10/07/94
L126	2254981	72.0	33	F	08/12/93	09/05/94	13.0	10/10/94
L127	2255758	72.0	33	CM	08/13/93	09/05/94	12.9	10/10/94
L128	2259494	54.0	33	F	08/18/93	09/05/94	12.8	10/10/94
L129	2263629	58.5	67	CM	08/25/93	09/05/94	12.5	10/10/94

APPENDIX B

Appendix B. Irradiation Procedure

1. Record beginning beam time.
2. Position table at 90 degrees.
3. Position gantry head at 0 degrees.
4. Anesthetize dog and place in dorsal recumbency in cradle. Straighten dog so his chest is vertical.
5. Position the cradle so that treatment field is over the racquet.
6. Use white tape to extend the dog's forelimbs cranially and secure to the table.
7. Set collimator to proper field size.
8. Level the table.
9. Set height of table using ruler to position isocenter.
10. Level table again (level seems to change as table is raised and lowered).
11. Check table height again.
12. Align marks on opposite sides of cradle with lasers.
13. Check table height again.
14. Position cranial edge of light field according to set up information for each dog. For most dogs position is 1 cm caudal to the cranial tip of the sternum.
15. Align dog so that the lengthwise crosshair is centered on midline, aligned on the center of the sternum and the tip of the xiphoid process.
16. When alignment is complete, recheck:

    leveling of the table
    table height
    field size
    cranial field placement
    alignment

Appendix B. Irradiation Procedure (continued)

17. Irradiate AP field

18. Rotate gantry to 360 degrees.

19. Check alignment of lengthwise crosshair with mark on bottom of cradle. This allows you to do some "quality control" of repeatability.

20. Irradiate PA field.

21. When all dogs are finished, record ending beam time and total MU used.

22. If no other users are scheduled for that day, turn off the machine.

    Turn off lasers.
    Turn off console/camera power.
    Turn off accelerator power.

APPENDIX C

Appendix C. Procedures Schedule

Pre-treatment work-up
Bordetella vaccination
(repeat in 2 wks, 1 yr)
Body weight
Temperature
Heart rate
Respiratory rate
CBC, SADP, UA
Awake arterial blood gas
Thoracic radiographs
Alpha cradle fitting
CT scan
Perfusion (Q) scintigraphy
Perfusion SPECT (select dogs)
Awake art. blood gas (rm air)
Cardiopulm. fxn tests

3 months post end XRT
CBC, SADP, UA
Awake art. blood gas
Thoracic radiographs
Q scintigraphy
Q SPECT (select dogs)
Cardiopulm. fxn tests

1 year post end XRT
CBC, SADP, UA
Thoracic radiographs

2 years post end XRT
CBC, SADP, UA
Thoracic radiographs
Q scintigraphy
Cardiopulm. fxn tests
Necropsy

Cardiopulmonary function tests include:
ECG
Functional residual capacity
Static and dynamic compliance
R. ventricular pressure
Pulmonary artery pressure
Pulmonary arterial wedge pressure
Cardiac output
Paired arterial and venous blood gases
Indicator dilution assays
(serotonin uptake, extravascular water, cardiac output)

Physical Exam Schedule:
Pre-treatment
Weekly to 3 m post
Biweekly to 1 y post
Monthly after 1 y

* All dogs will receive supplementary feeding during their irradiation period
* All dogs will be observed on a daily basis
* Physical exams will be done on each dog according to the above schedule
* Dogs developing respiratory distress (respiratory rates greater than 150 bpm or arterial pO_2 less than 65 mm Hg) or significant weight loss will be evaluated for early necropsy.

APPENDIX D

Appendix D: Lung Assay Procedure
(Lung mechanics, hemodynamics, blood gases, indicator dilution assays)

Enter barometric pressure into blood gas machine.

Set up:
2 transducers
ice water bath (get ice and key in lunch room)
sterile saline w/ venocath (put in ice bath)
sterile "SAVE" syringes w/ 3 ml saline in ice bath
empty pan of fresh, dilute Nolvassan solution in sink
1 femoral a. catheter/dog, sterile gloves, 15 blade
1 jugular v. catheter/dog, sterile gloves, 15 blade
1 Swan-Ganz catheter/dog
2 sterile towel packs/dog
Marquette: Set beagle ID #, time, date
Under "CO": Set vol = 3, cath size = 5 fr
"ART" gain = 150, "PA" gain = 30
tape cords to table
place temp. probe in ice bath, under water

Draw up:
10 heparinized saline flushes
two 3 cc heparinized syringes for blood gas/dog
one 12 cc heparinized syringe for standard/dog
anesthetic drugs for each dog

Place cephalic v. catheter, record pre-treatment PCV/TP.

Induce anesthesia with thiopental. **DO NOT GIVE ATROPINE FIRST!** Reserve atropine until the cardiac catheterization procedure has been completed, then administer only if needed.

Clip hair for femoral a. and jugular v. catheter placement.

Attach the 5 ECG leads (chest lead goes caudal to the R olecranon). With HR below 150, print strip with leads II, V, I and III. Change lead I to lead AVF on the Marquette and print another strip.

Appendix D: Lung Assay Procedure (continued)

Functional Residual Capacity

Empty reservoir bag into the scavengingsystem to minimize waste anesthetic gas exposure. Unhook the E.T. tube and transfer the dog to the FRC chamber. Attach the E.T. tube to the port in the FRC chamber and seal the box. Work with the engineer to calibrate the box and obtain FRC readings. When finished, remove beagle from FRC box and reattach anesthesia machine and ECG lead II.

Dynamic Compliance

Pass esophageal balloon. Remove stylet and fill balloon with air three times, allowing it to deflate each time. This assures good contact between balloon and esophageal wall. Work with the engineer to obtain dynamic compliance readings. Remove balloon when finished.

Cardiac Catheterization

Scrub jugular v. and femoral a. catheter sites and place catheters.

Inflate balloon of Swan-Ganz catheter with 3/4 ml air to make sure it is intact, then deflate. Flush yellow (distal lumen) and blue (proximal lumen) ports of S-G catheter, leaving syringe on blue port. Attach yellow port to PA transducer and flush through transducer. Zero the PA pressure reading. Connect thermistor lumen port to monitor.

Insert and position the S-G catheter.

Print graphs of:
- RV pressures and waveform (Diastolic pressure = 0)
- PA pressures and waveform
- pulmonary wedge pressure (usually around 6 to 8)
- cardiac output (vol = 3, size = 5 fr)

Draw paired blood gas samples: One from PA, one from femoral artery. Draw 12 ml blood sample from femoral a. into heparinized syringe for indicator dilution assay standards. Run PCV and TP on this sample and record on anesthetic record. Attach PA and FA blood gas results to anesthetic record.

Indicator Dilution Assay

Start dog on the ventilator for this portion of the procedure. Everyone must wear gloves for the remainder of the procedure. Connect dog to fraction collector pump and complete indicator dilution assay. The dog's blood and secretions are now radioactive and gloves must be worn when handling him. Hold off femoral artery with an ice pack and very firm pressure for 30 minutes after removing catheter. Hold off jugular catheter site with firm pressure.

Give 250 ml LRS SQ to each dog.

Appendix D: Lung Assay Procedure (continued)

Set up for second dog.
Make sure blood gas results (PA and FA) get attached to the anesthesia record immediately.

These dogs are confined to the "radioactive" metabolic cages for 4 days following this procedure.

APPENDIX E

Appendix E. Indicator Dilution Assay Procedure

SAMPLE COLLECTION

Three-Headed Pump

#1 – Infuses saline and injectate into jugular vein (tube 1/16 O.D.)
#2 – Withdraws from the femoral artery (tube 1/16 O.D.)
#3 – Delivers EtOH to the fraction collector (tube 1/8 O.D.)

- Tubing from pump 1 and 2 are joined with a "Y" connector for collection into vials.
- Isotopes are injected upstream of pump head #1 at the start of the run.

Collection Vials

- 45 numbered collection vials are used per study.
- 5 vials are weighed prior to the study. The weight is recorded on the vials and on the data sheet. The same 5 vials are reweighed after the study.

Injectate – Preparation for two dogs

- Always wear gloves when handling isotopes and work over a tray.
- Add 2.5 ml sterile H_2O to a 25 mg vial of Cardiogreen (Sigma). Cardiogreen must be kept in the dark and cannot be used after 10 hours.
- Add 500 µl Cardiogreen to a 15 ml tube. (250 µl for one dog)
- Add 80 µl ^{14}C 5-hydroxytriptamine (5-HT) (4 µCi) (40 µl for one dog)
- Add 40 µl ^{3}H H_2O (20 µCi) (20 µl for one dog)
- Add 2000 µl sterile H_2O (1000 µl for one dog)
- Mix gently and draw solution into a 3 ml syringe.
- Filter through a syringe filter into a sterile vacutainer.
- Label two 1 ml syringes and draw to 1 ml of injectate into each syringe.
- There must be enough injectate left in the tube for the standards (~ 250 µl).
- Weigh each syringe and record weight on data sheet.
- Place the syringes in the dark in the cabinet for later use.
- Reweigh the syringes after injection – always record post weight on data sheet.
- Discard all contaminated materials in the radioactive materials (RAM) waste.

Standards

- Prepare three 50 ml centrifuge tubes: one with 10 µl, one with 20 µl and one with 30 µl of injectate.
- Add 190 µl of saline to each tube.
- Draw 12 ml of arterial blood from subject prior to the run to use for standards.
- Add 3 ml arterial blood to each of the three 50 ml standard tubes and mix well.
- Add 12 ml 100% EtOH to each standard tube and mix well.

Appendix E. Indicator Dilution Assay Procedure (continued)

- Centrifuge standards for 30 min at 1000 RPM.
- Freeze standards along with samples from indicator dilution assay run (-20°C).

Samples

- Mix each sample in its collection vial and pour into a snap top centrifuge tube.
- Transfer the vial number from the vial to the tube.
- Centrifuge samples for 30 min at 1000 RPM.
- Freeze samples and standards for at least two days prior to analysis (-20°C).

ANALYSIS

Optical Density

- Optical density is read using a Spectronic 21D spectrophotometer. Turn the machine on and allow to warm up for 30 minutes prior to reading samples.
- Remove samples from freezer and centrifuge for 30 min at 1000 RPM.
- Pour off supernatant into square spectrophotometer cuvettes. Transfer centrifuge tube number to a scintillation vial (place label on cap).
- Read OD at 780 nm. Record tube number and OD on a data sheet. Use the first vial (lowest sample number) to zero the spectrophotometer. There will be no Cardiogreen or radioactivity in the first several samples.
- Save supernatant for the next step!

Scintillation Counting

- Transfer 1.5 ml of supernatant to a scintillation vial.
- Add 10 ml Ecolite scintillation fluid to vial.
- Place screw cap with sample number on vial.
- Repeat above for each sample.
- Crossover standards: To the first vial (lowest sample number) add 20 µl ^{14}C crossover standard. To the second vial add 20 µl ^{3}H crossover standard. Label these vials and place them at the beginning of the sample counting racks.
- Count radioactivity in the Beckman LS 6000 SE scintillation counter. The machine is programmed to count ^{14}C and ^{3}H in the indicator dilution assay samples on user card number 6.
- Place the user card on the front of the first rack to be counted.
- Place a halt card on the red rack and place it at the end of the run.
- Check to make sure that the printer is on line.
- Press start for automatic counting.

Appendix E. Indicator Dilution Assay Procedure (continued)

- When counting is completed, review results before discarding samples. Samples may be re-counted if there are any problems.
- Discard fluids in the sink with the water running. Place the empty vials in the RAM waste. Only dry waste may be disposed of in these containers.

APPENDIX F

Appendix F. Indicator Dilution Assay Data Form

DATA SHEET: LUNG METABOLISM OF VASOACTIVE HORMONES

DATE OF EXPERIMENT_____

IMPERMEABLE INDICATOR: Cardiogreen dye
PERMEABLE INDICATOR: ^{14}C serotonin
EXTRAVASCULAR INDICATOR tritiated water

BOLUS INJECTION NO. / NAME_____

TOTAL NUMBER OF SAMPLES USED FOR CURVE_____

ID NO. OF FIRST SAMPLE USED (ABOVE BACKGROUND)_____

ID NO. OF FIRST SAMPLE COLLECTED AT INJECTION_____

SAMPLING TIME INCREMENT (sec) 0.6 Snap Tubes (5) Post wt. _____

Pre wt. _____

TOTAL FLOW (IF KNOWN) XXXXXXX Net wt. _____

VOLUME COLLECTED IN EACH SAMPLE (ml) _____* HEMATOCRIT_____

*VOLUME = (W/5) (0.256 / 1.045) where W = weight of 5 samples.

INJECTED DOSE OF PERMEABLE INDICATOR (nmol) _____

INJECTED VOLUME (ml) _____

BACKGROUND COUNTS: IMPERMEABLE INDICATOR_____
BACKGROUND COUNTS: PERMEABLE INDICATOR_____
BACKGROUND COUNTS: EXTRAVASCULAR INDICATOR_____

FOR STANDARD VOLUMES PIPETTED INTO SAMPLES:

HOW MANY STANDARDS 3

VOLUME OF SAMPLE (ml) 3

	1	2	3
VOLUME OF INJECTATE ADDED TO SAMPLE (µl)	10	20	30

P_a_____ P_w_____ R_{dyn}_____ C_{dyn}_____
Body wt_____ Body temp_____ FRC_____

Blood chemistry on Air:
P_aO_2_____ P_aCO_2_____ pH_a_____ $[HCO_3^-]_a$_____
T_aCO_2_____ Hb_a gm%_____ Hb_a %sat_____ C_aO_2_____

Blood chemistry on 100% O2:
P_aO_2_____ P_aCO_2_____ pH_a_____ $[HCO_3^-]_a$_____
T_aCO_2_____ Hb_a gm%_____ Hb_a %sat_____ C_aO_2_____
P_vO_2_____ P_vCO_2_____ pH_v_____ $[HCO_3^-]_v$_____
T_vCO_2_____ Hb_v gm%_____ Hb_v %sat_____ C_vO_2_____

APPENDIX G

Appendix G. Radiographic Evaluation Form

Dog ID number _____Volume_____ Time point_____

NB: Review pre & post tx thoracic radiographs (VD, R lat, L lat) and port films for evaluation of changes in and out of field.

1) Mediastinal shift (VD) Right_____ Left_____ None_____

2) Pleural changes VD LAT
Fissure lines Grade_____ Grade_____
(0 = absent, 1 = mild, 2 = moderate, 3 = severe).

Rounded margins	Yes_____	No_____	Yes_____	No_____
Pneumothorax	Yes_____	No_____	Yes_____	No_____

3) Lung changes

A) Decreased vascular detail (LAT)

None	_____	(0)
Mild (3° vessels obscured)	_____	(1)
Moderate (2° vessels obscured)	_____	(2)
Severe (1° vessels obscured)	_____	(3)

B) Increased opacity

None	VD_____	LAT_____	(0)
Mild	VD_____	LAT_____	(1)
Moderate	VD_____	LAT_____	(2)
Severe	VD_____	LAT_____	(3)

Distribution

VD	In field_____	Out of field_____	100%_____
	Cranial_____	Middle_____	Caudal _____
LAT	Cranial_____	Middle_____	Caudal _____

	VD		LAT	
C) Peribronchial changes	Yes_____	No_____	Yes_____	No_____
D) Air bronchograms	Yes_____	No_____	Yes_____	No_____

Reviewer_____Date_____

APPENDIX H

Appendix H. Radiographic Grading Criteria

Fissure lines: visualized

Grade 0) Absent

Grade 1) Mild: Barely visible

Grade 2) Moderate: Distinct, easily

Grade 3) Severe: Full margin of the lung lobe visible.

Decreased vascular detail (LAT)

Mild (3° vessels obscured): Can see 2° vessels, but 3° vessels have indistinct margins.

Moderate (2° vessels obscured): Cannot see 3° vessels. 2° vessels have indistinct margins. Indistinct larger vessels, but still visible:
aorta
m pulmonary a
cr vena cava
cd vena cava
cr lobar aa
vessels over heart

Severe (1° vessels obscured): Non-visualization of:
aorta
m pulmonary a
cr vena cava
cd vena cava
cr lobar aa
vessels over heart

Increased opacity (VD):

None: Mediastinum clearly visible. No increased opacity.

Mild: Mediastinal line still distinct.

Moderate: Mediastinal line still visible, but indistinct.

Severe: Medistinal line not visible. Cd vena cava (VC) and aorta obscured.

Increased opacity (LAT)

None: Cr VC, Cr border of the heart, and Cd VC clearly visible.

Mild: Cr VC, Cr border of the heart, and Cd VC still distinct.

Moderate: Cr VC, Cr border of the heart, and Cd VC still visible, but indistinct.

Severe: Cr VC, Cr border of the heart, and Cd VC not visible.

APPENDIX I

Appendix I. Necropsy Form

Date_____

Beagle No._____ Signalment_____ Body wt._____

Percent volume irradiated _____ Time post XRT_____

Lung (weight in g)

Right Cranial_____ Left Cranial and Middle_____

Right Middle_____ Left Caudal_____

Right Caudal_____

Accessory_____

Heart (weight in g)

Right Auricle_____ Right Ventricle_____

Left Auricle_____ Left Ventricle_____

Septum_____

Liver (weight in g)_____

Other Tissues Collected:

Pericardium_____ Esophagus_____

Stomach (cardia)_____ Trachea_____

Liver in field_____

Liver out of field_____

Gross Lesions_____
_____